# The Role of MMPs, Smad3 and Heat Shock Proteins in TGF-β-Induced Anterior Subcapsular Cataract Development

by

**Alice Banh**

A thesis

presented to the University of Waterloo

in fulfillment of the

thesis requirement for the degree of

Doctor of Philosophy

in

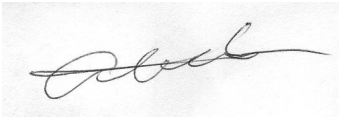Vision Science and Biology

Waterloo, Ontario, Canada, 2007

# Author's Declaration

I hereby declare that I am the sole author of this thesis.  This is a true copy of thesis,

Including any required final revisions, as accepted by my examiners.

I understand that my thesis may be made electronically available to the public.

Signature

# Abstract

Transforming growth factor beta (TGF-β) has been implicated in anterior subcapsular cataract (ASC) development. In the first section of this thesis, an *in-vitro* rat lens model was used to determine the role of matrix metalloproteinases during TGF-β-induced ASC. In the second part, an *in-vivo* TGF-β transgenic and Smad3 knockout model was used to examine the role of Smad3 signaling pathway in TGF-β-induced ASC development. Lastly, an *in-vitro* rat lens epithelial explant culture model was used to investigate the potential role of heat shock proteins (Hsps) in TGF-β-induced epithelial-mesenchymal transition (EMT). Optical, morphological and molecular changes were analyzed in theses studies.

Results from cultured rat lenses show a significant increase of back vertex distance variability (decrease of sharpness and focus) during ASC development. Inhibition of MMPs eliminated the TGF-β-induced plaque formation. Similarly, the overexpression of TGF-β1 in transgenic mouse lenses leads to ASC formation and a decrease in lens optical quality in comparison to wild-type lenses, while TGF-β1/Smad3$^{-/-}$ (null) lenses show diminished TGF-β-induced effects. The plaques formed in the TGF-β1/Smad3$^{-/-}$ lenses are substantially smaller than in the TGF-β1/Smad3$^{+/+}$ lenses. The morphological and molecular changes of TGF-β2/FGF-2 treated rat lens epithelial explants are similar to those found in the TGF-β2 treated rat lenses and transgenic TGF-β1 mouse lenses. Heat shock treatment prior to TGF-β treatment significantly reduced the effects of EMT in rat LECs.

In conclusion, MMP inhibition prevented TGF-β-induced ASC formation whereas heat shock treatment and the absence of Smad3 protein expression only reduced the severity of TGF-β-induced effects.

# Acknowledgements

I would like to thank my supervisor, Dr. Jacob Sivak, who is always available to provide guidance and encouragement. Dr. Sivak inspired me to keep on pursuing my interest in scientific research.

Special thanks to Dr. Judy West-Mays at McMaster University for her tremendous help and inspiration and for providing unlimited resources that made it possible for me to conduct my research studies.

I would like to also thank my committee members, Dr. Anthony Cullen and Dr. Mathilakath M. Vijayan for their help and guidance.

Thanks to Paula Deschamps and Dale Weber for their technical support.

I would like to acknowledge all my fellow graduate students (past and present) from both the Sivak and West-Mays labs for providing a friendly and supportive research environment.

# Table of Contents

**Chapter 2: Lens Specific Expression of TGF-β induces Anterior Subcapsular in the Absence of Smad3**……..……………………………...…….31

**Chapter 3: Lens Role of Molecular Chaperones in TGF-β-induced Epithelial-Mesenchymal Transition in Rat Lens Epithelial Explants**

# List of Figures

# List of Tables

# List of Abbreviations

α-crystallin     alpha crystallin

αSMA             alpha smooth muscle actin

ASC              anterior subcapsular cataract

BVD error        back vertex distance variability

β-actin          beta actin

β-crystallin     beta crystallin

ECM              extracellular matrix

EMT              epithelial-to-mesenchymal transition

FGF              fibroblast growth factor

Hsps             heat shock proteins

LECs             lens epithelial cells

MMPs             matrix metalloproteinases

PCO              posterior capsular opacification

PCR              polymerase chain reaction analysis

TGF-β            transforming growth factor beta

TIMPs            tissue inhibitors of metalloproteinases

TUNEL            terminal deoxynucleotidyl transferase mediated dUTP nick end labeling

# General Introduction

The ocular lens is a transparent structure that provides part of the refractive power needed to focus images on the retina of the human eye. The lens grows throughout life by the continuous addition of new fibre cell layers on top of older fibres, with minimal protein turnover.[1] Therefore, the cells in the lens nucleus were formed during the early phase of embryonic development and the cells in the cortex are the newest. It is important that the lens maintains its native protein organization to function as an optical device.[1, 2] A cataract results in reduced transparency of the lens and this leads to vision loss.[3] Anterior subcapsular cataracts (ASC) are cataracts that involve the formation of opacities in the epithelial cells following ocular trauma and eye surgery.[4] They are characterized by capsular wrinkling, formation of spindle-shaped cells, and the accumulation of extracellular matrix (ECM).[4, 5] The formation of this type of cataract may be associated with abnormal expressions of growth factors within the lens.

Transforming growth factor beta (TGF-β) is a secreted polypeptide that is involved in various cellular processes, including cell proliferation, differentiation, apoptosis, migration and ECM formation.[5-9] TGF-β has been shown to be promote wound healing by stimulating the production and deposition of ECM, which are essential to normal tissue repair after injury.[10] The profibrotic actions of TGF-β have also been implicated in fibrotic pathogenesis in the eye such as glaucoma and ASC.[4, 11-13] Past studies have found that the over expression of active TGF-β proteins in rat lens epithelial explants and cultured rat and transgenic mice lenses induces the formation of fibrotic plaques and morphological changes similar to those of ASCs in human lenses.[4, 5, 14-16] As

1

in anterior subcapsular cataract, both alpha smooth muscle actin ($\alpha$-SMA) and type I collagen are found in the TGF-$\beta$-induced plaques.[4]   Thus, both $\alpha$-SMA and type I collagen have been used as molecular markers to identify capsular plaques that are associated with subcapsular cataract because these proteins are not usually present under normal conditions.[14, 17]   Previous *in-vitro* TGF-$\beta$ experiments with cultured rat lenses showed that there are both a gender and an age effect in relation to cataract development when exposed to TGF-$\beta$.[17, 18]   However, the mechanisms involved in TGF-$\beta$-induced cataract formation are still unclear.

The focus of this dissertation is to explore the potential TGF-$\beta$ mechanisms involved in subcapsular cataract development in three different rodent models.  The morphological and molecular effects of TGF-$\beta$ were analyzed by use of histology, immunohistochemistry, Western blot protein analysis, TUNEL assay and optical analysis. The first chapter examines the optical effects of TGF-$\beta$-induced subcapsular cataract formation in cultured rat lenses using a laser scanning instrument.  The role of matrix metalloproteinases (MMPs) with respect to TGF-$\beta$-induced subcapsular cataract development was also investigated.  The purpose of the second chapter was to directly determine the requirement for Smad3 (TGF-$\beta$ signaling protein) in ASC formation using an *in-vivo* transgenic TGF-$\beta$1/Smad3 knockout mouse model.  Evidence of ASC formation in TGF-$\beta$1/Smad3$^{-/-}$ (null) mice and their TGF-$\beta$1/Smad$^{+/+}$ (wild-type) littermates was evaluated histologically using EMT (epithelial-to-mesenchymal transition) markers which include $\alpha$-SMA as well as fibronectin, collagen type I and IV as fibrotic markers.  Formation of ASC in mice was also evaluated using a quantitative

measure of lens optical quality. Finally chapter three used the *in-vitro* rat lens epithelial explant model to investigate the effects of heat shock treatment and the role of molecular chaperones on TGF-β2-induced EMT. The morphological and molecular changes of the rat lens epithelial explants were examined. The expressions of α-SMA, F-actin, and E-cadherin were used as indicators of EMT. The protein expression levels of Hsp70, Hsp90 and αA- and αB-crystallin and apoptotic cell loss were also determined.

*Note: The references for general introduction and conclusion is on pg.159

# Chapter 1

## The Role of Matrix Metalloproteinases in TGF-β-induced Anterior Subcapsular Cataract Development

All of the work involved in chapter one was done by Alice Banh. A majority of the data and results from chapter 1 was published in a manuscript as part of a collaborative effort with the West-Mays group at McMaster University. Please refer to Dwivedi et al. American Journal of Pathology, Vol. 168, No.1, Jan. 2006 (p.69-79).

## 1.1 Introduction

The crystalline lens is a transparent structure that provides part of the refractive power needed to focus images on the retina of the human eye. The embryonic lens arises from the primitive head ectoderm overlying the optic vesicle. The head ectoderm is stimulated by the optic vesicle to proliferate and thicken into a placode, which eventually forms a hollow lens vesicle. The lumen of the vesicle is then filled by growth of the posterior vesicle cells to form the primary lens fibre cells. Continued development of the lens is a result of mitosis of epithelial cells located at the lens equator.[1, 2] The proliferated epithelial cells become the secondary fibre cells. The lens grows throughout life by the continuous addition of new fibre cell layers on top of older fibres, with minimal protein turnover.[1] The cells that form the deeper fibres lose their nuclei and mitochondria. Therefore, the cells in the lens nucleus were formed during the early phase of embryonic development and the cells in the cortex are the newest. It is important that the lens maintains its native protein organization to function as an optical device.[1, 3]

A cataract results in reduced transparency of the ocular lens and this leads to vision loss. Many factors such as UV radiation, congenital cataracts, eye injuries and age-related changes may cause the onset of cataracts.[4] However, the causes of cataracts are still not fully understood and there is a need to investigate the molecular mechanisms that are involved in cataract formation. Anterior subcapsular cataracts are common cataracts that involve the formation of opacities in the epithelial cells following ocular trauma and eye surgery.[5] They are characterized by capsular wrinkling, formation of

spindle-shaped cells, and the accumulation of extracellular matrix (ECM).[5, 6] The formation of this type of cataract may be associated with abnormal expressions of growth factors within the lens.

Transforming growth factors beta (TGF-β) are secreted polypeptides that play crucial roles in cell proliferation, differentiation, migration and ECM formation in the lens. There are three functionally and structurally related species of TGF-β: TGF-β1, TGF-β2 TGF-β3.[6] TGF-β is involved in wound healing processes by promoting the production and deposition of the extracellular matrix, which is essential to normal tissue repair after injury.[7] In normal mature lenses, TGF-β proteins are secreted as inactive complexes and remain latent.[6] Interestingly, past studies have found that the over expression of active TGF-β proteins in rat lens epithelial explants and cultured rat and transgenic mice lenses induces the formation of fibrotic plaques and morphological changes similar to those of anterior subcapsular cataracts in human lenses.[5, 6, 8-10] As in anterior subcapsular cataract, both alpha smooth muscle actin (α-SMA) and type I collagen are found in the TGF-β-induced plaques.[5] Thus, α-SMA and type I collagen have been used as molecular markers to identify capsular plaques that are associated with subcapsular cataract because these proteins are not usually present under normal conditions.[8, 11] Previous *in-vitro* TGF-β experiments with cultured rat lenses showed that there are both a gender and an age effect in relation to cataract development when exposed to TGF-β.[11, 12] However, the mechanisms involved in TGF-β-induced cataract formation are still unclear.

Matrix metalloproteinases (MMPs) are a family of enzymes that consist of 25 homologues which share many common properties, including a zinc binding region located at the active site of the enzyme.[13-15] As in the case of TGF-β, MMPs and tissue inhibitors of metalloproteinases (TIMPs) are responsible for remodeling and turnover of extracellular matrices.[14-16] MMPs are found in many tissues of the eye such as, the vitreous humour, aqueous humour, retina, cornea, and lens.[17-22] A previous study demonstrated that MMPs and TIMPs are expressed in the lens epithelial cells of human lenses after cataract surgery and during the early phase of capsular healing.[23] Experiments using porcine capsular bags showed that there is an increased expression of both MMP-2 and MMP-9 in the lens during pathological conditions, such as cataract and posterior capsule opacification.[24] MMP-2 and MMP-9 are also involved in the wound healing process of corneal ulceration in mice.[21] Cell-surfaced localized MMP-2 and MMP-9 can activate latent TGF-β.[25] On the other hand, an experiment with chicken lens annular pad cells demonstrated that treatment with TGF-β is required to stimulate secretion of MMP-2 and MMP-9.[14] These various findings revealed the complexity of the relationship between MMPs and TGF-β and further investigation is necessary to uncover the regulation and activation of MMPs and TGF-β that leads to lens epithelial opacity.

The purpose of this study is to analyze the optical effects of TGF-β-induced subcapsular cataract formation in cultured rat lenses using a laser scanning instrument. Another objective is to investigate the potential role of MMPs with respect to TGF-β-

induced subcapsular cataract development. Thus, Ilomastat (an MMP inhibitor) treatment is used to examine the inhibitory effect on subcapsular cataract development.

## 1.2 Materials and Methods

Lenses were dissected from two to six month old male Wistar rats after euthanization with $CO_2$. The lenses were cultured in specialized serum-free medium M199 with Earl's salts and L-glutamine (product number 11150-059, Invitrogen Inc., ON. Canada) containing 0.1% bovine serum albumin (A-2058, Sigma, MO. USA), 50 IU/ml penicillin, 50 ug/ml streptomycin and 2.5 ug/ml amphotericin B (Fungizone).[12] Lenses were incubated at 37 °C with 4.0% $CO_2$ for 24 hours before any treatment to ensure that they were not damaged during the dissection. The lenses were kept in a sterile environment to prevent contamination. A total of 67 lenses were used in this study. The lenses were divided into three separate experiments that investigate both the optical effects of TGF-β2 (product number 302-B2, R&D Systems Inc. MN. USA) treated lenses and the inhibiting potential of Ilomastat (GM6001, Chemicon International, CA. USA) on TGF-β2 treated lenses. In addition to the laser scanner, a digital camera mounted to a dissecting scope was used to photograph the visual appearance of each lens as a comparisons to the optical quality measured by the laser scanner.

### 1.2.1 Experiment 1. TGF-β2 and Ilomastat Treatment

Lenses (n=20) were obtained as described above and separated into 3 treatment groups: control (culture medium, n=6), treatment with TGF-β2 (1 ng/ml, n=8), and treatment with TGF-β2 (1 ng/ml) + Ilomastat (25 μM, n=6). After 24 hours of initial incubation, the culture medium was removed and 4 ml of appropriate treatment media

was added to the tissue culture plates. The rat lenses remained in their respective treatment media for 6 days prior to optical analysis. The lenses were then transferred to a specialized glass chamber filled with culture medium to be analyzed with a laser scanner.

*1.2.2 Experiment 2. Concentration Effect of TGF-β2*

This experiment was performed to examine the optical changes and subcapsular cataract formation in rat lenses treated with two different TGF-β2 concentrations: 1 ng/ml and 2 ng/ml. A total of 33 lenses were divided into 5 different treatment groups: control group (culture medium, n=8), TGF-β2 (1 ng/ml, n=4), TGF-β2 (1 ng/ml) + Ilomastat (25 μM, n=4), TGF-β2 (2 ng/ml, n=9), and TGF-β2 (2 ng/ml) + Ilomastat (25 μM, n=8). Each lens was optically scanned at 4 time points (initial scan prior to treatment, 2, 4, and 6 days after initial treatment) to examine the temporal effects of the treatment. Each lens was temporarily removed from the treatment medium during the scanning process and then replaced back into the appropriate medium and incubated until the following scan point. Representative lenses from each group were photographed on each day.

*1.2.3 Experiment 3. Effect of Ilomastat Concentration*

This study was performed to ensure that the optimal concentration of Ilomastat was used and that no lens damage is caused by the Ilomastat itself. Ilomastat is dissolved in an aqueous solution (containing DMSO), therefore an Ilomastat negative control is

used to show that the effect of treatment is not due to the dissolving solution. Subcapsular cataract development in rat lenses was evaluated in lenses treated with TGF-β2 (2 ng/ml) in combination with 4 different Ilomastat concentrations (10,15, 20 and 25 μM). A total of 14 lenses were divided into 8 groups which consisting of: a control group (with culture medium, n = 2), 25 μM Ilomastat only (n = 1), TGF-β2 (n = 2), TGF-β2 + Ilomastat negative control (GM6001 negative control, Calbiochem, CA. USA; n = 1), TGF-β2 + 10 μM Ilomastat (n = 2), TGF-β2 + 15 μM Ilomastat (n = 2), TGF-β2 + 20 μM Ilomastat (n = 2), and TGF-β2 + 25 μM Ilomastat (n = 2). Optical analysis was performed 6 days after initial treatment. These lenses were treated in the same manner as described in the above experiments.

*1.2.4 Laser Scanning Instrument*

The laser scanning system (ScanTox™) consists of a collimated helium neon (HeNe) laser source (on an X-Y table) that projects a beam onto a mirror mounted at 45 ° on a carriage assembly. The reflected beam then goes up through the scanner table surface and through the lens under examination. Digital cameras capture images of the light beam refracted by the lens as it scans across it. The information collected by the digital cameras is transferred to a computer, and the refracted direction for each of the beam positions is recorded with respect to the optical center, the point at which the slope of the laser beam approaches zero. Each scan involved 20 laser positions across a 3 mm diameter span with a step size of 0.15 mm. The measurements made included average back vertex distance (BVD, a measure of focal length), and back vertex distance

11

variability (BVD error or sharpness of focus) as well as relative transparency (or scatter).[26-28] BVD error is the most sensitive measurement in detecting optical changes in subcapsular cataract development in the rat lens and thus, the results will focus on the changes in BVD error as an indication of decrease lens optical quality.

*1.2.5 Statistical Analysis*

The repeated-measures analysis of variance (repeated-measures ANOVA) and the unpaired student's t-test (SPSS™ 11.0 statistical software) were used to assess treatment, concentration, and temporal effects on the back vertex variability. A probability value (p-value )≤ 0.05, indicating a 95% confidence interval, was considered to be significant.

## 1.3 Results

The results of this study demonstrate that treatment of cultured rat lenses with TGF-β2 induces the formation of anterior subcapsular cataracts (Figures 1-4). The first experiment studies the optical effects of TGF-β2 (1ng/ml) and the addition of Ilomastat (25 μM) to TGF-β2 treatment. Figures 1 and 2 show that TGF-β2-induced subcapsular cataracts increased the light scattering properties of the lens. The TGF-β2 treatment group has a significantly (paired student's test: $p \leq 0.05$) larger BVD error ($0.196 \pm 0.003$ mm) relative to the control lenses ($0.101 \pm 0.005$ mm) and TGF-β2 + Ilomastat ($0.110 \pm 0.004$ mm) groups. Treatment with Ilomastat (MMP inhibitor) effectively inhibits subcapsular cataract formation and the lenses show optical measurements that are similar to those of the control lenses.

Figure 3 shows the appearances of lenses at 0, 2, 4 and 6 days after treatment. Lenses from the control and TGF-β2 + Ilomastat group remained clear throughout the experiment, while TGF-β2 treated lenses remained clear up to day 4 with lens opacities appearing on day 6. The optical measurements in Figure 4 show the changes in back vertex variability at the time points described when treated with two different concentrations of TGF-β2 (1 ng/ml and 2 ng/ml). Repeated-measures ANOVA of the BVD error measurements show that there is both a treatment and temporal effect ($p \leq 0.05$). The BVD errors for the control lenses (range from $0.068 \pm 0.004$ mm to $0.082 \pm 0.003$ mm) and did not change significantly from day 0 to 6. Rat lenses treated with Ilomastat: TGF-β2 1 ng/ml + Ilomastat show BVD errors ranging from $0.078 \pm 0.018$

13

mm to 0.084 ± 0.001 mm, while those treated with TGF-β2 2 ng/ml + Ilomastat show errors ranging from 0.071 ± 0.002 mm to 0.079 ± 0.006 mm. The results from both Ilomastat groups are similar to the values for the control lenses.  Both treatment with 1 ng/ml TGF-β2 (errors ranging from 0.073 ± 0.001 mm to 0.122 ± 0.003 mm) and 2 ng/ml TGF-β2 (errors ranging from 0.075 ± 0.014 mm to 0.142 ± 0.009 mm) cause a significant increase in BVD error on day 6.  The TGF-β2 groups (1 ng/ml and 2 ng/ml) also show significant optical change relative to the control and both Ilomastat groups. However, there is no significant difference between TGF-β2 (1 ng/ml) and TGF-β2 (2 ng/ml).

Figures 5 and 6 show optical measurements from lenses treated with different concentrations of Ilomastat: 10 μM (0.332 ± 0.029 mm), 15 μM (0.310 ± 0.029 mm), 20 μM (0.115 ± 0.011 mm) and 25 μM (0.097 mm) in addition to TGF-β2.  The lower Ilomastat concentrations (10 μM and 15 μM) are unable to prevent subcapsular cataract development, while lenses treated with the higher concentrations (20 μM and 25 μM) are as transparent as the control lenses and show similar BVD error (0.085 ± 0.001 mm). Also treatment with 25 μM Ilomastat (0.108 mm) only had no effect on the lens, while treatment with the negative control for Ilomastat + TGF-β2 (0.254 mm) demonstrate similar effects as the TGF-β2 (0.334 ± 0.031 mm) treated lens
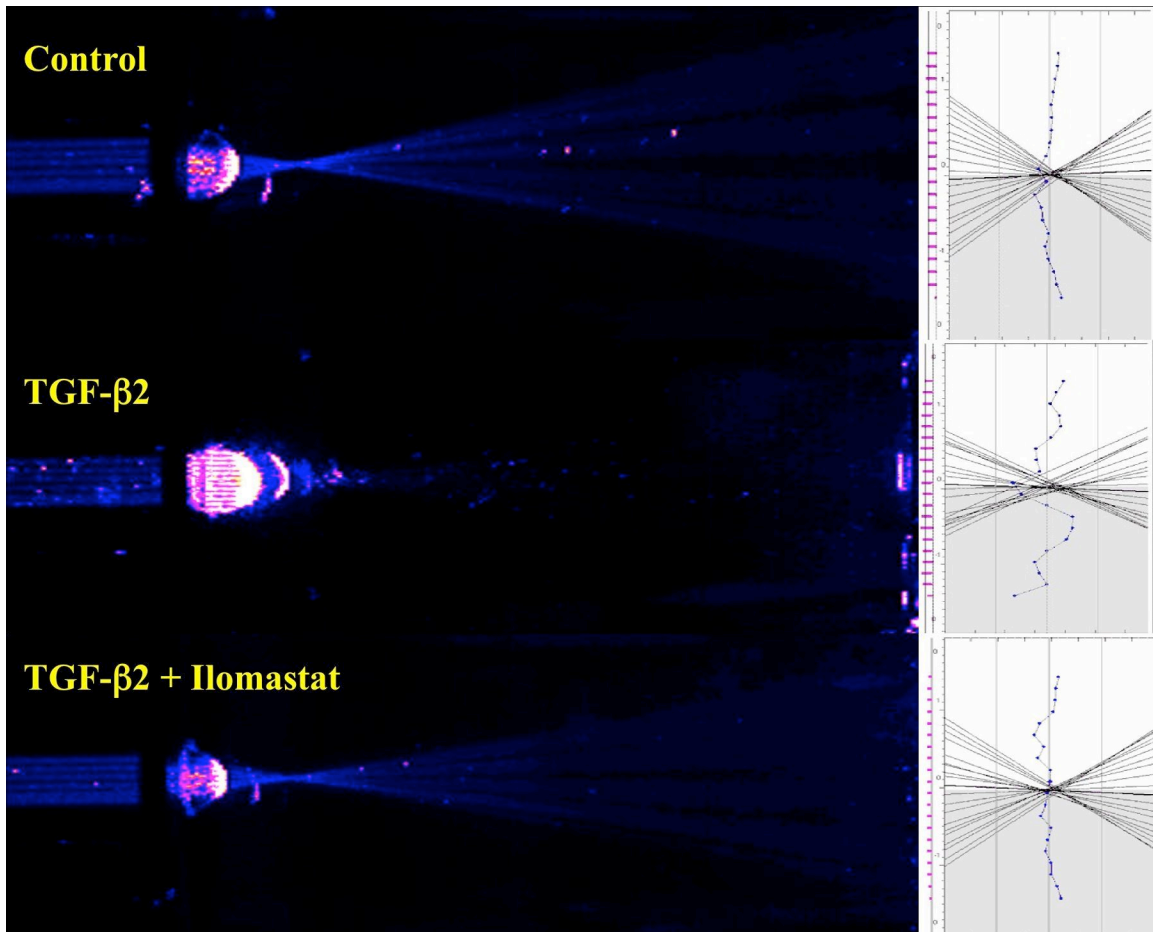
Figure 1. Optical scans of rat lenses

The images above shows the transmittance of the laser source through a control, TGF-β2, and TGF-β2 + Ilomastat treated rat lens. The refracted beams through the control lens and TGF-β2 + Ilomastat lens are focused and relatively straight. The TGF-β2 treated lens show increase scatter and the refracted light is less focused then the other lenses. The scatter plots on the right represents the back vertex distance (focal length measurements) for the corresponding lens. Each point on the scatter plot represents the back vertex distance from each beam location. Increased variability in the back vertex distance within a lens indicates a decrease in sharpness of focus.

**A**



**B**
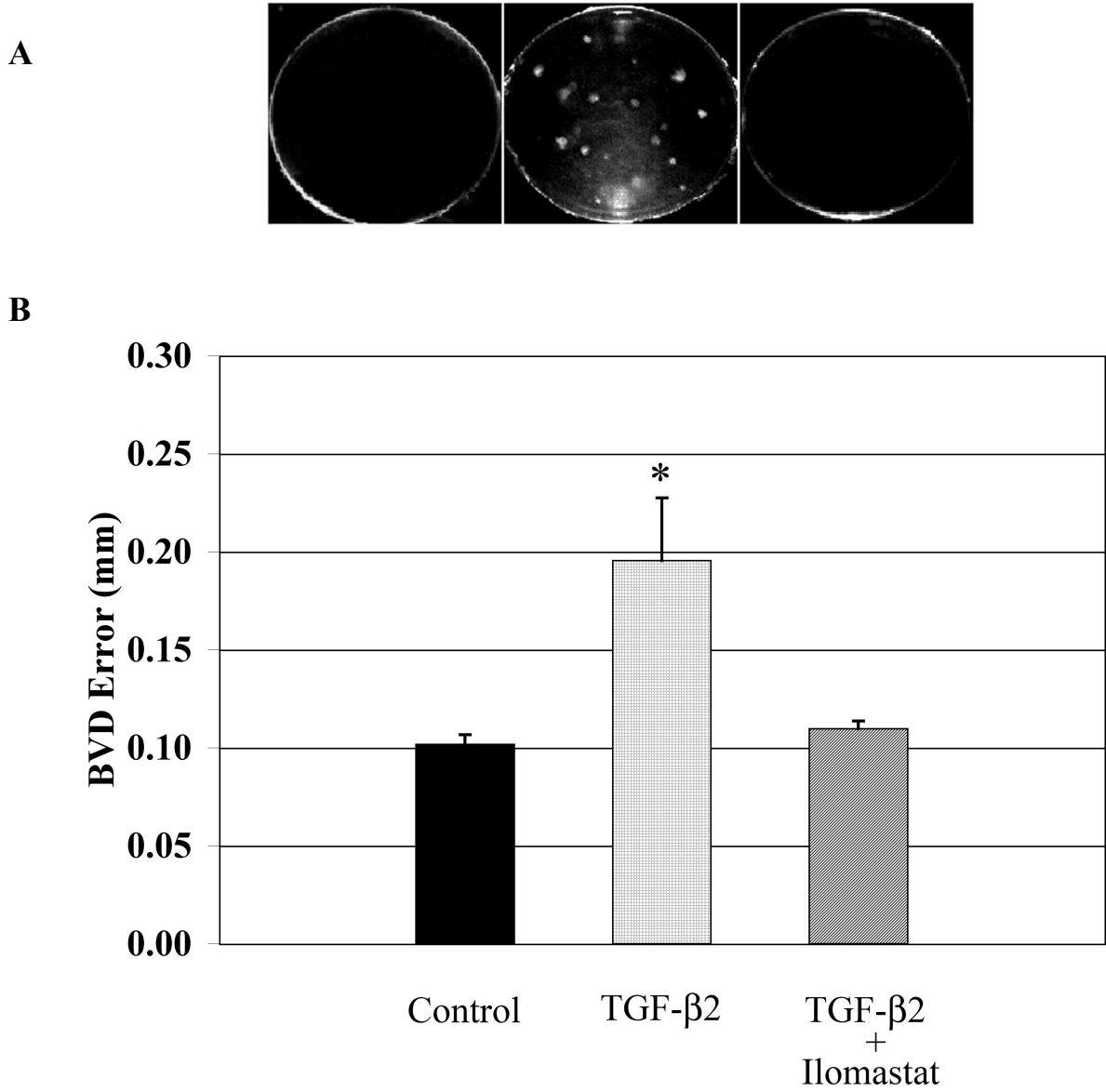


Figure 2. TGF-β2 induced subcapsular cataract formation

The top panel (A) are digital photographs representing a control (left), TGF-β2 (center), and TGF-β2 + Ilomastat (right) lens. The TGF-β2 treated lens shows subcapsular plaques while the control lens and TGF-β2 + Ilomastat treated lens remained transparent. The bar graph (B) shows the back vertex variability measurements (BVD error, mm ± SEM) for each treatment group. *Statistical analysis (unpaired student's t-test: $p \leq 0.05$)

shows that treatment with TGF-β2 (0.196 ± 0.032) significantly increased the BVD error

(decreased sharpness of focus) when compared to the control (0.102 ± 0.005) and TGF-

β2 + Ilomastat (0.110 ± 0.004) groups.
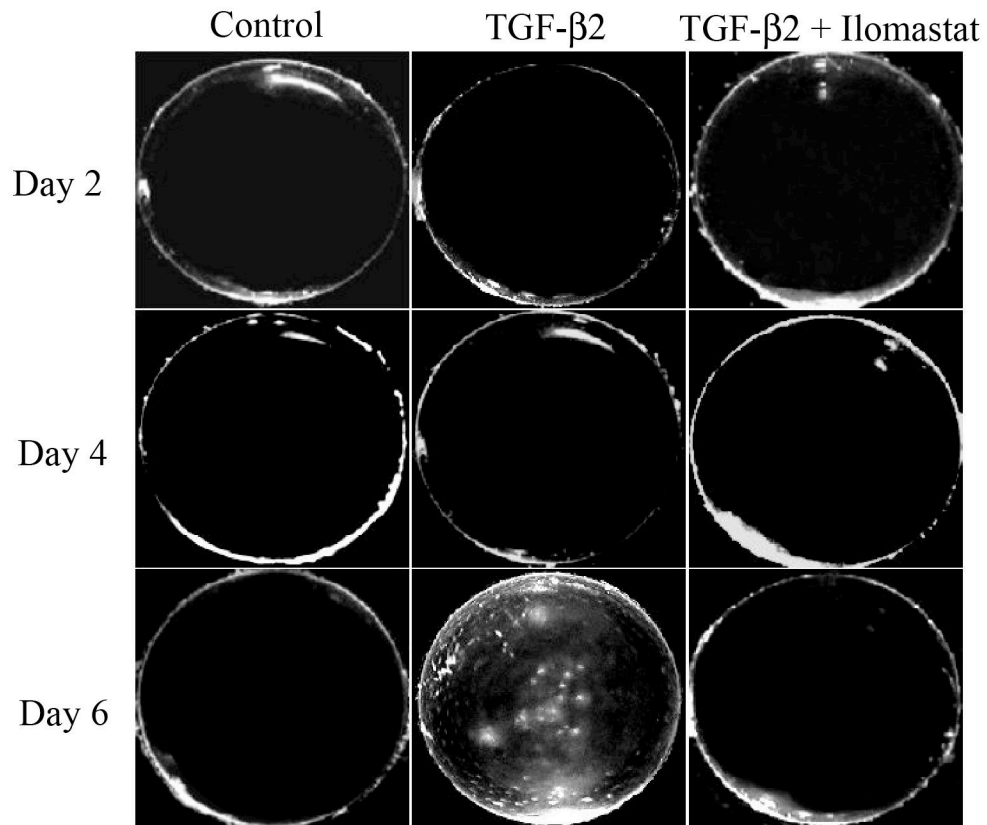
Figure 3. Rat lenses at different time points

The photographs display the appearance of lenses from each experimental group (control, TGF-β2 and TGF-β2 + Ilomastat) at days 2, 4, and 6 after initial treatment. Subcapsular plaques were found in TGF-β2 lenses at day 6 while the control and TGF-β2 + Ilomastat treated lenses are clear. At days 2 and 4 all lenses appear to be similar.
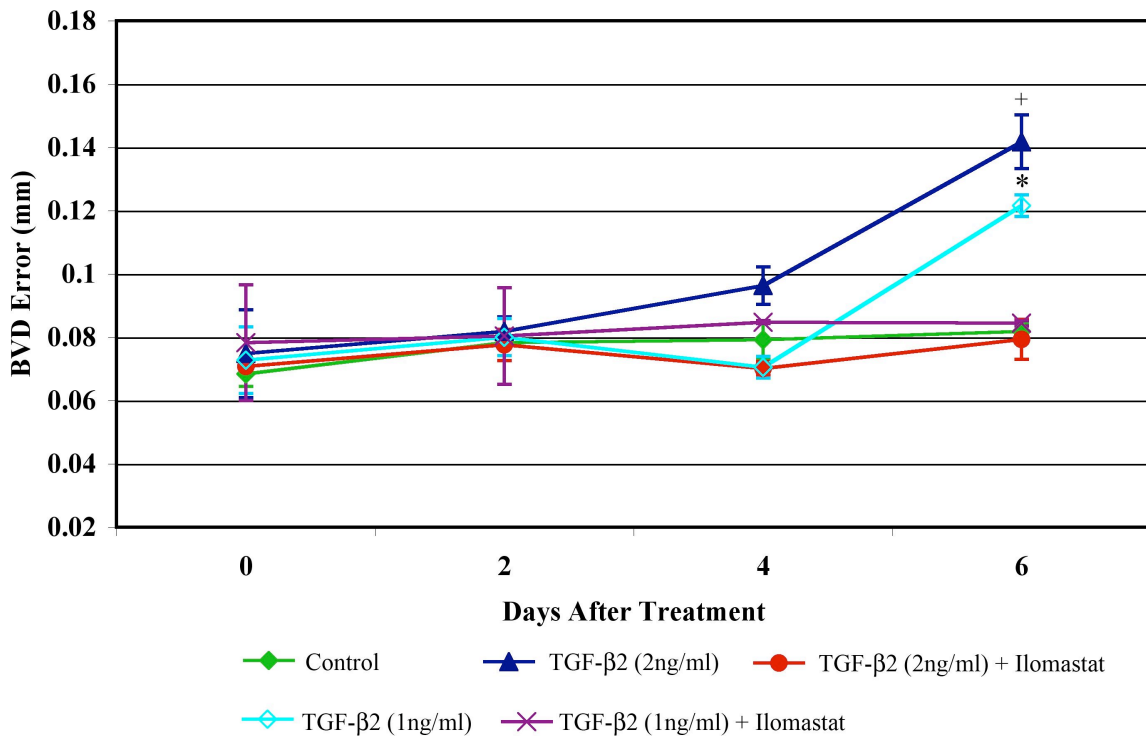
Figure 4. TGF-β concentration effects

The graph shows the changes in back vertex variability (BVD error, mm ± SEM) from day 0 (initial measurements prior to treatment) to 2, 4, and 6 days after initial treatment. Two concentrations of TGF-β2 (1 ng/ml and 2 ng/ml) were used in this experiment. Repeated-measures analysis of variance demonstrated that there is both a treatment and temporal effect ($p \leq 0.05$). $*$ $^{+}$ At day 6 after initial treatment both concentrations of TGF-β2 (1 ng/ml and 2 ng/ml) show significantly higher BVD error measurements than other treatment groups (control, TGF-β2 (1 ng/ml) + Ilomastat and TGF-β2 (2 ng/ml) + Ilomastat). However, there are no significant differences between TGF-β2 (1 ng/ml) and TGF-β2 (2 ng/ml). The control, TGF-β2 (1 ng/ml) + Ilomastat and TGF-β2 (2 ng/ml) + Ilomastat groups did not show significant changes in BVD error.

19
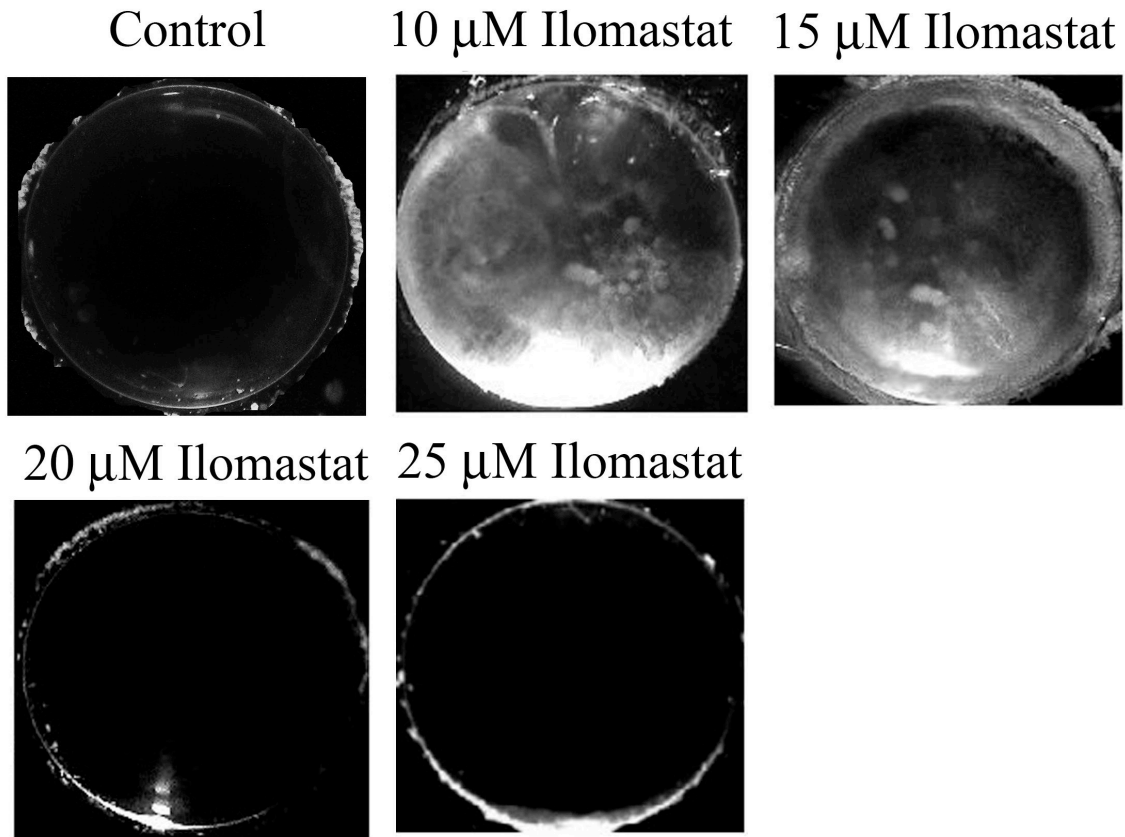
Figure 5. Ilomastat treatment

The pictures demonstrate the effects of TGF-β2 (2 ng/ml) in combination with four different concentrations of Ilomastat (10 μM, 15 μM, 20 μM and 25μM) in comparisons to the control (culture medium only) lens. The lens treated with TGF-β2 + 5 μM Ilomastat shows distinctive plaques and opacification. Both TGF-β2 + 10 μM Ilomastat and TGF-β2 + 15 μM Ilomastat-treated lenses show overall opacities. The photographs also show that the control, TGF-β2 + 20 μM Ilomastat and TGF-β2 + 25 μM Ilomastat lenses are clear.
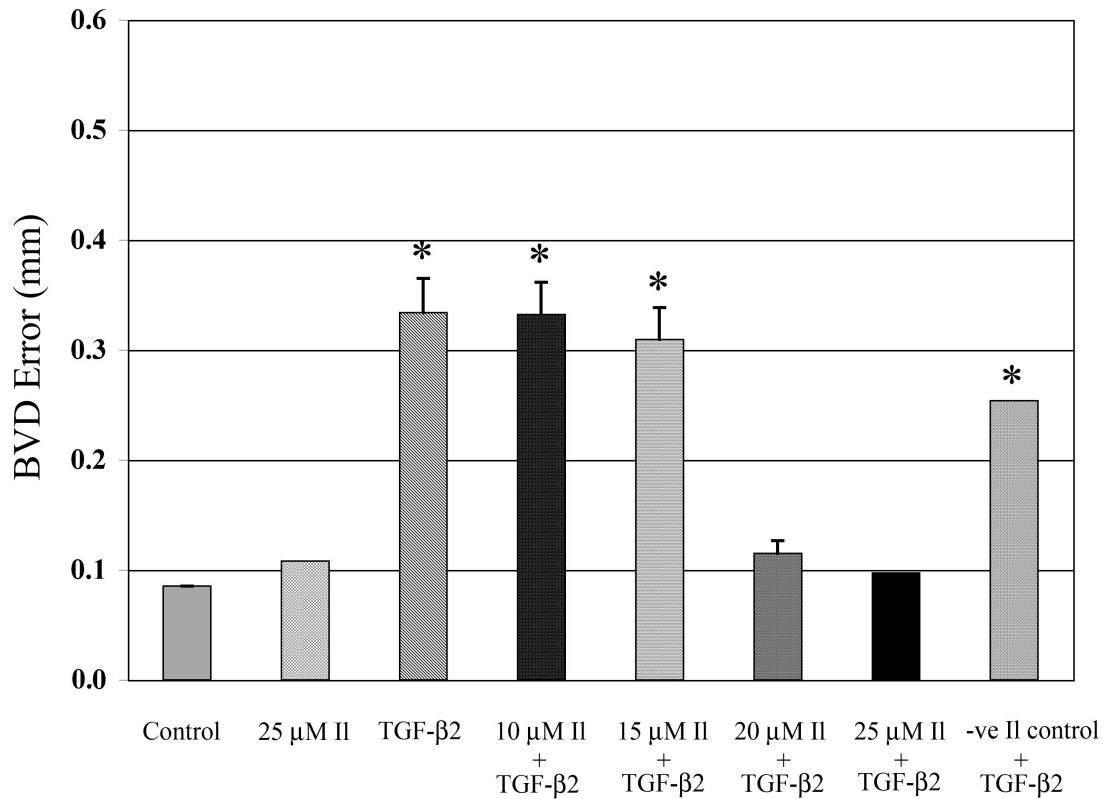
Figure 6. Ilomastat inhibition effect

This bar graph represents the back vertex variability (BVD error, mm) of lenses treated

with TGF-β2 (2 ng/ml) alone and with four different concentrations of Ilomastat (10 μM,

15 μM, 20 μM and 25 μM) as well as control lenses (culture medium only), TGF-β2,

negative control of Ilomastat and 25 μM Ilomastat treated lenses.  These measurements

show a decrease in BVD error as the Ilomastat concentration increases to 25 μM.  BVD

errors from lenses treated with 25 μM Ilomastat only, TGF-β2 + 20 μM Ilomastat and

TGF-β2 + 25 μM Ilomastat are not significantly different from the control lenses.  * The

data also show that lenses treated with TGF-β2 only, with negative control Ilomastat +

TGF-β2 and 10, and 15μM Ilomastat + TGF-β2 have BVD errors that are significantly

different from control lenses.

## 1.4 Discussion

Anterior subcapsular cataracts are associated with many pathological ocular conditions such as iritis and atopic dermatitis, as well as chemical and mechanical trauma.[29] The development of these cataracts involves epithelial-mesenchymal transition (EMT). EMT progression is characterized by the transdifferentiation of lens epithelial cells into myofibroblastic cells, which causes the accumulation of ECM molecules.[12, 29, 30] TGF-β can induce morphological and molecular changes similar to those of human anterior subcapsular cataract.[5] *In-vitro* rat lens culture and lens epithelial explants have shown that all three TGF-β isoforms (TGF-β1, TGF-β2 and TGF-β3) can induce cataractous changes. However, TGF-β1 is 10 times less potent than TGF-β2 and TGF-β3.[8]

TGF-β can promote and inhibit cell growth depending on the cell type. In general TGF-β has inhibitory effects on cells of epithelial origin, while it is mitogenic for smooth muscle and fibroblasts.[31] This is supported by the increase in expression of α-SMA in the lens epithelium during subcapsular cataract development. As mentioned before in the introduction, α-SMA is not found under normal lens conditions. TUNEL (TdT-dUTP terminal nick-end labeling) staining of TGF-β1 transgenic mice lenses and *in-vitro* human lens epithelial cell culture show that TGF-β also causes apoptosis in the lens epithelium.[30, 31]

22

The susceptibility of the lens to TGF-β-induced cataractous changes is dependent on the number of TGF-β receptors type I and II (TβRI and TβRII) present.[29] In contrast to rat lenses (which have both TβRI and TβRII), prolonged exposure of clear undamaged human lenses (TβRII only) to TGF-β2 did not induce EMT and α-SMA expression associated with anterior subcapsular cataract formation. However, traumatized human lenses treated with TGF-β2 did show increased in expression of α-SMA and multilayering of epithelial cells, which could be due to an increased expression of both TβRI and TβRII.[29] It has also been shown that there is increased sensitivity to TGF-β induction as the age of the rat increases.[12] Another study proved that estrogen plays a protective role in female rats against TGF-β-induced cataracts.[32] TGF-β has been detected endogenously within the lens cells as well as in the aqueous and vitreous humors. TGF-β modified ECM by inducing the expression of MMPs and other enzymes involved in matrix remodeling.[14]

This study focuses on the optical changes in rat lenses treated with TGF-β2. TGF-β2 effectively induced the formation of anterior subcapsular cataracts in rat lenses as shown in previous studies.[8, 9] A laser scanning instrument was used to objectively measure the back vertex variability (BVD error) in the lenses. As shown in the results, TGF-β2 (1 ng/ml and 2 ng/ml) treated lenses show significantly larger BVD errors (decreased sharpness of focus) relative to the BVD errors of the control lenses. However, there are no significant differences between the 1 ng/ml TGF-β2 lenses and 2 ng/ml TGF-β2 lenses. The higher concentration of TGF-β2 (2 ng/ml) demonstrated a greater change in BVD errors, compared to all other treatment groups at day 6 after initial treatment.

An MMP inhibitor (Ilomastat) was also used in this experiment to investigate the role of MMPs in TGF-β-induced subcapsular cataract development. Through the breakdown and remodeling of extracellular matrix, MMPs play an essential role in normal physiological processes such as embryonic development, morphogenesis, reproduction, and tissue resorption and remodeling.[33] MMPs are secreted as inactive zymogens (pro-MMPs) and require proteolytic removal of an amino-terminal pro-sequence for them to function.[15] Various growth factors, hormones, cytokines, cell-to-matrix, cell-to-cell interactions and cellular transformation transcriptionally regulate MMP expression.[16, 33] It has been suggested that over-expression of MMPs can promote tumor invasion and angiogenesis.[25] Interestingly, MMP2 (gelatinase A, 72 kD) and MMP9 (gelatinase B, 92 kD) are the most widely studied members of the MMP family in the eye.[14, 20] Both MMP2 and MMP9 are up-regulated during abnormal ocular conditions such as posterior capsule opacification, proliferative diabetic retinopathy and epithelial wound healing.[19, 23, 24, 34] The expression of MMP2 and MMP9 is both positively and negatively regulated by TGF-β.[14]

The results from this experiment show that prolonged exposure (6 days) of cultured rat lenses to TGF-β2 plus 25 μM Ilomastat effectively inhibited the formation of subcapsular plaques and lens opacities. Optical analysis demonstrated that there are no significant differences in BVD errors between the TGF-β2 + 25 μM Ilomastat-treated lenses and control lenses. Also the treatment with Ilomastat significantly reduced the effects of TGF-β2 on cultured rat lenses, as shown in the optical results. This is the first

experiment that used cultured rat lenses to investigate the inhibitory effects of Ilomastat on subcapsular cataract development. Ilomastat is a general MMP inhibitor that has been shown to prevent lens capsule contraction, and human lens and corneal epithelial cell migration.[22, 35] However, the mechanisms that are involved in subcapsular cataract formation with respect to the relationship between MMPs and TGF-β are still not fully understood.

In conclusion, this study has demonstrated that the cultured rat lens model can be used to investigate the role of TGF-β and MMP involvement in anterior subcapsular cataract development. Further studies will provide more insight as to the specific MMPs involved in this process. Also *in-vivo* transgenic mice models can be use to verify the results of the *in-vitro* rat lens culture model.

## 1.5 References

1.      Harding JJ, Dilley KJ. Structural proteins of the mammalian lens: a review with emphasis on changes in development, aging and cataract. *Exp Eye Res* 1976;22:1-73.

2.      West-Mays JA, Coyle BM, Piatigorsky J, Papagiotas S, Libby D. Ectopic expression of AP-2alpha transcription factor in the lens disrupts fiber cell differentiation. *Dev Biol* 2002;245:13-27.

3.      Bagchi M, Katar M, Maisel H. Heat shock proteins of adult and embryonic human ocular lenses. *J Cell Biochem* 2002;84:278-284.

4.      WHO. Blindness and visual disability. World Health Organization; 1997.

5.      Lovicu FJ, Schulz MW, Hales AM, et al. TGFbeta induces morphological and molecular changes similar to human anterior subcapsular cataract. *Br J Ophthalmol* 2002;86:220-226.

6.      Srinivasan Y, Lovicu FJ, Overbeek PA. Lens-specific expression of transforming growth factor beta1 in transgenic mice causes anterior subcapsular cataracts. *J Clin Invest* 1998;101:625-634.

7.      Lee EH, Seomun Y, Hwang KH, et al. Overexpression of the transforming growth factor-beta-inducible gene betaig-h3 in anterior polar cataracts. *Invest Ophthalmol Vis Sci* 2000;41:1840-1845.

8.      Gordon-Thomson C, de Iongh RU, Hales AM, Chamberlain CG, McAvoy JW. Differential cataractogenic potency of TGF-beta1, -beta2, and -beta3 and their expression in the postnatal rat eye. *Invest Ophthalmol Vis Sci* 1998;39:1399-1409.

9.      Hales AM, Chamberlain CG, McAvoy JW. Cataract induction in lenses cultured with transforming growth factor-beta. *Invest Ophthalmol Vis Sci* 1995;36:1709-1713.

10.     de Iongh RU, Lovicu FJ, Overbeek PA, et al. Requirement for TGFbeta receptor signaling during terminal lens fiber differentiation. *Development* 2001;128:3995-4010.

11.     Sun JK, Iwata T, Zigler JS, Jr., Carper DA. Differential gene expression in male and female rat lenses undergoing cataract induction by transforming growth factor-beta (TGF-beta). *Exp Eye Res* 2000;70:169-181.

12.     Hales AM, Chamberlain CG, McAvoy JW. Susceptibility to TGFbeta2-induced cataract increases with aging in the rat. *Invest Ophthalmol Vis Sci* 2000;41:3544-3551.

13.     Sternlicht MD, Werb Z. How matrix metalloproteinases regulate cell behavior. *Annu Rev Cell Dev Biol* 2001;17:463-516.

14.     Richiert DM, Ireland ME. Matrix metalloproteinase secretion is stimulated by TGF-beta in cultured lens epithelial cells. *Curr Eye Res* 1999;19:269-275.

15.     Smine A, Plantner JJ. Membrane type-1 matrix metalloproteinase in human ocular tissues. *Curr Eye Res* 1997;16:925-929.

16.     Brew K, Dinakarpandian D, Nagase H. Tissue inhibitors of metalloproteinases: evolution, structure and function. *Biochim Biophys Acta* 2000;1477:267-283.

17.     Reviglio VE, Rana TS, Li QJ, Ashraf MF, Daly MK, O'Brien TP. Effects of topical nonsteroidal antiinflammatory drugs on the expression of matrix metalloproteinases in the cornea. *J Cataract Refract Surg* 2003;29:989-997.

18.     Agapova OA, Kaufman PL, Lucarelli MJ, Gabelt BT, Hernandez MR. Differential expression of matrix metalloproteinases in monkey eyes with experimental glaucoma or optic nerve transection. *Brain Res* 2003;967:132-143.

19.     Noda K, Ishida S, Inoue M, et al. Production and activation of matrix metalloproteinase-2 in proliferative diabetic retinopathy. *Invest Ophthalmol Vis Sci* 2003;44:2163-2170.

20.     Wormstone IM. Posterior capsule opacification: a cell biological perspective. *Exp Eye Res* 2002;74:337-347.

21.     Xue ML, Wakefield D, Willcox MD, et al. Regulation of MMPs and TIMPs by IL-1beta during corneal ulceration and infection. *Invest Ophthalmol Vis Sci* 2003;44:2020-2025.

22.     Daniels JT, Limb GA, Saarialho-Kere U, Murphy G, Khaw PT. Human corneal epithelial cells require MMP-1 for HGF-mediated migration on collagen I. *Invest Ophthalmol Vis Sci* 2003;44:1048-1055.

23.     Kawashima Y, Saika S, Miyamoto T, et al. Matrix metalloproteinases and tissue inhibitors of metalloproteinases of fibrous humans lens capsules with intraocular lenses. *Curr Eye Res* 2000;21:962-967.

24.     Tamiya S, Wormstone IM, Marcantonio JM, Gavrilovic J, Duncan G. Induction of matrix metalloproteinases 2 and 9 following stress to the lens. *Exp Eye Res* 2000;71:591-597.

25.     Yu Q, Stamenkovic I. Cell surface-localized matrix metalloproteinase-9 proteolytically activates TGF-beta and promotes tumor invasion and angiogenesis. *Genes Dev* 2000;14:163-176.

26.     Bantseev V, McCanna D, Banh A, et al. Mechanisms of ocular toxicity using the in vitro bovine lens and sodium dodecyl sulfate as a chemical model. *Toxicol Sci* 2003;73:98-107.

27.     Oriowo OM, Cullen AP, Chou BR, Sivak JG. Action spectrum and recovery for in vitro UV-induced cataract using whole lenses. *Invest Ophthalmol Vis Sci* 2001;42:2596-2602.

28.     Priolo S, Sivak JG, Kuszak JR, Irving EL. Effects of experimentally induced ametropia on the morphology and optical quality of the avian crystalline lens. *Invest Ophthalmol Vis Sci* 2000;41:3516-3522.

29.     Marcantonio JM, Syam PP, Liu CS, Duncan G. Epithelial transdifferentiation and cataract in the human lens. *Exp Eye Res* 2003;77:339-346.

30.     Lee JH, Wan XH, Song J, et al. TGF-beta-induced apoptosis and reduction of Bcl-2 in human lens epithelial cells in vitro. *Curr Eye Res* 2002;25:147-153.

31.     Flugel-Koch C, Ohlmann A, Piatigorsky J, Tamm ER. Disruption of anterior segment development by TGF-beta1 overexpression in the eyes of transgenic mice. *Dev Dyn* 2002;225:111-125.

32.     Chen Z, John M, Subramanian S, Chen H, Carper D. 17Beta-estradiol confers a protective effect against transforming growth factor-beta2-induced cataracts in female but not male lenses. *Exp Eye Res* 2004;78:67-74.

33.     Nagase H, Woessner JF, Jr. Matrix metalloproteinases. *J Biol Chem* 1999;274:21491-21494.

34.     Wormstone IM, Tamiya S, Anderson I, Duncan G. TGF-beta2-induced matrix modification and cell transdifferentiation in the human lens capsular bag. *Invest Ophthalmol Vis Sci* 2002;43:2301-2308.

35.     Wong TT, Daniels JT, Crowston JG, Khaw PT. MMP inhibition prevents human lens epithelial cell migration and contraction of the lens capsule. *Br J Ophthalmol* 2004;88:868-872.

# Chapter 2

# Lens Specific Expression of TGF-β Induces Anterior Subcapsular Cataract Formation in the Absence of Smad3

Alice Banh[1], Paula A. Deschamps[2], Jack Gauldie[2], Paul A. Overbeek[3], Jacob G. Sivak[1], Judith A. West-Mays[2*]

[1]School of Optometry, University of Waterloo, Waterloo, ON, Canada; [2]Pathology and Molecular Medicine, McMaster University, Hamilton, ON, Canada; [3]Molecular and Cellular Biology, Baylor College of Medicine, Houston, TX, USA.

## 2.1 Introduction

Transforming growth factor beta (TGF-β) is a secreted polypeptide that is involved in various cellular processes, including cell proliferation, differentiation, apoptosis, migration and extracellular matrix (ECM) formation.[1-5]   TGF-β has been shown to promote wound healing by stimulating the production and deposition of ECM, which are essential to normal tissue repair after injury.[6]   The profibrotic actions of TGF-β have also been implicated in fibrotic pathogenesis in the eye such as glaucoma and anterior subcapsular cataracts (ASC).[7-10]

The ocular lens is a transparent structure that provides part of the refractive power needed to focus images on the retina of the human eye.  A cataract involves a reduction in transparency of the lens, which can lead to vision loss.  Specifically, ASC can occur following ocular trauma, ocular surgery or in conjunction with diseases like atopic dermatitis and retinitis pigmentosa.[11, 12]   The development of ASC involves the transformation and proliferation of the anterior epithelial cells of the lens into plaques of large "spindle shaped" cells, or myofibroblasts, through a phenomenon known as epithelial-to-mesenchymal transition (EMT).[13-15]   The appearance of the myofibroblasts promotes lens capsule wrinkling and an aberrant deposition of extracellular matrix (ECM), both of which are features of ASC.[1, 7, 16, 17]   Similarly, in secondary cataract (also known as posterior capsular opacification (PCO)), a complication that develops after cataract surgery, lens epithelial cells that remain within the capsule are triggered to

proliferate and migrate to the posterior lens capsule where they transition into myofibroblasts through EMT.[18, 19]

Under physiological conditions, TGF-β in the lens and ocular media mainly exists in its latent form, whereas biologically active TGF-β has been detected in the ocular media from patients suffering with ASC.[20, 21] There are three functionally and structurally related species of TGF-β: TGF-β1, TGF-β2 and TGF-β3.[22] Studies using *in-vitro* rat lens cultures and lens epithelial explants have shown that all three TGF-β isoforms can induce cataractous changes similar to those observed in humans. However, TGF-β1 is 10 times less potent than TGF-β2 and TGF-β.[23] The *in-vivo* expression of self-activating TGF-β1 in a transgenic mouse model has been useful for examining the morphological and molecular changes involved in ASC formation, which closely resemble human ASCs.[1, 7, 24] However, the TGF-β-mediated signaling pathways regulating fibrosis including those governing ASC formation have not been clearly defined.

Smad proteins are intracellular molecules involved in TGF-β signal transduction from the receptors to the target genes in the nucleus.[22, 25, 26] Upon ligand binding and TGF-β receptor activation, phosphorylation of receptor-regulated Smad2 and Smad3 occurs, which leads to the formation of hetero-oligomeric complexes with Smad4 (Co-Smad).[22, 25, 26] The Smad complexes then translocate into the nucleus, where they regulate target gene expression in collaboration with other coactivators and corepressors. The Smad3 knockout mouse model has been useful for determining TGF-β-mediated

33

fibrotic events requiring Smad3 signaling.[27-30]  Importantly, ablation of Smad3 in mice

was also shown to prevent the EMT of lens epithelial cells that occurs upon injury to the

lens capsule [31], suggesting that EMT in the lens may be entirely Smad3-dependent.

However, the effect of TGF-β on ASC formation in the absence of Smad3 has not been

directly tested.


In the current study we directly determined the requirement for Smad3 in ASC

formation using an *in-vivo* transgenic TGF-β1/Smad3 knockout mouse model.  Evidence

of ASC formation in TGF-β1/Smad3$^{-/-}$ mice and their TGF-β1/Smad wild-type

littermates was evaluated histologically using a EMT marker such as α-SMA as well as

fibronectin, collagen type I and IV as fibrotic markers.  Formation of ASC in mice was

also evaluated using a quantitative measure of lens optical quality.  The results show that

EMT and the formation ASC plaques occurs in the TGF-β1/Smad3$^{-/-}$ mice, accompanied

by a significant decrease in optical quality of the lens.  However, the plaques in the TGF-

β1/Smad3$^{-/-}$ mice were smaller, contained a greater number of apoptotic cells and

substantially less collagen compared to their Smad3 heterozygote and wild-type

littermates.  Together these findings demonstrate that while Smad3 signaling contributes

to TGF-β1-induced ASC formation, it is not necessary and additional Smad3-

independent pathways are involved in this ocular fibrotic disease.

## 2.2 Materials and Methods

*2.2.1 Generation of transgenic TGF-β1/Smad3 knockout mice*

All animal studies were carried out according to the Canadian Council on Animal Care Guidelines and the Association for Research in Vision and Ophthalmology (ARVO) Statement for the Use of Animals in Ophthalmic and Vision Research. The transgenic TGF-β1 mice contain a human TGF-β1 cDNA construct with an αA-crystallin promoter designed for lens specific expression of active TGF-β1 [1] on a FVB/N/C57BL/6J background. The Smad3 null mutant was generated by the deletion of exon 8 of the Smad3 gene, which truncated 89 amino acids from the C-terminal end.[32] Exon 8 contains an SSVS consensus phosphorylation site and an L3 loop which are essential for interaction with the TGF-β receptor [2]. TGF-β1 transgenic mice were bred with Smad3 null and heterozygous mice on a SvEv/C57BL background to generate mice with the following genotypes: TGF-β1/Smad3$^{-/-}$ (null), TGF-β1/Smad3$^{+/-}$ (heterozygous), TGF-β1/Smad3$^{+/+}$, Smad3$^{-/-}$ and non-transgenic/Smad$^{+/+}$ (wild-type). Wild-type littermates were used to insure that results were not due to the various differences between the strains of mice.

*2.2.2 Genotype analysis*

DNA extraction and purification from mouse ear tissue was performed using the Qiagen DNeasy tissue kit (Qiagen Inc.,On. Canada). Genotypes were determined by polymerase chain reaction (PCR) analysis. The TGF-β1 transgene was identified by using primers specific for the simian virus 40 (SV40) sequences in the transgene: the sense primer (5′-GTGAAGGAACCTTACTTCTGTGGTG-3′) and the antisense primer (5′-GTCCTTGGGGTCTTCTACCTTTCTC-3′) yield a 300 bp fragment in the PCR reactions [33]. PCR reactions were carried out for 36 cycles using the following conditions: initial heating for 3 minutes at 94°C (only for cycle 1); denaturation for 30 seconds at 94°C; annealing for 1 minute at 57°C; and extension for 1 minute at 72°C. A final extension was carried out for 2 minutes at 72°C. Agarose gel electrophoresis (1.5% agarose) with ethidium bromide (EtBr) detection was used to visualize the PCR reaction products.

The Smad3 wild-type and knockout alleles were detected using three primers. The Smad3 wild-type allele is detected by using primer 1 (5′-CCACTTCATTGCCATATGCCCTG-3′) and primer 2 (5′-CCCGAACAGTTGGATTCACACA-3′). Primer 1 (located 5′ to the deletion) and primer 2 (located within the deletion) amplify a 400 bp fragment from wild-type and heterozygous knockout mice.[32] The Smad3 knockout allele was detected by using primer 1 and primer 3 (5′CCAGACTGCCTTGGGAAAAGC-3′ (located in the pLoxpneo)) to yield a 250 bp fragment, which is detected in both the heterozygous and homozygous

Smad3 knockout mice.[32]   PCR reactions were carried out for 31 cycles using the following conditions: initial heating for 2 minutes at 94°C (only for cycle 1); denaturation for 30 seconds at 94°C; annealing for 30 seconds at 60°C; and extension for 2 minutes at 72°C.  A final extension was carried out for 2 minutes at 72°C.  A 2% agarose gel electrophoresis with EtBr detection was used to visualize the PCR reaction products.

*2.2.3 Histology and immunohistochemistry staining*

Whole eyes were dissected from 2-3 month old mice of each genotype and fixed in 10% neutral formalin buffer for 24 hours, then dehydrated, processed and embedded in paraffin.  Paraffin sections of 5 μm thickness were used for either Hematoxylin and Eosin (H&E), Mason's Trichrome (collagen deposition), or immunohistochemistry staining (α-SMA, fibronectin and β-crystallin).  Fresh eyes from each genotype were also embedded in OCT and frozen sections (5 μm thickness) were used to stain for collagen type I and IV.  Staining was visualized with a Leica microscope equipped with an immunofluorescence attachment and images were captured using a high-resolution camera and associated software (OpenLab; Quorum Technologies). Images were reproduced for publication using Adobe Photoshop 9.0.1 (Adobe Systems Incorporated).

For α-SMA, fibronectin, and β-crystallin immunoflourescence localization, paraffin sections were deparaffinized, rehydrated and incubated with 5% normal goat serum for 20 minutes at room temperature.  The sections were then incubated either with mouse anti-α-SMA monoclonal antibody (1:100; Sigma-Aldrich Inc., MO. USA), rabbit

anti-mouse fibronectin (1:500; Cedarlane Laboratories Ltd., ON Canada) or rabbit anti-β-crystallin (1:200; donation from J. Samuel Zigler, National Eye Institute) at room temperature for 1 hour.  The bound primary antibodies were visualized with either a fluorescein-isothiocyanate (FITC) conjugated goat anti-mouse secondary antibody, goat anti-rabbit FITC secondary antibody or tetramethyl rhodamine isothiocyanate (TRITC) conjugated goat anti-rabbit secondary antibody (Jackson ImmunoResearch Laboratories Inc., PA. USA).  All sections were mounted in Vectashield mounting medium with 4',6-Diaminodino-2-Phenylindol (DAPI, Vector Laboratories Inc., CA. USA) to visualize the nuclei.

Frozen tissue sections were thawed at room temperature, fixed with acetone for 20 minutes at –20 °C and used for immunofluorescence localization of collagen type I or IV. The sections were incubated with 5% normal goat serum for 20 minutes at room temperature followed by rabbit anti-collagen type I, or rabbit anti-collagen type IV primary antibody (1:100; Cortex Biochem, CA. USA) at room temperature for 1 hour.  A goat anti-rabbit FITC secondary antibody was used to visualize the bound primary antibodies.  All sections were mounted in Vectashield mounting medium with DAPI and photographed as mentioned above.

*2.2.4 TUNEL assay*

TUNEL (terminal deoxynucleotidyl transferase mediated dUTP nick end labeling) labeling was used to examine cell death in the lens epithelium of each genotype. Paraffin sections were deparaffinized and the ApopTag plus flourescein *in-situ* apoptosis detection kit (Chemicon International Inc., CA. USA) was used to detect apoptotic nuclei. The TUNEL procedure was carried out in accordance with the manufacturer's instructions. A positive control was prepared by treating a sample with DNaseI prior to TUNEL staining. All sections were mounted in Vectashield mounting medium with DAPI and photographed as mentioned above. For quantitative analysis, the percentage of TUNEL-positive cells among 150 lens epithelial cells in three fields per slide was determined at 400-fold magnification in three different samples from each genotype.

*2.2.5 Western blot analysis*

Four lenses from each genotype including TGF-β1/Smad3$^{-/-}$, TGF-β1/Smad3$^{+/-}$, TGF-β1/Smad3$^{+/+}$, Smad3$^{-/-}$ and wild-type mice were collected and pooled for Western blot analysis of phosphorylated Smad3 (pSmad3) protein expression. In addition two lenses from each genotype were collected and pooled for Western blot analysis of α-SMA protein expression. The lenses were homogenized in Triton-X100 lysis buffer containing protease inhibitor cocktail (Roche Applied Science, IN. USA). The total protein concentration was determined by the Bradford protein assay [34]. Equal amounts of

total protein from each group of lenses were electrophoresed on 10% tris-tricine polyacrylamide gel (pSmad3) or 10% SDS polyacrylamide gel (α-SMA).  The proteins were electro-transferred onto a nitrocellulose membrane (Pall Corporation, NY. USA). Membranes were blocked with 5% skimmed milk powder in Tris-buffered saline (50mM Tris base, NaCl pH 8.5) + 0.1% Tween-20 and then incubated overnight at 4°C with either a rabbit anti-phospho-Smad3/Smad1 antibody (1:1000; Cell Signaling Inc., MA. USA) or mouse anti-α-SMA monoclonal antibody (1:1000).  Following this incubation, membranes were probed with the appropriate HRP-conjugated anti-rabbit or anti-mouse secondary antibodies (1:5000; Amersham Biosciences, NJ. USA) and ECL detection reagents (Amersham Biosciences, NJ. USA).  The Western blots were visualized by x-ray film exposure.  The α-SMA membranes were stripped and reprobed with mouse anti-β-actin antibody (1:1000; Cedarlane Laboratories Ltd., On Canada) as a loading control. The secondary detection for β-actin followed the same procedures as mentioned above.

*2.2.6 Optical analysis*

Lenses were dissected from 2-3 month old mice after euthanization with $CO_2$. The lenses were cultured in specialized serum-free medium M199 with Earl's salts and L-glutamine (product no. 11150-059, Invitrogen Inc., ON. Canada) containing penicillin/streptomycin. Lenses were incubated at 37°C with 4.0% $CO_2$ for 24 hours prior to optical analysis to ensure that no damage occurred during the dissection.  A total of 33 lenses were used for optical measurements: TGF-β1/Smad3$^{-/-}$ (n = 8), TGF-β1/Smad3$^{+/-}$ (n = 8), TGF-β1/Smad3$^{+/+}$ (n = 11) and wild-type (n = 6) lenses.  A laser scanning system

(ScanTox™) developed at the University of Waterloo, was used to analyze the quality of the lenses [35-37]. The laser scanner consists of a collimated helium neon (HeNe) laser source (on an X-Y table) that projects a beam onto a mirror mounted at 45 ° on a carriage assembly. The reflected beam then goes up through the scanner table surface and through the lens under examination. There are two digital cameras that capture images of the light beam being through the lens. The image information collected by the digital cameras is transferred to a computer, and the refracted direction for each of the beam positions is recorded with respect to the optical center, the point at which the slope of the laser beam approached zero.[35-37] Each scan involved 20 laser positions across a 2 mm diameter with a step size of 0.10 mm. The measurements made included average back vertex distance (BVD, a measure of focal length), and back vertex distance variability (BVD error or sharpness of focus) and relative transparency (or scatter). The BVD error is the most sensitive measurement in detecting optical changes in subcapsular cataract development in the mouse lens. Thus, the results will focus on the changes in BVD error as an indication of decreased optical quality in the lens.

*2.2.7 Statistical analysis*

The analysis of variance (ANOVA; SPSS™ 11.0 statistical software) was used to assess the optical effects (back vertex variability) of cataract formation between each group of mouse lenses. The unpaired student's t-test was used to analyze the apoptotic cell counts for the TUNEL assay. A p-value ≤ 0.05 was considered to be significant with a 95% confidence interval.

## 2.3 Results

*2.3.1 Generation of transgenic TGF-β1/Smad3 KO mice*

Figure 1 represents the PCR results for 2-3 month old offspring generated from crosses between the Smad3$^{+/-}$ and TGF-β1 transgenic mice. The genotype of the mice was determined based on detection of the TGF-β1 transgene (300 bp) (top gel) and the Smad3 wild-type (400bp) and Smad3 knockout (250bp) alleles (bottom gel). TGF-β1/Smad3$^{+/-}$ mice show all three bands (lane 3) while TGF-β1/Smad3$^{-/-}$ and TGF-β1/Smad3$^{+/+}$ mice exhibit 2 bands, the transgene and either the wild-type allele or the knockout allele (lanes 2 and 4, respectively). Non-transgenic Smad3$^{+/+}$ and Smad3$^{-/-}$ mice exhibit a single band at 400 and 250bp respectively (lanes 1 and 5).

Western blot analysis for phosphorylated Smad3 provides verification that Smad3 signaling is absent in the lenses of Smad3 knockout mice (Fig. 2). The antibody used for pSmad3 (Ser433/435) detection cross reacts with pSmad1 (Ser463/465; 65 kDa) which was detected in all lenses examined and thus acted as a positive internal control. Both the TGF-β1/Smad3$^{+/+}$ and TGF-β1/Smad3$^{+/-}$ lenses exhibited pSmad3 (58 kDa) in contrast to the non-transgenic wild-type and Smad3$^{-/-}$ lenses, which did not. p-Smad1 expression was also increased in the TGF-β1/Smad3$^{+/+}$ and TGF-β1/Smad3$^{+/-}$ lenses. Smad1 is a mediator activated mainly by BMP (bone morphogenetic protein) receptors.[38, 39] Interestingly, extracellular signal-regulated kinases (ERK) have been shown to phosphorylate Smad1 at the linker region, preventing the transcriptional activation by

BMP in R-1B/L17 cells.[39] Thus, the increase in pSmad1 observed in our western may be due to TGF-β-induced mitogen activated protein kinases (MAPK) signaling. Importantly, even in the presence of the TGF-β1 transgene, Smad3^{-/-} mice did not show any detectable pSmad3. Therefore the deletion of exon 8 of the Smad3 gene completely inhibited TGF-β1-mediated Smad3 phosphorylation in the lens.

*2.3.2 Histological and immunohistochemical analyses of the TGF-β1/Smad3 lenses*

Histological examination of eyes from 3 month old TGF-β1 transgenic mice on all three Smad3 backgrounds (TGF-β1/Smad3^{+/+}, TGF-β1/Smad3^{-/-} and TGF-β1/Smad3^{+/-} (latter not shown) revealed distinct evidence of ASC formation including extensive multi-layering of cells forming plaques beneath the anterior lens capsule (Fig. 3). In contrast to the cataracts of TGF-β1/Smad3^{+/+} and TGF-β1/Smad3^{+/-} mice, which typically spanned nearly the full width of the anterior region of the lens, the subcapsular plaques in the TGF-β1/Smad3^{-/-} lenses were substantially smaller. In addition, cells in the Smad3-deficient plaques exhibited a more rounded appearance than their wild-type and heterozygote littermates (Compare Fig. 3 J, K). In addition to lens plaque formation, TGF-β1/Smad3^{+/+} and TGF-β1/Smad3^{+/-} (latter not shown) mice exhibited overt defects in the cornea including increased thickness and cellularity of the corneal stroma that often resulted in the corneal endothelium adhering to the lens capsule (Fig. 3 B, F). The corneal phenotype in the TGF-β1/Smad3^{-/-} mice was much less severe and the cornea did not come into contact with the lens. Finally, vacuole formation and nucleation in the posterior cortex of the mature TGF-β1/Smad3^{+/+} and TGF-β1/Smad3^{+/-} lenses was

43

observed, while these features were substantially reduced or absent in the TGF-β1/Smad3$^{-/-}$ lenses (Fig. 4).

The expression of α-SMA was examined since this is a commonly used marker for the EMT that occurs in TGF-β-induced ASC formation (Fig. 5). Expression of α-SMA was observed in the subcapsular plaques of the TGF-β1/Smad3$^{+/+}$, and TGF-β1/Smad3$^{+/-}$ (latter not shown) lenses whereas no α-SMA expression was detected in the non-transgenic wild-type and Smad3$^{-/-}$ lenses (Fig. 5). Importantly, α-SMA expression was also detected in the plaques of lenses from the TGF-β1/Smad3$^{-/-}$ mice, although immunoreactivity appeared reduced as compared to the mice with Smad3 wild-type or heterozygote backgrounds. Staining in the iris of the non-transgenic wild-type and Smad3$^{-/-}$ served as a positive control for α-SMA expression. Results from western blot analysis of α-SMA (42 kDa) expression in lens extracts (Fig. 6) confirmed the immunostaining results. While all TGF-β1 transgenic mice exhibit distinct expression of α-SMA, lenses from TGFβ1/Smad3$^{-/-}$ mice show reduced levels compared to the TGF-β1/Smad3$^{+/+}$ and TGF-β1/Smad3$^{+/-}$ mice. β-actin (42 kDa) protein was used as loading control and showed equal levels of expression in all samples examined.

Fibronectin is a fibrotic marker known to be expressed in ASC plaques.[40-43] We therefore examined the expression of fibronectin in the TGF-β1/Smad3 lenses. Unlike non-TGF-β1 transgenic mice where fibronectin expression was found to be confined to the lens capsule, the cells within the subcapsular plaques of the TGF-β1/Smad3$^{+/+}$, TGF-β1/Smad3$^{-/-}$ and TGF-β1/Smad3$^{+/-}$ (not shown) lenses exhibited immunoreactivity to

fibronectin (Fig.7). However, as was shown earlier for α-SMA, the intensity of the immunoreactivity to fibronectin in the cells of the subcapsular plaques of TGF-β1/Smad3^{-/-} lenses was reduced when compared to the TGF-β1/Smad3^{+/+} and TGF-β1/Smad3^{+/-} lenses.

Mason's Trichrome stain was next used to observe total collagen deposition (collagen stains blue or aqua) in the mouse lenses (Fig. 8). In the normal lens, collagen expression is confined to the lens capsule, whereas aberrant collagen deposition has been observed in ASC plaques.[43] The expression of the TGF-β1 transgene resulted in substantial collagen deposition in the plaques of TGF-β1/Smad3^{+/+} and TGF-β1/Smad3^{+/-} (latter not shown) mice as previously reported.[1, 7] In contrast, much less collagen deposition was observed in the subcapsular plaques of the TGF-β1/Smad3^{-/-} mice. Further analysis of collagen type I and IV expression was performed using specific antibodies (Fig. 9 and 10), since these isoforms are known to be expressed in ASC.[43] Expression of collagen type I was detected in the subcapsular plaques of all the transgenics including TGF-β1/Smad3^{+/+}, TGF-β1/Smad3^{-/-} and TGF-β1/Smad3^{+/-} (latter not shown) (Fig. 9), whereas non-TGF-β1 transgenic lenses showed no expression of collagen type I. Interestingly, the intensity of immunoreactivity for type I collagen was similar for all the TGF-β1/Smad3^{-/-}, TGF-β1/Smad3^{+/+} and TGF-β1/Smad3^{+/-} (latter not shown) lenses. Normal expression of type IV collagen was observed in the lens capsule of all mice examined [44] (Fig. 10). A substantial level of collagen type IV immunoreactivity in the subcapsular plaques of TGF-β1/Smad3^{+/+} and TGF-β1/Smad3^{+/-}

(latter not shown) lenses was observed. In contrast, the plaques of TGF-β1/Smad3$^{-/-}$ mice exhibited little to no type IV collagen staining.

Previous studies have shown that TGF-β-induced subcapsular plaques consist of a heterogeneous population of cells that are either immunoreactive to a-SMA or to β-crystallin, a lens fibre specific marker.[45] Expression of β-crystallin was therefore examined to further characterize the cellular makeup of the plaques in the TGF-b1 transgenic lenses (Fig. 11). Expression of β-crystallin was detected in the posterior part of subcapsular plaques (away from the lens capsule) in the TGF-β1/Smad3$^{+/+}$, and TGF-β1/Smad3$^{+/-}$ (latter not shown) lenses. These results correspond to the β-crystallin immunoreactivity in previously detected in larger human ASC plaques.[45] Interestingly, the TGF-β1/Smad3$^{-/-}$ lenses also exhibited immunoreactivity to β-crystallin demonstrating that although these plaques are reduced in size they still contain a heterogeneous population of cells similar to their wild-type and heterozygote littermates.

*2.3.3 Apoptotic cell death analyses of TGF-β1/Smad3 lenses*

Since the ASC plaques observed in the TGF-β1/Smad3$^{-/-}$ mice are smaller than their wild-type littermates and apoptosis has been reported to occur in TGF-β-induced ASC,[8, 46] we utilized TUNEL labeling to examine the level of apoptosis in the different experimental groups. Both the non-transgenic wild-type and Smad3 null lenses did not exhibit TUNEL-positive nuclei (not shown). TUNEL-positive nuclei were found in the subcapsular plaques of all the TGF-β transgenic mice including the TGF-β1/Smad3$^{+/+}$,

TGF-β1/Smad3$^{+/-}$ (latter not shown) and TGF-β1/Smad3$^{-/-}$ mice (Fig. 12). Importantly, TGF-β1/Smad3$^{-/-}$ lenses demonstrate a significantly higher percentage of TUNEL-positive cells (20.3±5.8%) as compared to the TGF-β1/Smad3$^{+/+}$ (6.1±1.1 %) lenses (unpaired student's t-test: $p \le 0.05$). The TUNEL positive cells of TGF-β1/Smad3$^{-/-}$ lenses are mainly situated at the posterior aspect of the plaque, abutting the lens fibre cell mass.

*2.3.4 Effect of the TGF-β1 and Smad3 on the optical quality of the mouse lens*

A laser scanning system was next employed to determine quantitative differences in the optical quality of the lenses of TGF-β1 transgenic mice on the different Smad3 backgrounds. As described in detail in the methods, the automated laser scanning system consists of a scanning helium-neon laser source, which is projected through the lens to measure lens optical qualities (the average back vertex distance, BVD) and sharpness of focus (BVD error).[35-37] The bar graph in figure 13 represents the back vertex distance variability (BVD error, mm ± SEM) for wild-type, TGF-β1/Smad3$^{+/+}$, TGF-β1/Smad3$^{+/-}$, and TGF-β1/Smad3$^{-/-}$ mouse lenses. An increase in BVD error signifies a decrease in sharpness of light focus through the lens. The TGF-β1/Smad3$^{+/+}$ and TGF-β1/Smad3$^{+/-}$ lenses showed the most significant (ANOVA: $p \le 0.05$) BVD errors (0.531±0.071 mm and 0.486 ±0.040 mm respectively) when compared to wild-type (0.067±0.002 mm) lenses, indicating that lens optical quality was reduced in the presence of subcapsular plaques in the TGF-β1 transgenic mice. The TGF-β1/Smad3$^{-/-}$ (0.099±0.005 mm) lenses also showed a significantly greater BVD error when compared to the wild-type lenses,

47

however, this was significantly lower than the TGF-$\beta$1/Smad3$^{+/+}$ and TGF-$\beta$1/Smad3$^{+/-}$

lenses.  Thus, the optical results correspond with the morphological findings.
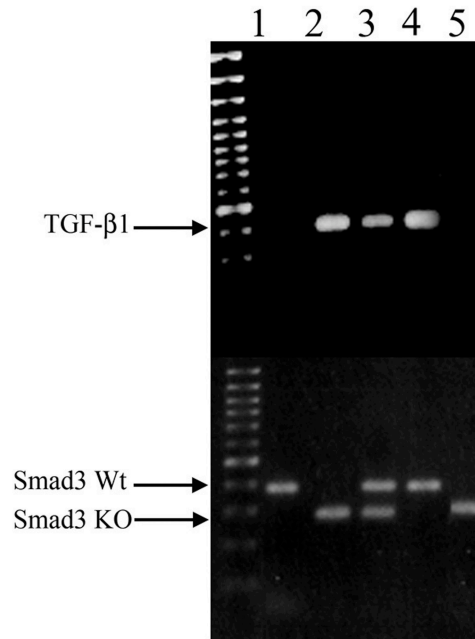
Figure 1. Genotyping for TGF-β1/Smad3 KO mice

The top gel shows PCR results for the TGF-β1 (300 bp) transgene, while the bottom gel shows PCR results for the Smad3 wild-type (Wt, 400b bp) and Smad3 knockout (KO, 250 bp) alleles. The mice have the following genotypes: wild-type (lane 1), TGF-β1/Smad3$^{-/-}$ (lane 2), TGF-β1/Smad3$^{+/-}$ (lane 3), TGF-β1/Smad3$^{+/+}$ (lane 4) and Smad3$^{-/-}$ (lane 5).
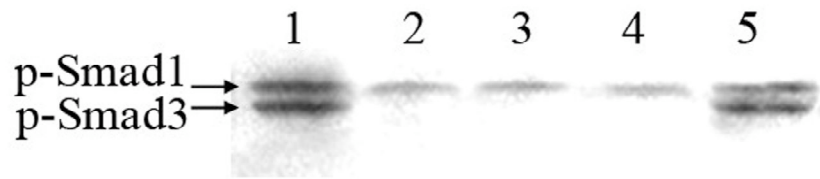
Figure 2. Phosphorylated Smad3

Western blot analysis using an anti-pSmad3/Smad1 antibody for the detection of pSmad3 (58 kDa) protein expression in lens extracts. The antibody cross reacts with phosphorylated Smad1 (65 kDa) protein, which served as an internal positive control. The lanes show the level of phospho-Smad3 protein in TGF-β1/Smad3$^{+/+}$ (lane 1), wild-type (lane 2), TGFβ1/Smad3$^{-/-}$ (lane 3), Smad3$^{-/-}$ (lane 4) and TGF-β1/Smad3$^{+/-}$ (lane 5) mouse lenses. Both TGF-β1/Smad3$^{+/+}$ and TGF-β1/Smad3$^{+/-}$ lenses show the presence of pSmad3, whereas wild-type and Smad3 null (TGF-β1/Smad3$^{-/-}$ and Smad3$^{-/-}$) lenses did not.
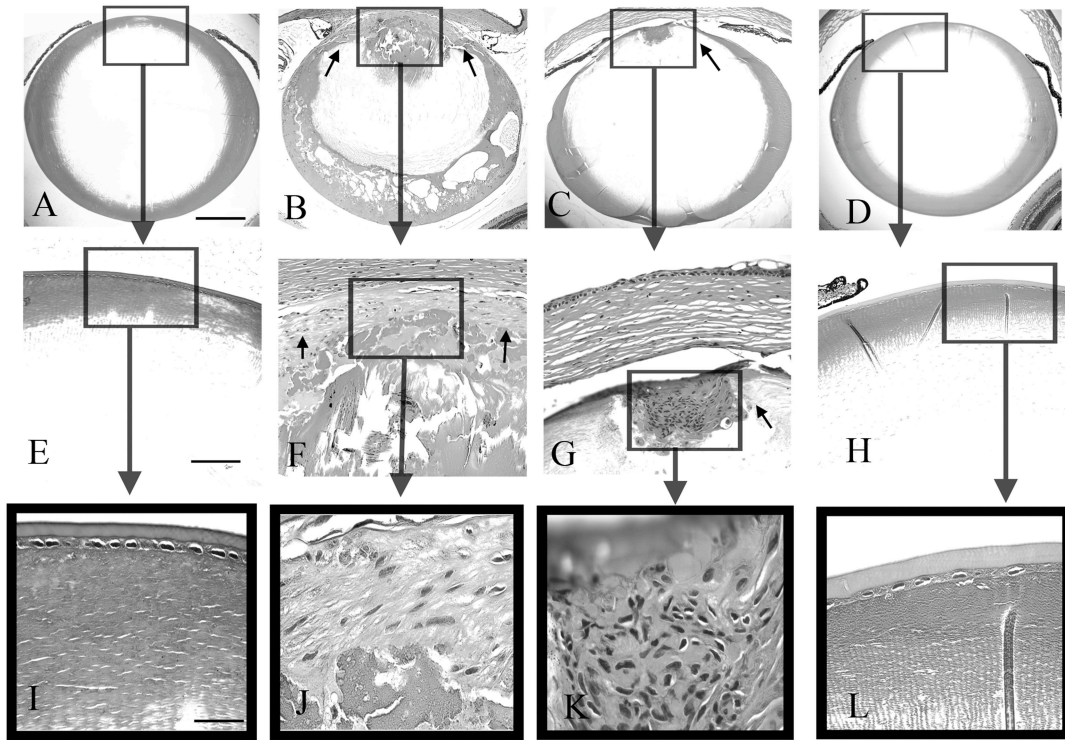
Figure 3. Histological analysis of the TGF-β1/Smad3 lenses

Wild-type (A, E and I), TGF-β1/Smad3$^{+/+}$ (B, F and J), TGF-β1/Smad3$^{-/-}$ (C, G and K), and a Smad3$^{-/-}$ (D, H and L,) lenses are shown.  The boxes show the areas of magnification.  The expression of the TGF-β1 transgene induced subcapsular plaque formation in the TGF-β1/Smad3$^{+/+}$ and TGF-β1/Smad3$^{-/-}$ lenses (F, G, small arrows). The subcapsular plaques in TGF-β1/Smad3$^{-/-}$ lenses were smaller than those in the TGF-β1/Smad3$^{+/+}$ lenses.  Both the wild-type and Smad3$^{-/-}$ lenses show normal morphology of the lens epithelium.  The scale bars represent 400 μm (A-D), 100 μm (E-H) and 50 μm (I-L) respectively.
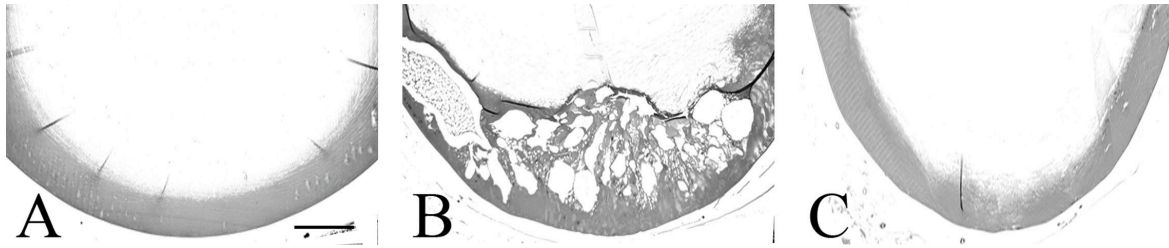
Figure 4. Vacuole formation in the TGF-β1/Smad3 lenses

The posterior lens cortex of wild-type (A), TGF-β1/Smad3$^{+/+}$ (B) and TGF-β1/Smad3$^{-/-}$ (C) lenses are shown. The expression of TGF-β1 induced nucleation and vacuole formation in the TGF-β1/Smad3$^{+/+}$ lenses. Both the wild-type and TGF-β/Smad3$^{-/-}$ lenses show normal morphology of the posterior lens cortex. Scale bar represents 200 μm.
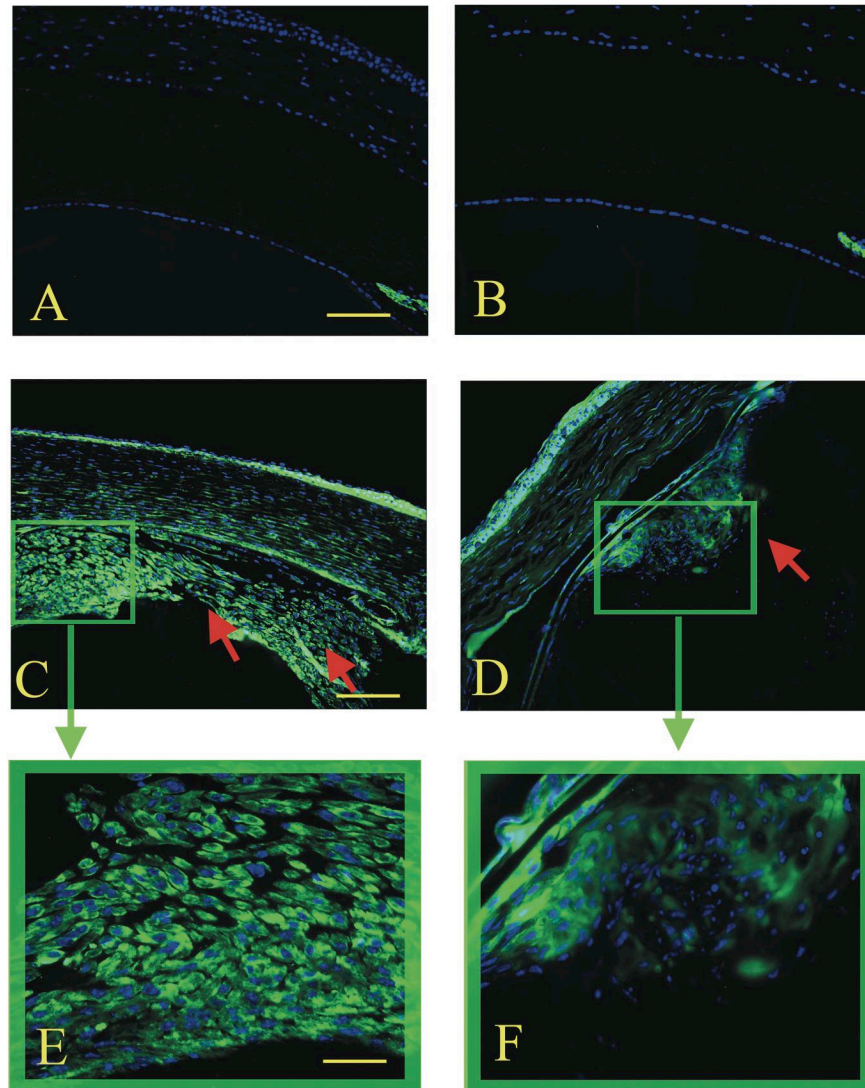
Figure 5. Immunohistochemical analysis of α-smooth muscle actin expression (FITC)

Wild-type (A), Smad3$^{-/-}$ (B), TGF-β1/Smad3$^{+/+}$ (C and E) and TGF-β1/Smad3$^{-/-}$ (D and F) lenses are shown. The arrows (red) indicate the subcapsular plaques. Expression of α-smooth muscle actin (α-SMA) was detected in the subcapsular plaques of the TGF-β1/Smad3$^{+/+}$ and TGF-β1/Smad3$^{-/-}$ lenses. However, there was less α-SMA immunoreactivity detected in TGF-β1/Smad3$^{-/-}$ lenses. Both the wild-type and Smad3$^{-/-}$

lenses show no expression of α-SMA in the lens and normal expression in the iris (positive control). The scale bars represent 100 μm (A-D) and 50 μm (E and F).
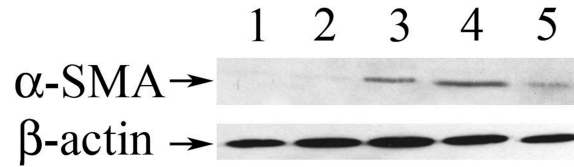
Figure 6. α-Smooth muscle actin protein expression

Western blot analysis using an anti-α-smooth muscle actin (α-SMA) antibody for the detection of α-SMA (42 kDa) protein expression in lens extracts. The membrane was stripped and reprobed for β-actin, which served as a loading control. Lanes 1-5 show α-SMA and β-actin protein expression in wild-type, Smad3$^{-/-}$, TGF-β1/Smad3$^{+/-}$, TGF-β1/Smad3$^{+/+}$, and TGFβ1/Smad3$^{-/-}$ lenses respectively. The β-actin signal shows that equal amounts of protein were loaded in all lanes. TGF-β1/Smad3$^{+/+}$, TGF-β1/Smad3$^{+/-}$ and TGFβ1/Smad3$^{-/-}$ lenses show expression of α-SMA, whereas wild-type and Smad3$^{-/-}$ lenses do not. The TGFβ1/Smad3$^{-/-}$ lenses show reduced levels of α-SMA compared to both the TGF-β1/Smad3$^{+/+}$ and TGF-β1/Smad3$^{+/-}$ lenses.
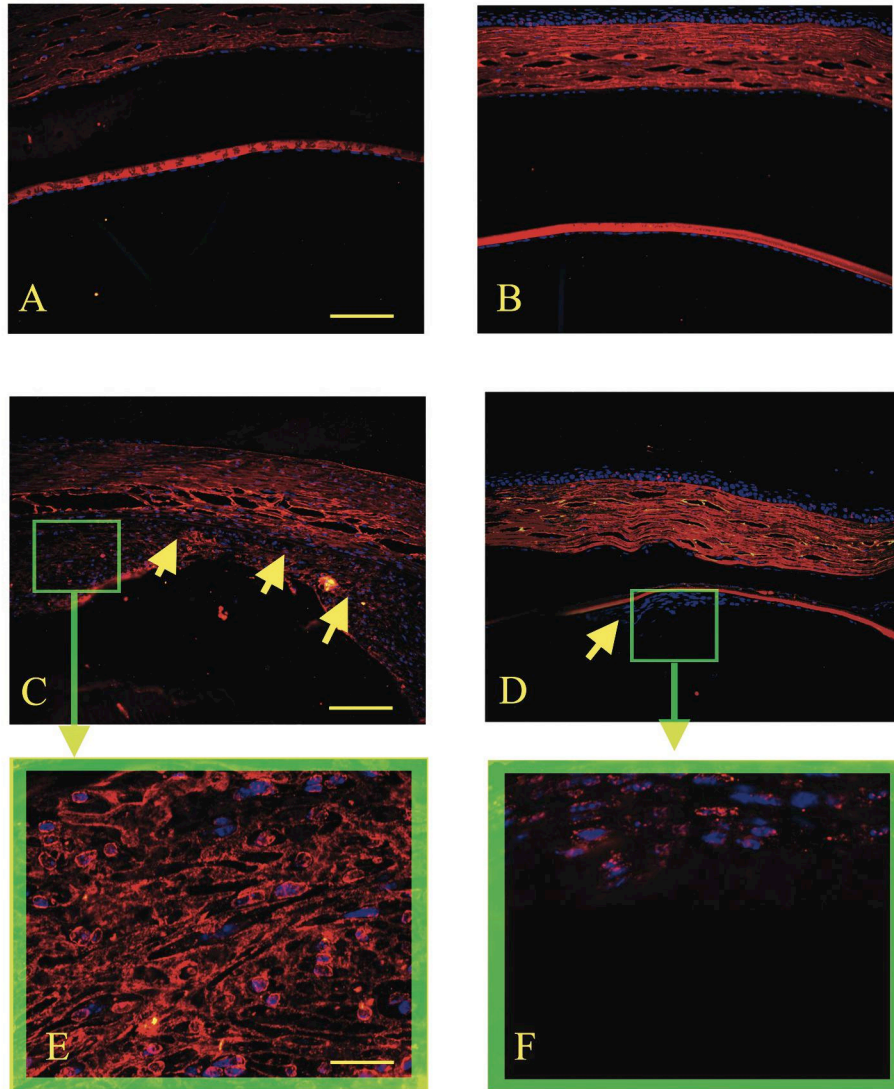
Figure 7. Immunohistochemical analysis of fibronectin expression (TRITC)

Wild-type (A), Smad3$^{-/-}$ (B), TGF-β1/Smad3$^{+/+}$ (C and E) and TGF-β1/Smad3$^{-/-}$ (D and F) lenses are shown. The arrows (yellow) indicate location of subcapsular plaques. There was detectable expression of fibronectin in the subcapsular plaques of the TGF-β1/Smad3$^{+/+}$ and TGF-β1/Smad3$^{-/-}$ lenses. The intensity of fibronectin immunoreactivty in the subcapsular plaques of TGF-β1/Smad3$^{-/-}$ lenses was reduced when compared to the TGF-β1/Smad3$^{+/+}$ lenses. Both the wild-type and Smad3$^{-/-}$ lenses showed normal

expression of fibronectin in the lens capsule.  The scale bars represents 100 μm (A-D)

and 50 μm (E and F).
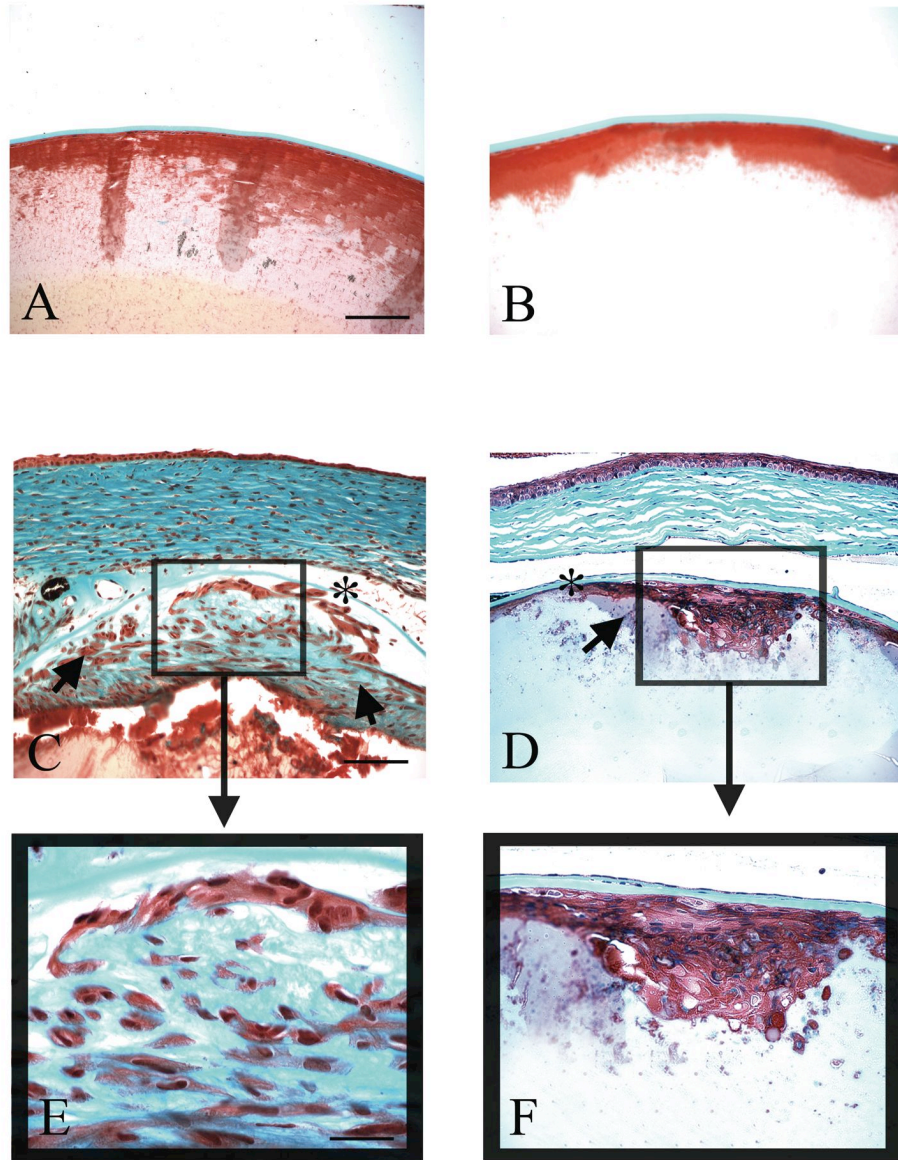
Figure 8. Mason's Trichrome staining for collagen

Wild-type (A), Smad3$^{-/-}$ (B), TGF-β1/Smad3$^{+/+}$ (C and E) and TGF-β1/Smad3$^{-/-}$ (D and F) lenses are shown. The arrows (black) indicate location of subcapsular plaques and * asterisks indicate collagen expression in the lens capsules. The expression of TGF-β1 increased collagen formation in the TGF-β1/Smad3$^{+/+}$ and TGF-β1/Smad3$^{-/-}$ lens epithelium. However, the collagen deposition in the subcapsular plaques of TGF-

β1/Smad3$^{-/-}$ lenses was substantially reduced as compared to the TGF-β1/Smad3$^{+/+}$ lenses. Both the wild-type and Smad3$^{-/-}$ lenses showed normal collagen expression in the lens capsule. The scale bars represent 100 μm (A-D) and 50 μm (E and F).
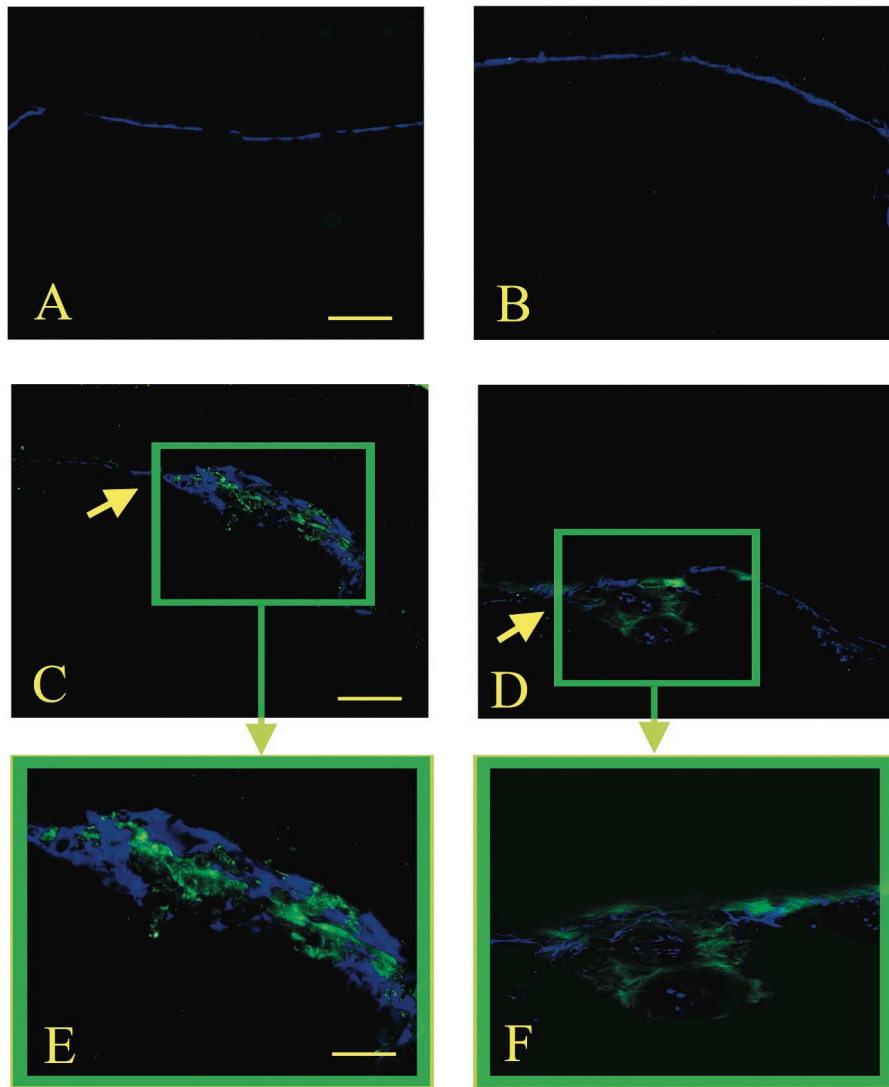
Figure 9. Immunohistochemical analysis of collagen type I expression (FITC)

Wild-type (A), Smad3$^{-/-}$ (B), TGF-β1/Smad3$^{+/+}$ (C and E) and TGF-β1/Smad3$^{-/-}$ (D and F) lenses are shown. The arrows (yellow) indicate location of subcapsular plaques. Expression of collagen type I was detected in the subcapsular plaques of the TGF-β1/Smad3$^{+/+}$and TGF-β1/Smad3$^{-/-}$ lenses. There was no observable difference in collagen I expression between the TGF-β1/Smad3$^{-/-}$ and TGF-β1/Smad3$^{+/+}$ lenses. Both the wild-type and Smad3$^{-/-}$ lenses show no expression of collagen type I in the lens. The

scale bars represents 100 μm (A-D) and 50 μm (E and F).
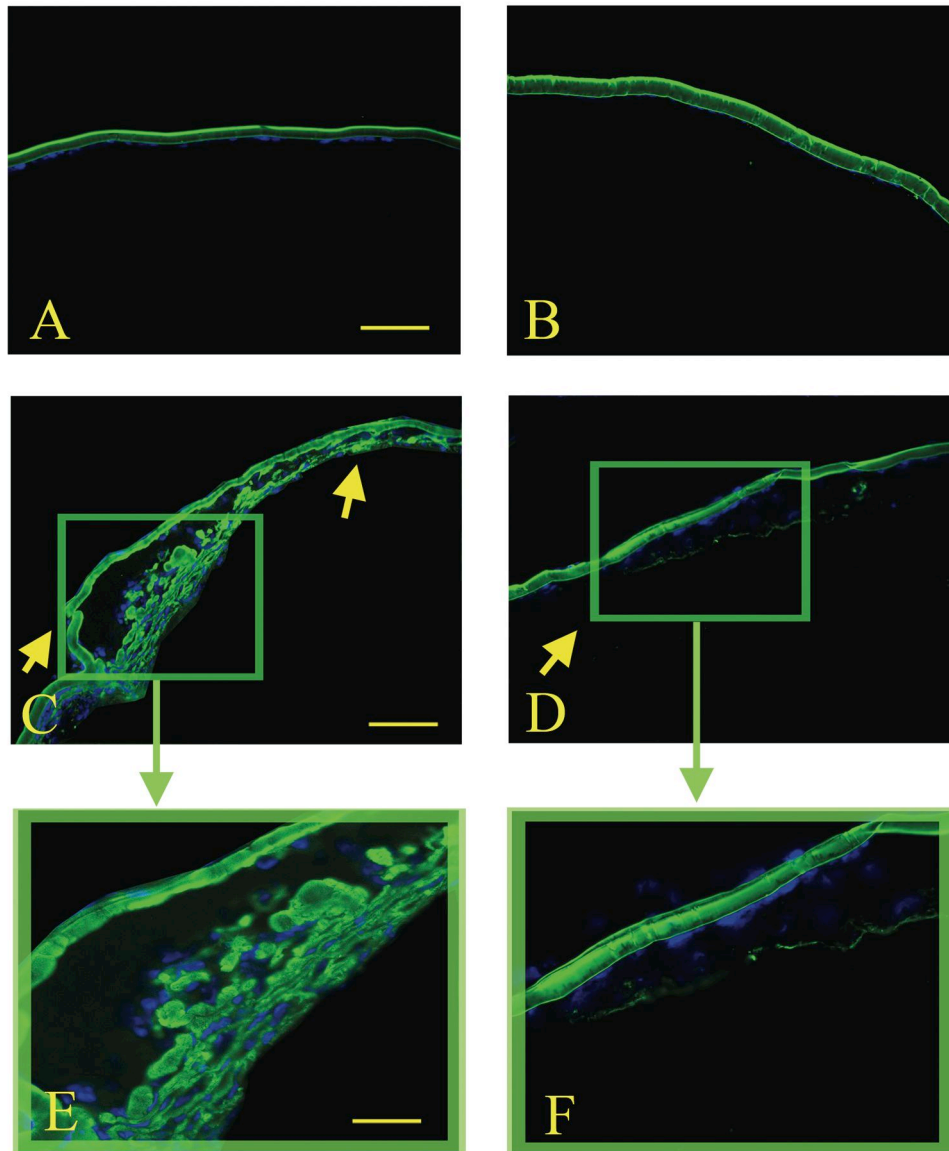
Figure 10. Immunohistochemical analysis of collagen type IV expression (FITC)

Wild-type (A), Smad3$^{-/-}$ (B), TGF-β1/Smad3$^{+/+}$ (C and E) and TGF-β1/Smad3$^{-/-}$ (D and F) lenses are shown. The arrows (yellow) indicate the location of subcapsular plaques. Expression of collagen type IV was detected in the subcapsular plaques of the TGF-β1/Smad3$^{+/+}$ and TGF-β1/Smad3$^{-/-}$ lenses. There was considerable reduction in collagen IV immunoreactivity in the TGF-β1/Smad3$^{-/-}$ lenses when compared to the TGF-

β1/Smad3$^{+/+}$ lenses.  Both the wild-type and Smad3$^{-/-}$ lenses show collagen type IV present in the lens capsule.  The scale bars represent 100 μm (A-D) and 50 μm (E and F).
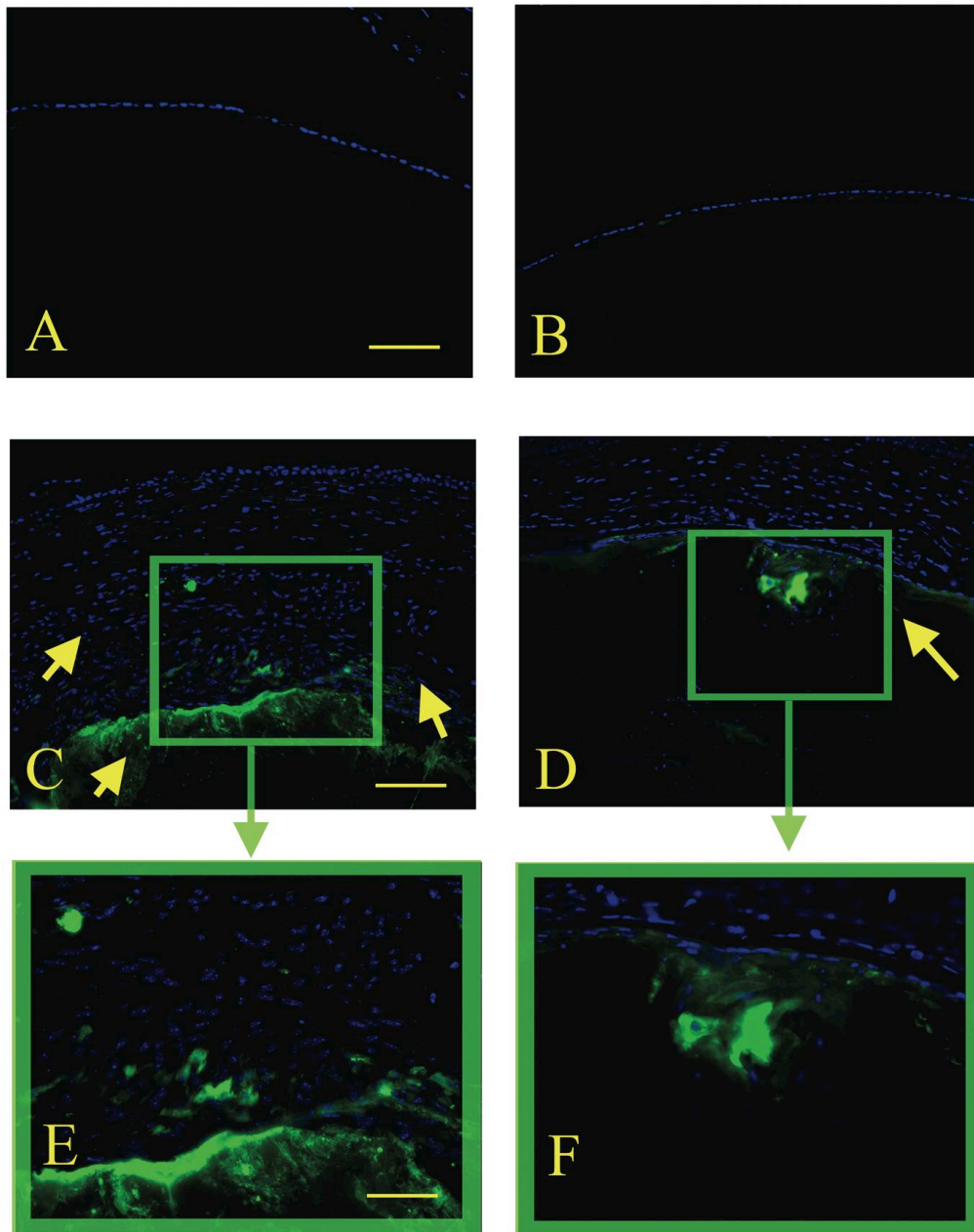
Figure 11. Immunohistochemical analysis of β-crystallin expression (FITC)

The photographs represents: a wild-type (A), Smad3$^{-/-}$ (B), TGF-β1/Smad3$^{+/+}$ (C and E)

and a TGF-β1/Smad3$^{-/-}$ (D and F) mouse lens. The arrows (yellow) indicate location of

subcapsular plaques. Expression of β-crystallin was detected in the posterior aspect

(abutting the lens fibre cell mass) of the subcapsular plaques in both the TGF-β1/Smad3$^{+/+}$ and TGF-β1/Smad3$^{-/-}$ lenses.  Both the wild-type and Smad3$^{-/-}$ lenses show no expression of β-crystallin in the lens epithelium. The scale bars represents 100 μm (A-D) and 50 μm (E and F).
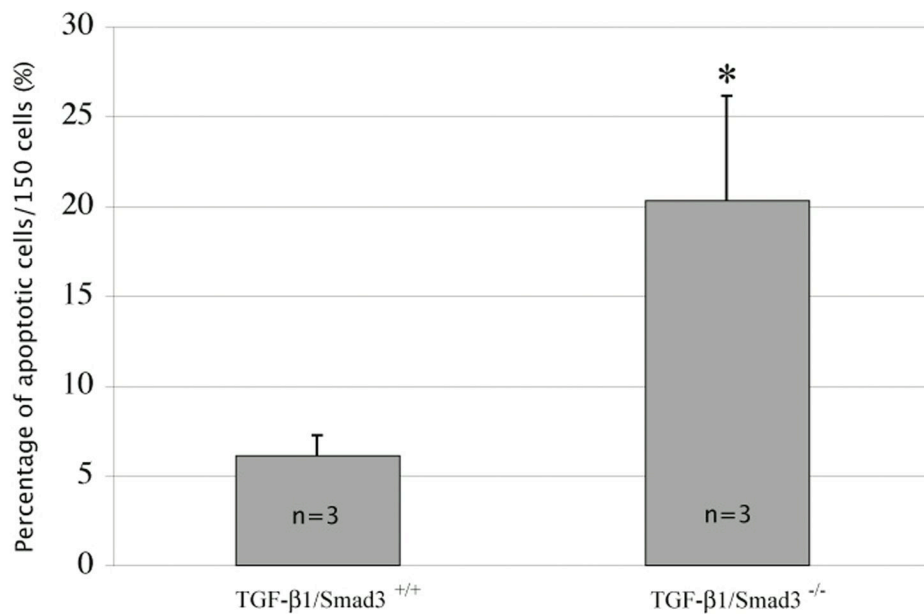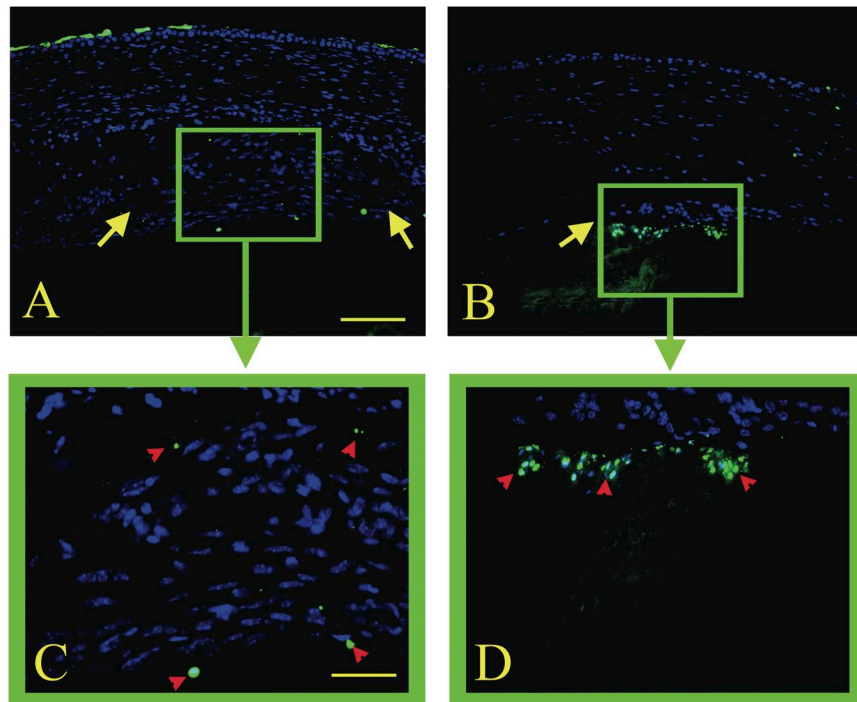
Figure 12. TUNEL staining of apoptotic nuclei (FITC) in TGF-β1/Smad3 lenses

The photographs represent: a TGF-β1/Smad3^{+/+} (A and C) and a TGF-β1/Smad3^{-/-} (B and

D) mouse lens. The yellow arrows indicate the location of subcapsular plaques and the red arrowheads indicate the location of TUNEL-positive nuclei. The TGF-β1/Smad3$^{+/+}$ lenses showed a few TUNEL-positive nuclei located in the anterior and posterior regions of the plaques (A and C). The TGF-β1/Smad3$^{-/-}$ lenses exhibited more TUNEL-positive nuclei. The scale bars represent 100 μm (A and B) and 50 μm (C and D). The bar graph represents the percentage of apoptotic nuclei per 150 cells. *The TGF-β1/Smad3$^{-/-}$ lenses have significantly more apoptotic nuclei (20.3±5.8%) than the TGF-β1/Smad3$^{+/+}$ (6.1±1.1%) lenses (unpaired student's t-test: $p \leq 0.05$).
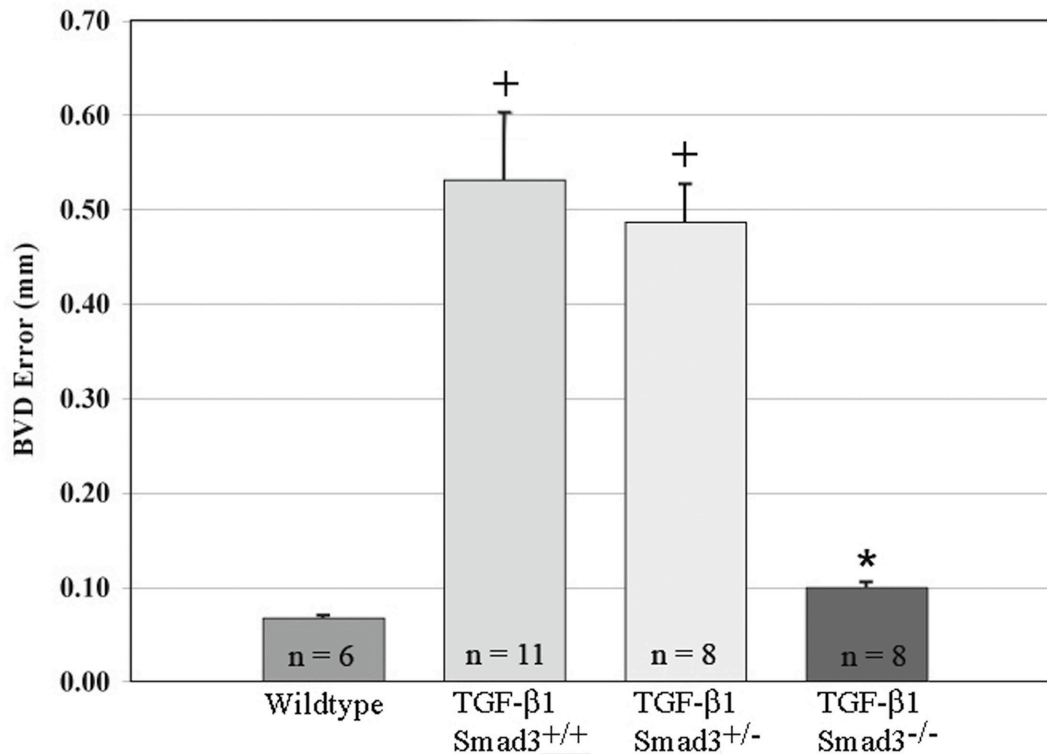
Figure 13. Optical effects of subcapsular cataract formation in mouse lenses

The bar graph represents the back vertex distance variability (BVD error, mm ± SEM) for wild-type, TGF-β1/Smad3^{+/+}, TGF-β1/Smad3^{+/-}, and TGF-β1/Smad3^{-/-} mouse lenses. An increased in BVD error signifies a decrease in sharpness of light focus through the lens. [+]Statistical analysis (ANOVA: $p \leq 0.05$) shows that the TGF-β1/Smad3^{+/+} and TGF-β1/Smad3^{+/-} lenses show the greatest BVD errors (0.531±0.071 mm and 0.486 ±0.040 mm respectively) when compared to the wild-type (0.067±0.002 mm) lenses. [*]The TGF-β1/Smad3^{-/-} (0.099±0.005 mm) lenses also show a significantly greater BVD error when compared to the wild-type lenses. However, the BVD error of TGF-β1/Smad3^{-/-} lenses is significantly lower than both TGF-β1/Smad3^{+/+} and TGF-β1/Smad3^{+/-} lenses.
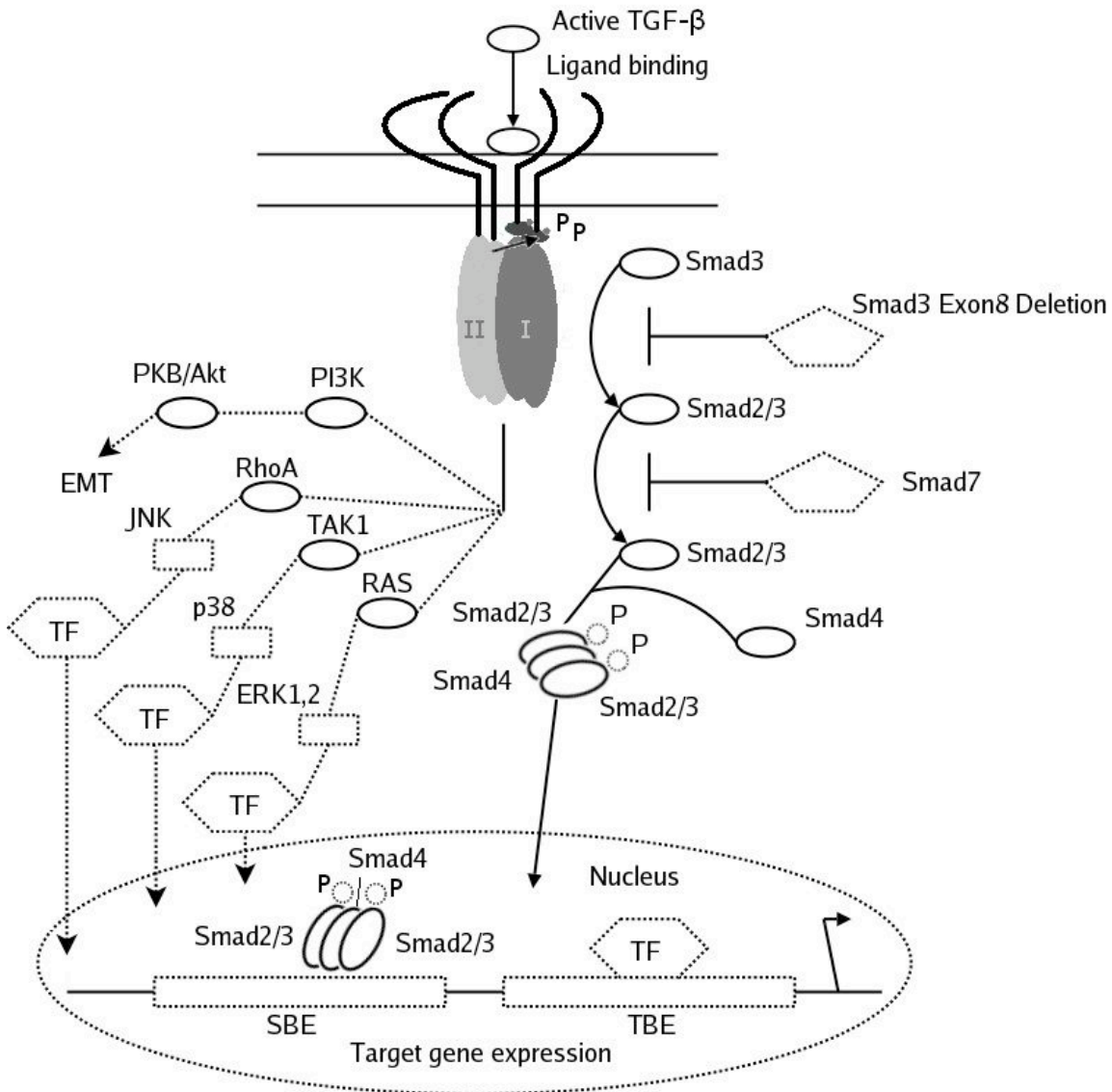
Figure 14. TGF-β induced Smad dependent and Smad independent signaling pathways

The above diagram is modified from A. Roberts and R. Derynck, 2001.[67] Upon ligand

binding, type I and type II receptors are activated and phosphorylation of R-Smads

(Smad2/3) occurs. Phosphorylated R-Smads form heterotrimeric complexes with Co-

Smad (Smad 4) and translocate to the nucleus. The Smad complexes interact with other

transcription factors (TF) at DNA sequence-specific binding sites (transcription factor

binding element (TBE); Smad binding element (SBE)) to regulate gene expression. Smad7 is an inhibitory Smad that prevents receptor activation of R-Smads. Smad3 phosphorylation is prevented in Smad3 null mice so TGF-β-induced responses are presumed to occur through activation of other TGF-β-induced signaling pathways. TGF-β also induces activation of mitogen activated protein kinase (MAPK) pathways (JNK, p38 and ERK1, 2) through upstream mediators: RhoA, Ras, and TAK1. Additional pathways involving PI3K have also been shown to mediate EMT.

## 2.4 Discussion

TGF-β plays crucial roles during development, homeostasis and pathological conditions, including ocular fibrotic diseases such as ASC formation and glaucoma.[1, 22, 24, 47] Typically, TGF-β has inhibitory effects on cells of epithelial origin, while it is mitogenic for smooth muscle cells and fibroblasts.[24, 48] In addition, TGF-β can cause an EMT for various types of epithelial cells in response to injury. This occurs in the lens where active TGF-β has been shown to promote the conversion of lens epithelial cells into myofibroblasts, which form ASC plaques.[1, 16, 20] Smad3 is an important mediator of TGF-β-induced fibrosis in the kidney and lung.[27, 30, 49] However, the requirement of Smad3 in the EMT of epithelial cells remains controversial.[50] In the current study we have shown that transgenic, expression of TGF-β1 in the lens promotes the formation of ASCs in the absence of Smad3, demonstrating that Smad3-independent signaling pathways are activated.

Smad2 is another receptor-mediated Smad that complexes with the Co-Smad (Smad4). Thus, one may surmise that Smad2 activation may have compensated for the loss of Smad3 and contributed to the TGF-β induced EMT in the TGF-β1/Smad3^{-/-} lens epithelium. However, although both Smad2 and Smad3 can mediate TGF-β and activin signaling, they clearly have non-redundant functions. For example, homozygous mice with targeted disruptions in the Smad2 gene exhibit embryonic lethality during gastrulation,[51, 52] whereas, homozygous Smad3 null mice are viable and survive to adulthood.[32, 53] Smad3 and Smad2 have also been shown to have different gene-

71

regulatory functions and Smad3, not Smad2, has been linked to fibrotic events.[25, 53, 54] Finally, pSmad2 has been shown to be constitutively expressed in the lens epithelium and unaffected by TGF-β signaling.[55]

While the predominant signaling pathways activated by TGF-β involve the Smads, additional Smad-independent TGF-β signaling pathways exist that could regulate the EMT of LECs. These include the mitogen activated protein kinases (MAPK), such as c-Jun-N-terminal protein kinases (JNK), extracellular signal-regulated kinases (ERK) and p38 MAPK.[50, 56-58] In particular, the p38 MAPK pathway has been shown to play a key role in TGF-β stimulated EMT and cell migration in many systems including mouse mammary and human breast epithelial cells.[56, 59] p38 activation occurs via the TGF-β activated kinase-1 (TAK1) upstream mediator.[57, 60] Interestingly, p38 has also been shown to converge with the Smad pathway in order to produce full effects of EMT in some cell lines.[61] This may explain why we observe a less severe corneal and lens phenotype, including smaller sized plaques, on the Smad3 null background. Phosphadtidyl-inositol 3-kinase (PI3K) and RhoA are also alternative parallel pathways shown to be involved in TGF-β mediated EMT of epithelial cells [62-64] and could therefore be candidate signaling molecules for the EMT of LECs in ASC formation (see Fig. 14). More recently, it has been shown that other growth factors may be able to mediate EMT independent of TGF-β signaling pathways (Garcia CM, et al. *IOVS* 2005;46:ARVO E-Abstract 4641).

The EMT of LECs into myofibroblasts has also been shown to occur in a lens injury model in which the lens capsule is disrupted with a hypodermic needle. Furthermore, lens injury-induced EMT in the lens was shown to be completely inhibited on the Smad3-null background.[31] This is in contrast to our current findings, which show evidence of EMT and ASC formation in the Smad3 null lens in the presence of the TGF-β1 transgene. Reasons for the difference in these findings likely relate to the difference in the mode of delivery of TGF-β between the two models that could affect the levels and exposure time of TGF-β. For example, the TGF-β1 transgenic model used in the current study involves the expression of active TGF-β1 in lens fibre cells, under the control of the αA-crystallin promoter, which is initiated during early embryogenesis and continues throughout life of the animal. In contrast, in the lens injury model, postnatal mice are utilized and latent TGF-β in lens cells or the aqueous humor is thought to be activated following a puncture wound to the capsule.[31] Crystallin promoters are typically strong promoters and when used to drive active TGF-β1 expression in the lens produce dramatic lens phenotypes and corneal defects including a thickened, hypercellular corneal stroma and lack of a stratified corneal epithelium.[1, 24] In comparison, in the lens injury model corneal phenotypes have not been reported. This may be due to the fact that the cornea is fully differentiated in the postnatal mice used for the injury studies. However, it may also reflect that the levels of TGF-β, and/or length of exposure may be greater in the transgenic models as compared to the lens injury model. As discussed above, it is becoming increasingly clear that additional, Smad-independent pathways can regulate EMT and fibrosis. Thus, it is possible that Smad-independent signaling pathways are

differentially induced in the two models, and that this results in EMT and subsequent ASC development in the absence of Smad3 in the transgenic model.

Aberrant ECM deposition is a typical feature of ASC plaques.[1, 7, 45] We observed ECM deposition in the subcapsular plaques of all of the TGF-β1 transgenic lenses examined. However, the plaques of TGF-β1/Smad3$^{-/-}$ lenses showed only trace amounts of collagen type IV and substantially less fibronectin staining as compared to the other TGF-β1 transgenic lenses. This reduced ECM deposition correlates with the smaller sized plaques in the TGF-β1/Smad3$^{-/-}$ mice. There are fewer myofibroblasts to secrete aberrant ECM. However, the fact that collagen type IV and fibronectin appeared to be selectively reduced, whereas collagen I expression did not seem to change dramatically, suggests that Smad3 controls specific aspects of the ASC phenotype. Selective changes in expression of ECM have been previously reported for the Smad3-null mice. For example, Smad3 null mice when challenged with streptozotocin to induce diabetes and glomerular fibrosis show attenuated induction of fibronectin and α3Col4 expression when compared to their wild-type littermates.[65] A selective induction of fibrotic markers, such as αSMA, has also been shown to occur following corneal injury in the Smad3-deficient mice.[66] Thus, while it is clear that TGF-β-induced EMT in the lens can occur in the absence of Smad3, other fibrotic gene programs induced during ASC formation may be Smad3-dependent.

Apoptosis has been shown to be an additional feature of both TGF-β-induced ASC and PCO.[7, 8, 46] In this study, we observed apoptotic figures in the plaques of the TGF-β1

transgenic mice with an increased number in the TGF-β1/Smad3^{-/-} mice as compared to transgenic wild-type littermates. This may explain why the plaques in the TGF-β1/Smad3^{-/-} mice remain small relative to their wild-type and heterozygote littermates. The mechanism by which TGF-β induces apoptosis in the lens is not known. However, epithelial cells when separated from their basement membrane have been shown to undergo apoptosis and specifically, type IV collagen, a component of the lens capsule (basement membrane), has been shown to protect LECs from undergoing Fas-stimulated apoptosis.[44] Thus, the deposition of type IV collagen within the plaques of the TGF-β transgenic mice, which has also been reported in human ASC samples,[43] may permit survival of these cells. The fact that we observed increased numbers of apoptotic cells in the TGF-β1/Smad3^{-/-} plaques, in which there was little to no type IV collagen deposition, further supports a role for type IV collagen in survival of the plaque cells.

We also employed a laser-scanning instrument (ScanTox™) to obtain quantitative measures of the optical quality of the TGF-β transgenic versus non-transgenic lenses. The optical measurements obtained were very consistent with the morphological and molecular data. For example, all of the TGF-β1 transgenic lenses, which exhibited ASC plaques, show significantly larger BVD errors (decreased sharpness of focus) relative to the BVD errors of the wild-type lenses, which are devoid of plaques. Importantly, the scanning laser instrument was able to discern the effects of size of the subcapsular plaques amongst the different genotypes on optical quality. This is likely to be a useful tool in future transgenic/KO lens studies requiring quantitative measures of lens optical quality.

75

In conclusion, the findings of the current study demonstrate that Smad3 deficiency does not prevent ASC formation in an *in-vivo* transgenic TGF-β1 mouse model. The fact that the subcapsular plaques were reduced in size in the TGF-β1 transgenic mice on the Smad3-null background with less type IV collagen and fibronectin deposition as compared to their wild-type and heterozygote littermates suggests that the Smad3 pathway may selectively regulate aspects of the ASC phenotype. Uncovering additional TGF-β signaling mechanisms may provide potential therapeutic targets to help prevent ASC and closely related ocular fibrotic diseases, such as secondary cataract or PCO.

## 2.5 References

1. Srinivasan Y, Lovicu FJ, Overbeek PA. Lens-specific expression of transforming growth factor beta1 in transgenic mice causes anterior subcapsular cataracts. *J Clin Invest* 1998;101:625-634.

2. Yang X, Letterio JJ, Lechleider RJ, et al. Targeted disruption of SMAD3 results in impaired mucosal immunity and diminished T cell responsiveness to TGF-beta. *Embo J* 1999;18:1280-1291.

3. Kurisaki A, Kose S, Yoneda Y, Heldin CH, Moustakas A. Transforming growth factor-beta induces nuclear import of Smad3 in an importin-beta1 and Ran-dependent manner. *Mol Biol Cell* 2001;12:1079-1091.

4. Qing J, Zhang Y, Derynck R. Structural and functional characterization of the transforming growth factor-beta -induced Smad3/c-Jun transcriptional cooperativity. *J Biol Chem* 2000;275:38802-38812.

5. Dunker N, Krieglstein K. Reduced programmed cell death in the retina and defects in lens and cornea of Tgfbeta2(-/-) Tgfbeta3(-/-) double-deficient mice. *Cell Tissue Res* 2003;313:1-10.

6. Lee EH, Seomun Y, Hwang KH, et al. Overexpression of the transforming growth factor-beta-inducible gene betaig-h3 in anterior polar cataracts. *Invest Ophthalmol Vis Sci* 2000;41:1840-1845.

7. Lovicu FJ, Schulz MW, Hales AM, et al. TGFbeta induces morphological and molecular changes similar to human anterior subcapsular cataract. *Br J Ophthalmol* 2002;86:220-226.

8.      Maruno KA, Lovicu FJ, Chamberlain CG, McAvoy JW. Apoptosis is a feature of TGF beta-induced cataract. *Clin Exp Optom* 2002;85:76-82.

9.      de Iongh RU, Wederell E, Lovicu FJ, McAvoy JW. Transforming growth factor-beta-induced epithelial-mesenchymal transition in the lens: a model for cataract formation. *Cells Tissues Organs* 2005;179:43-55.

10.     Dwivedi DJ, Pino G, Banh A, et al. Matrix Metalloproteinase Inhibitors Suppress Transforming Growth Factor-{beta}-Induced Subcapsular Cataract Formation. *Am J Pathol* 2006;168:69-79.

11.     Lang RA, McAvoy JW. Growth Factors in Lens Development. In: Lovicu FJ, Robinson ML (eds), *Development of the Ocular Lens.* New York: Cambridge University Press; 2004:261-289.

12.     Sasaki K, Kojima M, Nakaizumi H, Kitagawa K, Yamada Y, Ishizaki H. Early lens changes seen in patients with atopic dermatitis applying image analysis processing of Scheimpflug and specular microscopic images. *Ophthalmologica* 1998;212:88-94.

13.     Font R, SA B. A light and electron microscopic study of anterior subcapsular cataracts. *American Journal of Ophthalmology* 1974;78:972-984.

14.     Novotny GE, Pau H. Myofibroblast-like cells in human anterior capsular cataract. *Virchows Arch A Pathol Anat Histopathol* 1984;404:393-401.

15.     Hay ED. An overview of epithelio-mesenchymal transformation. *Acta Anat (Basel)* 1995;154:8-20.

16.     Hales AM, Schulz MW, Chamberlain CG, McAvoy JW. TGF-beta 1 induces lens cells to accumulate alpha-smooth muscle actin, a marker for subcapsular cataracts. *Curr Eye Res* 1994;13:885-890.

17.     Hales AM, Chamberlain CG, McAvoy JW. Cataract induction in lenses cultured with transforming growth factor-beta. *Invest Ophthalmol Vis Sci* 1995;36:1709-1713.

18.     Kappelhof JP, Vrensen GF. The pathology of after-cataract. A minireview. *Acta Ophthalmol Suppl* 1992;13-24.

19.     Marcantonio JM, Syam PP, Liu CS, Duncan G. Epithelial transdifferentiation and cataract in the human lens. *Exp Eye Res* 2003;77:339-346.

20.     Cousins SW, McCabe MM, Danielpour D, Streilein JW. Identification of transforming growth factor-beta as an immunosuppressive factor in aqueous humor. *Invest Ophthalmol Vis Sci* 1991;32:2201-2211.

21.     Wallentin N, Wickstrom K, Lundberg C. Effect of cataract surgery on aqueous TGF-beta and lens epithelial cell proliferation. *Invest Ophthalmol Vis Sci* 1998;39:1410-1418.

22.     Rooke HM, Crosier KE. The smad proteins and TGFbeta signalling: uncovering a pathway critical in cancer. *Pathology* 2001;33:73-84.

23.     Gordon-Thomson C, de Iongh RU, Hales AM, Chamberlain CG, McAvoy JW. Differential cataractogenic potency of TGF-beta1, -beta2, and -beta3 and their expression in the postnatal rat eye. *Invest Ophthalmol Vis Sci* 1998;39:1399-1409.

24.     Flugel-Koch C, Ohlmann A, Piatigorsky J, Tamm ER. Disruption of anterior segment development by TGF-beta1 overexpression in the eyes of transgenic mice. *Dev Dyn* 2002;225:111-125.

25.     Greene RM, Nugent P, Mukhopadhyay P, Warner DR, Pisano MM. Intracellular dynamics of Smad-mediated TGFbeta signaling. *J Cell Physiol* 2003;197:261-271.

26.     Attisano L, Wrana JL. Signal transduction by the TGF-beta superfamily. *Science* 2002;296:1646-1647.

27.     Inazaki K, Kanamaru Y, Kojima Y, et al. Smad3 deficiency attenuates renal fibrosis, inflammation,and apoptosis after unilateral ureteral obstruction. *Kidney Int* 2004;66:597-604.

28.     Ramirez AM, Takagawa S, Sekosan M, Jaffe HA, Varga J, Roman J. Smad3 deficiency ameliorates experimental obliterative bronchiolitis in a heterotopic tracheal transplantation model. *Am J Pathol* 2004;165:1223-1232.

29.     Sato M, Muragaki Y, Saika S, Roberts AB, Ooshima A. Targeted disruption of TGF-beta1/Smad3 signaling protects against renal tubulointerstitial fibrosis induced by unilateral ureteral obstruction. *J Clin Invest* 2003;112:1486-1494.

30.     Zhao J, Shi W, Wang YL, et al. Smad3 deficiency attenuates bleomycin-induced pulmonary fibrosis in mice. *Am J Physiol Lung Cell Mol Physiol* 2002;282:L585-593.

31.     Saika S, Kono-Saika S, Ohnishi Y, et al. Smad3 signaling is required for epithelial-mesenchymal transition of lens epithelium after injury. *Am J Pathol* 2004;164:651-663.

32.     Ashcroft GS, Yang X, Glick AB, et al. Mice lacking Smad3 show accelerated wound healing and an impaired local inflammatory response. *Nat Cell Biol* 1999;1:260-266.

33.     de Iongh RU, Lovicu FJ, Overbeek PA, et al. Requirement for TGFbeta receptor signaling during terminal lens fiber differentiation. *Development* 2001;128:3995-4010.

34.     Bradford MM. A rapid and sensitive method for the quantitation of microgram quantities of protein utilizing the principle of protein-dye binding. *Anal Biochem* 1976;72:248-254.

35.     Priolo S, Sivak JG, Kuszak JR, Irving EL. Effects of experimentally induced ametropia on the morphology and optical quality of the avian crystalline lens. *Invest Ophthalmol Vis Sci* 2000;41:3516-3522.

36.     Oriowo OM, Cullen AP, Chou BR, Sivak JG. Action spectrum and recovery for in vitro UV-induced cataract using whole lenses. *Invest Ophthalmol Vis Sci* 2001;42:2596-2602.

37.     Bantseev V, McCanna D, Banh A, et al. Mechanisms of ocular toxicity using the in vitro bovine lens and sodium dodecyl sulfate as a chemical model. *Toxicol Sci* 2003;73:98-107.

38.     Massague J, Seoane J, Wotton D. Smad transcription factors. *Genes Dev* 2005;19:2783-2810.

39.     Kretzschmar M, Doody J, Massague J. Opposing BMP and EGF signalling pathways converge on the TGF-beta family mediator Smad1. *Nature* 1997;389:618-622.

40.     Symonds JG, Lovicu FJ, Chamberlain CG. Posterior capsule opacification-like changes in rat lens explants cultured with TGFbeta and FGF: Effects of cell coverage and regional differences. *Exp Eye Res* 2006;82:693-699.

41.     de Jong-Hesse Y, Kampmeier J, Lang GK, Lang GE. Effect of extracellular matrix on proliferation and differentiation of porcine lens epithelial cells. *Graefes Arch Clin Exp Ophthalmol* 2005;243:695-700.

42.     Oharazawa H, Ibaraki N, Lin LR, Reddy VN. The effects of extracellular matrix on cell attachment, proliferation and migration in a human lens epithelial cell line. *Exp Eye Res* 1999;69:603-610.

43.     Ishida I, Saika S, Okada Y, Ohnishi Y. Growth factor deposition in anterior subcapsular cataract. *J Cataract Refract Surg* 2005;31:1219-1225.

44.     Futter CE, Crowston JG, Allan BD. Interaction with collagen IV protects lens epithelial cells from Fas-dependent apoptosis by stimulating the production of soluble survival factors. *Invest Ophthalmol Vis Sci* 2005;46:3256-3262.

45.     Lovicu FJ, Steven P, Saika S, McAvoy JW. Aberrant lens fiber differentiation in anterior subcapsular cataract formation: a process dependent on reduced levels of Pax6. *Invest Ophthalmol Vis Sci* 2004;45:1946-1953.

46.     Lee JH, Wan XH, Song J, et al. TGF-beta-induced apoptosis and reduction of Bcl-2 in human lens epithelial cells in vitro. *Curr Eye Res* 2002;25:147-153.

47.     Lutjen-Drecoll E. Morphological changes in glaucomatous eyes and the role of TGFbeta(2) for the pathogenesis of the disease. *Exp Eye Res* 2005;81:1-4.

48.     Horowitz JC, Lee DY, Waghray M, et al. Activation of the pro-survival phosphatidylinositol 3-kinase/AKT pathway by transforming growth factor-beta1 in mesenchymal cells is mediated by p38 MAPK-dependent induction of an autocrine growth factor. *J Biol Chem* 2004;279:1359-1367.

49.     Bonniaud P, Kolb M, Galt T, et al. Smad3 null mice develop airspace enlargement and are resistant to TGF-beta-mediated pulmonary fibrosis. *J Immunol* 2004;173:2099-2108.

50. Derynck R, Zhang YE. Smad-dependent and Smad-independent pathways in TGF-beta family signalling. *Nature* 2003;425:577-584.

51. Nomura M, Li E. Smad2 role in mesoderm formation, left-right patterning and craniofacial development. *Nature* 1998;393:786-790.

52. Weinstein M, Yang X, Li C, Xu X, Gotay J, Deng CX. Failure of egg cylinder elongation and mesoderm induction in mouse embryos lacking the tumor suppressor smad2. *Proc Natl Acad Sci U S A* 1998;95:9378-9383.

53. Datto MB, Frederick JP, Pan L, Borton AJ, Zhuang Y, Wang XF. Targeted disruption of Smad3 reveals an essential role in transforming growth factor beta-mediated signal transduction. *Mol Cell Biol* 1999;19:2495-2504.

54. Massague J. Wounding Smad. *Nat Cell Biol* 1999;1:E117-119.

55. Beebe D, Garcia C, Wang X, et al. Contributions by members of the TGFbeta superfamily to lens development. *Int J Dev Biol* 2004;48:845-856.

56. Bakin AV, Rinehart C, Tomlinson AK, Arteaga CL. p38 mitogen-activated protein kinase is required for TGFbeta-mediated fibroblastic transdifferentiation and cell migration. *J Cell Sci* 2002;115:3193-3206.

57. Hanafusa H, Ninomiya-Tsuji J, Masuyama N, et al. Involvement of the p38 mitogen-activated protein kinase pathway in transforming growth factor-beta-induced gene expression. *J Biol Chem* 1999;274:27161-27167.

58. Hayashida T, Poncelet AC, Hubchak SC, Schnaper HW. TGF-beta1 activates MAP kinase in human mesangial cells: a possible role in collagen expression. *Kidney Int* 1999;56:1710-1720.

59.     Kim MS, Lee EJ, Kim HR, Moon A. p38 kinase is a key signaling molecule for H-Ras-induced cell motility and invasive phenotype in human breast epithelial cells. *Cancer Res* 2003;63:5454-5461.

60.     Yamaguchi K, Shirakabe K, Shibuya H, et al. Identification of a member of the MAPKKK family as a potential mediator of TGF-beta signal transduction. *Science* 1995;270:2008-2011.

61.     Yu L, Hebert MC, Zhang YE. TGF-beta receptor-activated p38 MAP kinase mediates Smad-independent TGF-beta responses. *Embo J* 2002;21:3749-3759.

62.     Bakin AV, Tomlinson AK, Bhowmick NA, Moses HL, Arteaga CL. Phosphatidylinositol 3-kinase function is required for transforming growth factor beta-mediated epithelial to mesenchymal transition and cell migration. *J Biol Chem* 2000;275:36803-36810.

63.     Bhowmick NA, Zent R, Ghiassi M, McDonnell M, Moses HL. Integrin beta 1 signaling is necessary for transforming growth factor-beta activation of p38MAPK and epithelial plasticity. *J Biol Chem* 2001;276:46707-46713.

64.     Masszi A, Di Ciano C, Sirokmany G, et al. Central role for Rho in TGF-beta1-induced alpha-smooth muscle actin expression during epithelial-mesenchymal transition. *Am J Physiol Renal Physiol* 2003;284:F911-924.

65.     Fujimoto M, Maezawa Y, Yokote K, et al. Mice lacking Smad3 are protected against streptozotocin-induced diabetic glomerulopathy. *Biochem Biophys Res Commun* 2003;305:1002-1007.

66.    Stramer BM, Austin JS, Roberts AB, Fini ME. Selective reduction of fibrotic markers in repairing corneas of mice deficient in Smad3. *J Cell Physiol* 2005;203:226-232.

67.    Roberts AB, Derynck R. Meeting report: signaling schemes for TGF-beta. *Sci STKE* 2001;2001:PE43.

# Chapter 3

# The Role of Molecular Chaperones in TGF-β-induced Epithelial-Mesenchymal Transition in Rat Lens Epithelial Explants

Alice Banh[1], Paula A. Deschamps[2], Mathilakath M. Vijayan[3], Jacob G. Sivak[1], Judith A. West-Mays[2]

[1]School of Optometry, University of Waterloo, Waterloo, ON, Canada; [2]Pathology and Molecular Medicine, McMaster University, Hamilton, ON, Canada; [3]Biology, University of Waterloo, Waterloo, ON, Canada.

## 3.1 Introduction

The ocular lens is a transparent structure that provides part of the refractive power needed to focus images on the retina.  The lens is a polarized tissue consisting of a single layer of cuboidal epithelium in the anterior pole and lens fibre cells occupying the interior and posterior pole.[1]  The lens grows throughout life by the continuous addition of new fibre cell layers on top of older fibres, with minimal protein turnover.[2]  The cells that form the deeper fibres lose their nuclei and become metabolically inert.[3]  A cataract results in reduced transparency of the lens, which leads to vision loss.  Recently there has been great interest in human anterior subcapsular cataract (ASC) and posterior capsule opacification (PCO), which are secondary cataracts formed residual lens epithelial cells (LECs) after cataract surgery.[4, 5]  Understanding the mechanisms involved in these types of cataract development can lead to prevention and treatment.

Transforming growth factor beta (TGF-β) is a secreted polypeptide that is involved in various cellular processes, including cell proliferation, differentiation, apoptosis, migration and extracellular matrix (ECM) formation.[6-10]  Under physiological conditions, TGF-β in the lens and ocular media mainly exists in its latent form, whereas an increase of biologically active TGF-β has been detected in the ocular media from patients suffering with ASCs.[11, 12]  The three functionally related TGF-β isoforms (TGF-β1-3) [13] have been shown to induce cataractous changes in *in-vitro* rat lens cultures and lens epithelial explants.  However, TGF-β1 is 10 times less potent than TGF-β2 and TGF-β3.[14]  Previous *in-vivo* and *in-vitro* studies have shown that TGF-β-induced

87

epithelial-to-mesenchymal transition (EMT) in transgenic mouse and cultured rat LECs results in the formation of multilayer plaques and in the transdifferentiation of LECs to myofibroblasts/fibroblastic or spindle-like cells.  The EMT is also accompanied by capsular wrinkling, apoptosis, α-smooth muscle actin (α-SMA) expression and an aberrant deposition of ECM, such as collagen type I and III, fibronectin and tenacin.[5, 6, 15-18]  It has been established that these TGF-β induced cataractous changes are associated with ASC and PCO development.[4-6, 18-20]  However, the exact mechanisms involved in TGF-β induced EMT in LECs are still under investigation.

Fibroblast growth factor (FGF) also plays a role in lens cell survival, proliferation, migration and differentiation.[21]  Both FGF-1 (acidic) and FGF-2 (basic) are present continuously in the normal lens environment, with FGF-2 being the more potent isoform.[22]  Treatment with FGF-2 exacerbates the cataractous effects induced by TGF-β in cultured rat lenses and lens epithelial explants.[13, 22]  In addition, FGF-2 can reduce the loss of rat LECs on cultured explants caused by TGF-β induced apoptosis.  It is suggested that FGF along with TGF-β are involved in PCO development.[17, 23]

Heat shock proteins (Hsps) are molecular chaperones that were initially identified as protein expressed after exposure of cells to environmental stress.  However, it has been proven that Hsps also play a crucial role in proper protein assembly, folding, transport and degradation under normal conditions.[24, 25]  The heat shock proteins are divided into families that are classified according to their molecular weight,[25-27] and each family of Hsps recognizes and interacts with various non-native polypeptides through different

modes of binding.[28]  Previous studies have shown that molecular chaperoning activities of α-crystallin, Hsp70 and Hsp90 within the lens are critical in maintaining the supramolecular organization and lens transparency.[29-31]  However, the role of heat shock proteins in LECs during EMT is unclear.

The most abundant soluble protein in the mammalian lens is α-crystallin, which plays a prominent role in maintaining the transparency and refractive properties of the lens.[32, 33]  α-Crystallin (~ 800 kDa aggregate) is composed of two homologous subunits, αA and αB (each with a molecular mass of 20 kDa).[34-37]  Both αA- and αB- crystallin demonstrate chaperone-like activity and belong to the small heat shock protein family.[38-41]  α-Crystallin binds selectively to other unfolded or denatured lens proteins and suppresses non-specific aggregation.[42]  α-Crystallin also protects the lens from oxidative stress under physiological conditions.[43]  Furthermore, LECs collected from human anterior polar type cataracts demonstrate abnormal modification of α-crystallins.[41]

Hsp70 is another heat shock protein present in the lens epithelium and superficial cortical fibres in the adult human lens.[30]  Hsp70 is required for correct folding, assembly, intracellular targeting and degradation of polypeptides and oligomeric proteins.[44]  The constitutive (Hsc70) and inducible forms of Hsp70 are present in the lens under normal unstressed conditions.  It is suggested that the normal microenvironment of the lens is stressful, therefore requiring continuous expression of inducible Hsp70.[30, 45, 46]  Studies using bovine lenses, mouse LECs and rat lenses show that Hsp70 expression is up-regulated under heat, oxidative, osmotic, and mechanical stresses.[31, 47]  The chaperone

89

activities of Hsp70 require ATP and interaction with other chaperones such as Hsp40 and Hsp90.[48] It has been suggested that ATP initiates the interaction of Hsp70 with α-crystallin and sHsp bound intermediates to convert denatured proteins to their native state.[30, 42]

Hsp90 is one of the most abundant proteins in unstressed eukaryotic cells (1-2% of all cellular protein). In mammalian cells there are two functionally similar Hsp90 isoforms, Hsp90α and Hsp90β.[49] Hsp90 is involved in regulating the activity of intracellular proteins such as steroid hormone receptors and protein kinase.[49, 50] Interestingly, TGF-β has been shown to regulate the expression levels of both Hsp70 and Hsp90 in cultured CEC (chicken embryo cells).[51] Hence, heat shock protein may play a protective role in the LECs during TGF-β induced EMT.

The present study investigates the effects of heat shock treatment and the role of molecular chaperones in TGF-β2-induced EMT in rat lens epithelial explants. FGF-2 was also used to exacerbate the effects of TGF-β, as mentioned previously. The morphological and molecular changes of the rat lens epithelial explants were examined and the expressions of α-SMA, F-actin, and E-cadherin were used as indicators of EMT. The protein expression levels of Hsp70, Hsp90 and αA- and αB-crystallin and apoptotic cell loss were also analyzed. The findings of this study show that heat shock treatment reduces the effects of TGF-β-induced EMT in explanted rat LECs. Heat shocked TGF-β epithelial explants demonstrated lower α-SMA expression and greater retention of E-cadherin expression and organization than non-heat shocked TGF-β explants. TGF-β-

induced apoptosis was also reduced in the heat shock rat explants.  Interestingly, this study also shows that Hsp70, Hsp90 and $\alpha$A-crystallin protein expressions in the heat shock treated FGF-2, TGF-$\beta$, and TGF-$\beta$2/FGF-2 rat LECs are significantly lower than their respective non-heat shocked groups at four days after initial treatment.

## 3.2 Materials and Methods

### 3.2.1 In-vitro Rat lens epithelial explants

All animal studies were carried out according to the Canadian Council on Animal Care Guidelines and the Association for Research in Vision and Ophthalmology (ARVO) Statement for the Use of Animals in Ophthalmic and Vision Research. Lenses were dissected from Wistar rats (7-10 day old) after euthanization by cervical dislocation. The lens was placed with its anterior side down onto a 35 mm laminin coated culture dish (BD Biosciences, ON. Canada) containing specialized serum-free medium M199 with antibiotics.[52] Lens epithelial explants were prepared by peeling the posterior pole of the lens capsule and pinning the anterior capsule to the culture dish with the epithelial cells facing upwards. The lens fibre mass was removed and discarded.[13, 17] This provided a primary rat LEC culture on an intact anterior lens capsule serving as the substratum for the cells. The lens epithelial explants were incubated at 37 °C with 4.0% $CO_2$ for 24 hours before any treatment to ensure that they were not damaged during the dissection. Only explants with a confluent monolayer of LECs were used. The concentration of FGF-2 and TGF-β2 used for treatment were 10 ng/ml (FGF-2; PeproTech Inc., NJ. USA) and 8 ng/ml (TGF-β2; Cedarlane Laboratories Ltd., ON. Canada). The explants were divided into eight treatment groups: control (culture medium), FGF-2, TGF-β2 and TGF-β2/FGF-2 (simultaneous treatment with both TGF-β2 and FGF-2) under normal culture conditions and heat shocked control (culture medium), FGF-2, TGF-β2, and TGF-β2/FGF-2. The culture media was replaced 24 hours after dissection and replaced with 3.5 ml of the appropriate treatment media. The normal conditioned groups (control,

FGF-2, TGF-β2, and TGF-β2/FGF-2) were placed back into the incubator. The heat shocked explants were heat shocked at 45°C for 1 hour and stabilized 37 °C with 4.0% $CO_2$ for 3 hours prior to treatment with the respective media, as mentioned above. The explants were cultured for 4 days in the treatment media and then prepared for histological, immunohistochemical, Western blot and TUNEL analysis. A total of 440 rat epithelial explants were used for this study. All preparations were performed directly onto the culture dish where the whole epithelial explants remain attached and intact.

*3.2.2 Histology and immunohistochemistry staining*

A total of 128 rat epithelial explants were used for histological and immunohistochemical analysis). Four explants from each of the eight treatment groups were prepared for each of the four different staining procedures. The whole-mount of lens epithelial explants was used for either Hematoxylin and Eosin (H&E), or immunohistochemistry staining (F-actin, α-SMA and E-cadherin). The lens epithelial explants were fixed in 4% paraformaldahyde for 30 minutes, then permeablized with 0.1% TritonX-100 in 1X phosphate buffered saline solution (PBS) for 15 minutes at room temperature. H&E staining procedures were performed on the epithelial explants and after staining, the sides of the culture dish were removed and a round glass coverslip was applied. The epithelial explants were visualized with a Leica microscope and images were captured using a high-resolution camera and associated software (OpenLab; Quorum Technologies Inc., CA. USA). Images were reproduced for publication using Adobe Photoshop 9.0.1 (Adobe Systems Inc., CA. USA).

For α-SMA and E-cadherin immunoflourescence localization, the whole-mount lens epithelial explants were incubated with 5% normal goat serum for 30 minutes at room temperature.  The explants were then incubated overnight at 4 °C, either with mouse anti-α-SMA monoclonal antibody (1:400; Sigma-Aldrich Inc., MO. USA) or mouse anti-E-cadherin antibody (1:100; BD Biosciences, ON. Canada).  An Alexa Fluor 488 conjugated goat anti-mouse secondary antibody (1:100; Invitrogen Inc., ON. Canada) was used for detection of the bound primary antibodies.  All whole-mount explants were mounted in Vectashield mounting medium with 4',6-Diaminodino-2-Phenylindol (DAPI, Vector Laboratories Inc., CA. USA) to visualize the nuclei.  A round glass coverslip was applied and the sides of the culture dish were removed.  A Zeiss scanning laser confocal microscope (LSM 510 META) equipped with an Argon-Krypton laser was use to examine the immunoreactivity of the epithelial explants.  Cross-sections of the explants were visualized with confocal z-stack using an optical slice thickness of 0.3 μm, the images were captured using the Zeiss LSM software.  Adobe Photoshop 9.0.1 was also used to reproduce images for publication.

For F-actin localization, whole-mount lens epithelial explants were incubated with 5% normal goat serum for 30 minutes at room temperature.  The explants were then incubated with Alexa 546 phalloidin (1:50; Invitrogen Inc., ON. Canada) for 30 minutes at room temperature.  The epithelial explants were mounted in Vectashield mounting medium with DAPI to visualize the nuclei.  A round glass coverslip was applied and the

sides of the culture dish were removed. Laser scanning confocal microscopy was performed as described above.

*3.2.3 TUNEL assay*

TUNEL (terminal deoxynucleotidyl transferase mediated dUTP nick end labeling) labeling was used to examine cell death in three lens epithelial explants of each treatment group. A total of 24 explants were used. The whole-mount epithelial explants were fixed and permeablized as described above. The ApopTag plus flourescein *in-situ* apoptosis detection kit (Chemicon International Inc., CA. USA) was used to detect apoptotic nuclei and the TUNEL procedure was carried out in accordance with the manufacturer's instructions. A positive control was prepared by treating a sample with DNaseI prior to TUNEL staining. All sections were mounted in Vectashield mounting medium with DAPI and photographed using the laser scanning confocal microscope. For quantitative analysis, the percentage of TUNEL-positive cells among 150 lens epithelial cells in three fields per section was determined at 250-fold magnification.

*3.2.4 Western blot analysis*

Thirty-six epithelial explants from each of the eight treatment groups were collected and pooled (in groups of four explants) for Western blot analysis of $\alpha$-SMA, E-cadherin, $\alpha$A-crystallin, $\alpha$B-crystallin, Hsp70 and Hsp90 protein expression (total n=288). The lens epithelial explants were homogenized in Triton-X100 lysis buffer

containing protease inhibitor cocktail (Roche Applied Science, IN. USA). Total protein concentration was determined by the Bradford protein assay.[53] Equal amounts of total protein from each group of explants were electrophoresed on 10% SDS polyacrylamide gel. In addition, a heat shocked HeLa cell lysate (Stressgen Bioreagents, MI. USA) was loaded and used as a positive control for heat shocked proteins. The proteins were electro-transferred onto a nitrocellulose membrane (Pall Corporation, NY. USA). Membranes were blocked with 5% skimmed milk powder in Tris-buffered saline (50mM Tris base, NaCl pH 8.5) + 0.1% Tween-20 and then incubated overnight at 4°C with either a mouse anti-α-SMA monoclonal antibody (1:1000), rabbit anti-αA-crystallin polyclonal antibody (1:1000) or rabbit anti-αB-crystallin polyclonal antibody (1:1000). Following this incubation, membranes were probed with the appropriate HRP-conjugated anti-rabbit or anti-mouse secondary antibodies (1:5000; Amersham Biosciences, NJ. USA) and ECL detection reagents (Amersham Biosciences, NJ. USA). The Western blots were visualized by x-ray film exposure. The membranes were stripped and reprobed with either a mouse anti-E-cadherin antibody (1:2500), rabbit anti-Hsp70 polyclonal antibody (1:2000), or rabbit anti-Hsp90 polyclonal antibody (1:2000) followed by the appropriate secondary detection as mentioned above. The αA-crystallin, αB-crystallin, Hsp70, and Hsp90 antibodies were purchased from Stressgen Bioreagents (MI. USA). The membranes were stripped a second time and reprobed with a mouse anti-β-actin antibody (1:1000; Cedarlane Laboratories Ltd., ON Canada) as a loading control. The secondary detection for β-actin followed the same procedures as mentioned above. The bands were quantitated by densitometry and normalized with β-actin using ImageJ software (software available at http://rsb.info.nih.gov/ij/download.html; developed by

Wayne Rasband, National Institutes of Health, Bethesda, MD).  Protein expression is expressed as a percentage of normal control ± standard error of the mean (%±SEM).

*3.2.5 Statistical analysis*

The analysis of variance (ANOVA; SPSS™ 11.0 statistical software) was used to assess the treatment effects on protein expression and apoptotic cell death of rat lens epithelial explants.  The Tukey's post-hoc test was use to determine the significance between treatment groups.  A p-value ≤ 0.05 was considered to be significant with a 95% confidence interval.

## 3.3 Results

*3.3.1 Histological and immunohistochemical analysis of rat lens epithelial explants*

Histological examination of cultured lens epithelial explants from 7-10 day old rats treated with TGF-β2 and TGF-β2/FGF-2 under both normal and heat shocked conditions revealed distinct evidence of EMT including extensive multi-layering of cells forming plaques on the anterior lens capsule (Fig. 1 and 2 E-H). In contrast to the plaques formed on the TGF-β2/FGF-2 treated explants (Fig. 2 G, H), which are typically large and diffuse, the plaques in the TGF-β2 explants (Fig. 2 E, F) were substantially smaller. Capsular wrinkling as well as fibroblastic and spindle shaped cell formation also occurred in the TGF-β treated explants (not shown). The control and FGF-2 epithelial explants demonstrated a confluent monolayer of LECs with a cobblestone pattern and did not form multilayer plaques (Fig. 2 A-D). However the FGF-2 treated explants exhibited a more rounded cellular appearance and greater cell density per area than the controls. The cellular morphology of heat shocked groups (Fig. 2 B, D, F, H) did not differ significantly from the normal condition groups for each of the four conditions (Fig. 2 A, C, E, G). Heat shock treatment did not inhibit TGF-β induced plaque formation. But the plaques formed on the heat shocked TGF-β2/FGF-2 treated explants were less severe and spanned a smaller area of the explants when compared to the non-heat shocked TGF-β2/FGF-2 plaques.

98

The expression of F-actin and α-SMA were next examined since these are commonly used as markers for TGF-β-induced EMT (Figs. 3 and 4).[54] The control explants (Fig 3 A, B) demonstrate normal polygonal arrays of F-actin stress fibres underlying the apical location of the LEC membranes.[55] Interestingly, treatment with FGF-2 significantly reduced the F-actin immunoreactivity in the LEC cytoplasm and the F-actin expression was mainly confined to the cell borders. The TGF-β2 (Fig. 3 E, F) treated explants demonstrated a slight increase in F-actin immunoreactivity and stress fibre extension when compared to the controls (Fig. 3 A, B). Whereas the simultaneous treatment of epithelial explants with TGF-β2 and FGF-2 (Fig. 3 G, H) induced the formation of substantially longer peripheral extension of F-actin filaments in the plaques. There was no significant difference in F-actin immunoreactivity between the normal cultured explants (A, C, E and G) and heat shocked explants (B, D, F and H). The increase in stress fibre formation and reorganization in the lens epithelial explants demonstrates the occurrence of TGF-β-induced EMT in the LECs.

Expression of α-SMA was also observed in the multilayer plaques of the TGF-β2 and TGF-β2/FGF-2 lens epithelial explants, whereas no α-SMA expression was detected in the FGF-2 treated explants (Fig. 4). The control explants showed diffuse staining of α-SMA in the cytoplasm of some LECs (Fig. 4. A, B). The TGF-β2 treated explants (Fig 4. E, F) demonstrated greater α-SMA immunoreactivity and more filamentous expression of α-SMA in the apical portion of the cells. The simultaneous treatment of epithelial explants with TGF-β2 and FGF-2 (Fig. 4 G, H) induced the greatest α-SMA immunoreactivity, with the formation of substantially longer and extended α-SMA

99

filaments in the plaques.   Interestingly, the heat shocked epithelial explants (Fig. 4 B, F and H) show significantly lower α-SMA immunoreactivity than the same treatment groups under normal culture conditions (Fig. 4 A, E and G respectively).  Fewer cells from the heat shocked control explants show α-SMA staining when compared to the non-heat shocked control explants.  The heat shocked TGF-β2 and TGF-β2/FGF-2 explants show less filamentous α-SMA staining than the non-heat shocked TGF-β2 and TGF-β2/FGF-2 explants.   The results from Western blot analysis of α-SMA (42 kDa) expression in lens epithelial explants (Fig. 5, Table 1) confirmed the immunostaining results.  Statistical analysis (ANOVA: $p \leq 0.05$) shows that there is a significant treatment effect.   The heat shocked control (lane 2, 55.7±5.6%) epithelial explants show significantly lower levels α-SMA protein expression compared to the normal control (lane 1, 100%) epithelial explants, while the FGF-2 treated explants (normal (lane 3, 6.7±3.5%) and heat shocked (lane 4, 1.4±0.7%)) show negligible amounts of α-SMA. The treatment with TGF-β2 (normal (lane 5, 255.2±3.3%), heat shocked (lane 6, 170.0±.8.4%)) and TGF-β2/FGF-2 (normal (lane 7, 363.0±4.8%), heat shocked (lane 8, 293.4±.2.3%)) demonstrated a significant increase in α-SMA protein expression, with the greatest increase of α-SMA expression in the TGF-β2/FGF-2 explants.  In addition, the α-SMA expression of heat shock treated TGF-β2 and TGF-β2/FGF-2 explants are significantly lower than the same treatment groups under normal cultured conditions.  β-actin (42 kDa) protein, used as a loading control, showed equal levels of expression in all samples examined.  Therefore in contrast to F-actin expression, α-SMA expression is reduced in the heat shocked TGF-β groups.

E-cadherin is an epithelial marker which is localized at the adherence junctions and the disassembly of E-cadherin is associated with TGF-β-induced EMT.[56] Both the control (Fig. 6 A, B) and FGF-2 (Fig. 6 C, D) treated explants show normal E-cadherin expression at the cell-cell junction locations. The TGF-β2 (Fig. 6 E, F) treated explants demonstrated lower E-cadherin immunoreactivity and a loss of E-cadherin in some LECs when compared to the controls. The simultaneous treatment of epithelial explants with TGF-β2 and FGF-2 (Fig. 6 G, H) induced considerable loss of E-cadherin organization and diffused staining. Heat shock treatment did not affect the E-cadherin expression levels in both the control and FGF-2 epithelial explants. However, heat shock TGF-β2 and TGF-β2/FGF-2 (Fig. 6 F, H) demonstrated higher immunoreactivity and organization of E-cadherin than normal TGF-β2 and TGF-β2/FGF-2 (Fig. 6 E, G) explants respectively. Results from Western blot analysis of E-cadherin (120 kDa) expression in lens epithelial explants (Fig. 7, Table 1) confirmed the immunostaining results. Statistical analysis (ANOVA: $p \leq 0.05$) showed that there is a significant treatment effect. Both the normal control (lane 1, 100%) and heat shocked control (lane 2, 100.3±1.8%) explants expressed similar levels of E-cadherin protein. FGF-2 treatment (normal (lane 3, 119.5±8.5%) and heat shocked (lane 4, 126.6±5.9%)) induced significant increase of E-cadherin expression when compared to the normal control epithelial explants. Both treatment with TGF-β2 (normal (lane 5, 70.0±1.8%), heat shocked (lane 6, 86.7±.3.1%)) and TGF-β2/FGF-2 (normal (lane 7, 45.6±2.6%), heat shocked (lane 8, 72.6±.3.4%)) demonstrated a significant decrease in E-cadherin protein expression, with the greatest loss of E-cadherin expression in the normal TGF-β2/FGF-2 explants. However, the E-cadherin expression of heat shocked TGF-β2 and TGF-β2/FGF-2 explants were

101

significantly higher than the same treatment groups under normal culture conditions. β-actin protein expression showed that equal levels of total protein from each sample were loaded. The decrease in E-cadherin expression coincided with increased expression of F-actin and α-SMA in TGF-β treated explants. Therefore these results show that TGF-β induced EMT in the rat LECs. Although heat shock treatment did not inhibit TGF-β-induced multilayer plaque formation, it reduced the severity of EMT, as shown in the α-SMA and E-cadherin results.

*3.3.2 Apoptotic cell death in rat lens epithelial explants*

Since TGF-β induced multilayer plaque formation in lens epithelial explants, and apoptosis has been reported to occur in TGF-β-induced anterior subcapsular cataracts (ASC) [57, 58], we utilized TUNEL labeling to examine the level of apoptosis in the different experimental groups (Fig. 8). The photographs in figure 8 represent the TUNEL staining in a normal control (A) and TGF-β2/FGF-2 (B) explants. Both TGF-β2/FGF-2 and TGF-β2 (latter not shown) showed an increase of TUNEL-positive nuclei in the plaques when compared to the control, whereas the FGF-2 lens epithelial explants show negligible amounts of TUNEL-positive nuclei (photograph not shown). Statistical analysis (ANOVA: $p \leq 0.05$) shows that there is a significant treatment effect. The heat shocked control (2.3±0.6%) epithelial explants demonstrated less apoptotic cell death than the control (4.3±0.5%) explants under normal culture conditions, but the decrease is not significant. FGF-2 treatment (normal (1.9±0.6%) and heat shock (0.8±0.2%)) induced significant decreases in apoptotic cell death relative to the normal control

epithelial explants. The normal TGF-β2 (7.5±0.8%) and TGF-β2/FGF-2 (normal (9.6±0.6%), heat shocked (6.8±.0.5%)) explants demonstrated a significant increase in cell death. The increase of cell death in the heat shocked TGF-β2 (4.6±0.7%) explants is not significantly different from normal control explants. In addition, the heat shocked TGF-β2 and TGF-β2/FGF-2 explants demonstrated significantly lower apoptotic cell death than the same treatment groups under normal cultured conditions. Thus, TGF-β-induced apoptosis was reduced by heat shock treatment in rat lens epithelial explants.

*3.3.3 Effect of the TGF-β2 on heat shock protein expressions in rat lens epithelial explants*

As mentioned in the introduction, αA- and αB- crystallin demonstrate chaperone-like activity and belong to the small heat shock protein family. The decrease of α-crystallin chaperone activity has been attributed to the loss of lens transparency and cataract formation.[38-42] Thus, the expression levels of αA- and αB-crystallins were also investigated and the results are described in figures 9 and 10 (also see Table 1). The β-actin protein expression in both Western blot analyses showed that equal levels of total protein from each sample was loaded. The results of figure 9 show that heat shock treatment of control (lane 2, 48.9±1.3%), TGF-β2 (lane 6, 46.8±5.0%) and TGF-β2/FGF-2 (lane 8, 35.2±4.5%) epithelial explants significantly (ANOVA: $p \leq 0.05$) lower the levels of αA-crystallin (20 kDa) protein expression when compared to the normal control (lane 1, 100%) explants. There is also a decrease of αA-crystallin expression in normal

103

TGF-β2 (lane 5, 87.1±2.3%) and TGF-β2/FGF-2 (lane 7, 94.1±2.3%), but the decrease is not significant. In addition, the heat shock treated TGF-β2 and TGF-β2/FGF-2 explants demonstrated significantly lower αA-crystallin expression than the same treatment groups under normal culture conditions. In contrast, FGF-2 (normal (lane 3, 124.0±1.2%), heat shock (lane 4, 114.8±.4.3%)) treated explants demonstrate a significant increase of αA-crystallin protein expression when compared to normal control explants.

Unlike αA-crystallin, Western blot results of αB-crystallin protein expression of the different treatment groups did not show a significant treatment effect (ANOVA: $p \geq 0.05$). Results shown in figure 10 show that the control (lane 1, 100%), FGF-2 (lane 3, 112.0±2.3%), TGF-β2 (lane 5, 101.6±4.6%) and TGF-β2/FGF-2 (lane 7, 106.5±1.6%) explants under normal culture conditions are similar to the heat shocked explants: control (lane 2, 109.0±4.0%), FGF-2 (lane 4, 111.5±2.3%), TGF-β2 (lane 6, 99.5±3.5%) and TGF-β2/FGF-2 (lane 8, 101.3±2.7%).

Western blot analysis of Hsp70 (70 kDa, Fig. 11, Table 1) shows that there is a significant treatment effect (ANOVA: $p \leq 0.05$) between the different groups. A heat shocked HeLa cell lysate was used as a positive control. The β-actin protein expression also showed that equal levels of total protein were loaded for each sample. Heat shock treatment did not affect Hsp70 levels in the control epithelial explants (normal lane1, 100% and heat shocked lane 2, 99.6±2.7%). While Hsp70 expression significantly decreased in the normal FGF-2 (lane 3, 73.5±4.7%) and heat shocked FGF-2 (lane 4,

54.6±3.7%).  The heat shocked TGF-β2 (lane 6, 83.5±1.6%) treated explants also show significant decrease in Hsp70 expression when compared to the control explants.  In contrast, the normal TGF-β2 (lane 5, 118.0±3.3%) and TGF-β2/FGF-2 (normal (lane 7, 211.6±4.5%), heat shocked (lane 8, 124.7±.4.0%)) explants show significant increase of Hsp70 protein expression, with the greatest increase in the TGF-β2/FGF-2 explants.  In addition, the Hsp70 expression of heat shocked FGF-2, TGF-β2 and TGF-β2/FGF-2 explants are significantly lower than the same respective treatment groups under normal culture conditions.

The results from the Hsp90 protein analysis (90 kDa, Fig. 12, Table 1) also show significant treatment effect (ANOVA: $p \leq 0.05$).  As mentioned above, the HeLa cell lysate was used as a positive control.  The β-actin protein expression also showed that equal levels of total protein were loaded from each sample.  Heat shocked treatment significantly decreased the Hsp90 expression levels in the control (lane 2, 55.6±1.1%) and TGF-β2 (lane 6, 73.6±6.0%) epithelial explants when compared to normal control (lane 1, 100%) epithelial explants.  Although there is also a decrease of Hsp90 expression in the normal TGF-β2 (lane 5, 93.9±2.5%), it is not significant.  The FGF-2 (normal (lane 3, 172.6±2.5%), heat shocked (lane 4, 129.0±.3.3%)) and TGF-β2/FGF-2 (normal (lane 7, 187.0.±5.3%), heat shocked (lane 8, 157.0±5.3%)) explants show significant increase of Hsp90 protein expression, with the greatest increase in the TGF-β2/FGF-2 explants. Heat shock treatment also significantly decreased the Hsp90 expression levels of FGF-2, TGF-β2 and TGF-β2/FGF-2 explants when compared to the same treatment groups under normal culture conditions.   Interestingly, the heat shocked TGF-β (TGF-β2 and TGF-

β2/FGF-2) explants demonstrated lower levels of αA-crystallin, Hsp70 and Hsp90 than the TGF-β explants under normal culture conditions. This may be an indication that heat shock treatment reduced TGF-β-induced stress conditions in the epithelial explants. Thus, there is less up-regulation of molecular chaperone activities in the heat shocked TGF-β explants when compared to the TGF-β explants under normal conditions.
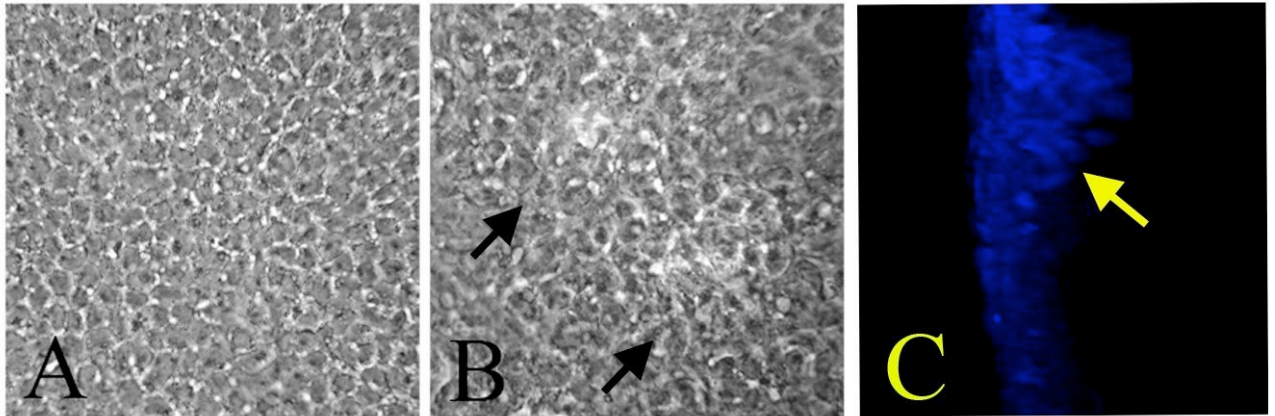
Figure 1. Cultured rat lens epithelial explants

The phase contrast photographs represent a control (A) and a TGF-β2/FGF-2 treated (B) lens epithelial explant.  Panel C shows a confocal z-stack section (a y-axis projection) of a TGF-β2/FGF-2 treated lens epithelial explant.  The control rat explant demonstrates a regular monolayer of lens epithelial cells, while the TGF-β2/FGF-2 (B and C) treated explants formed spindle shaped cells and mutilayer plaques (arrows).
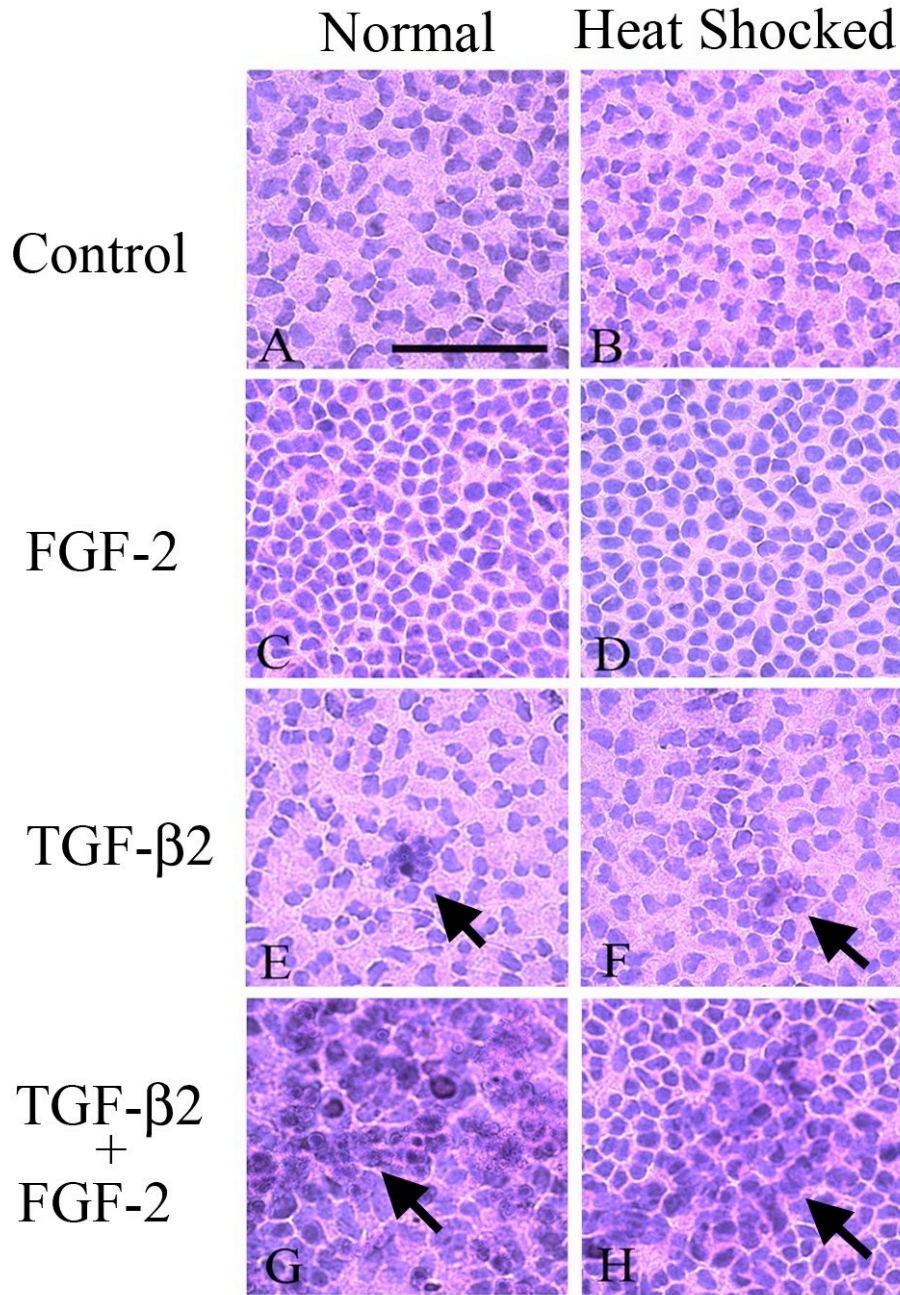
Figure 2. Histological analysis of rat lens epithelial explants

Control (A and B), FGF-2 (C and D), TGF-β2 (E and F) and TGF-β2/FGF-2 (G and H)

lens epithelial explants under normal conditions (A, C, E and G) and after heat shocked

(B, D, F and H) treatment are shown.   N=4 for each treatment group.   Control epithelial

cells (A and B) show normal morphology. FGF-2 treated explants (C and D) have rounder cells and also show greater cell density then the control explants. Treatment with TGF-β2 (E-H) induced formation of multilayer plaques (arrows). The simultaneous treatment of epithelial explants with TGF-β2 and FGF-2 (G and H) induced the formation of considerably larger and more diffused plaques than TGF-β2 (E and F) alone. Both the heat shocked and normal cultured explants show similar phenotype for each of the four conditions. However, the plaques formed on the heat shocked TGF-β2/FGF-2 explants are less severe and less expansive than the non-heat shocked TGF-β2/FGF-2 plaques. The scale bar represents 100 μm.
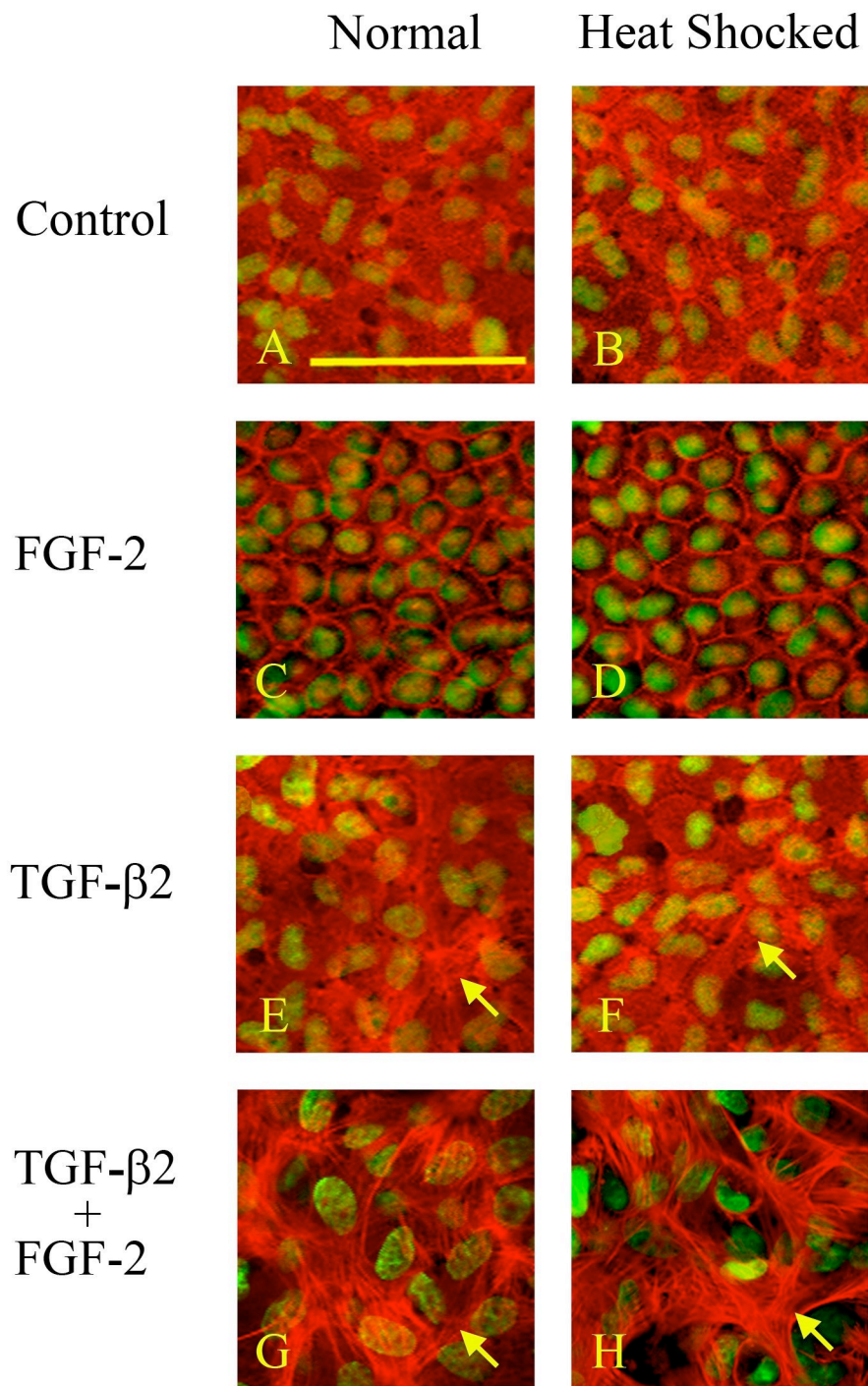
Figure 3. Immunohistochemical analysis of F-actin expression

F-actin was stained with Alexa 546 phalloidin and analyzed by confocal microscopy.

Control (A and B), FGF-2 (C and D), TGF-β2 (E and F) and TGF-β2/FGF-2 (G and H)

lens epithelial explants under normal conditions (A, C, E and G) and after heat shock (B, D, F and H) treatment are shown. N=4 for each treatment group.  Control epithelial cells (A and B) show normal expression of F-actin, while FGF-2 treated explants (C and D) show a significant decrease of F-actin immunoreactivity in the cytoplasm.  FGF-2 treated explants show F-actin staining mainly around the cell borders.  The TGF-β2 (E and F) treated explants demonstrate a slight increase (arrows) of F-actin immunoreactivity and stress fibre extension when compared to the controls (A and B).   Whereas the simultaneous treatment of epithelial explants with TGF-β2 and FGF-2 (G and H) induced the formation of substantially longer peripheral extensions of F-actin filaments in the plaques (arrows).    There is no significant difference of F-actin immunoreactivity between the normal cultured explants (A, C, E and G) and heat shocked explants (B, D, F and H) for each of the four conditions.  The scale bar represents 50 μm.
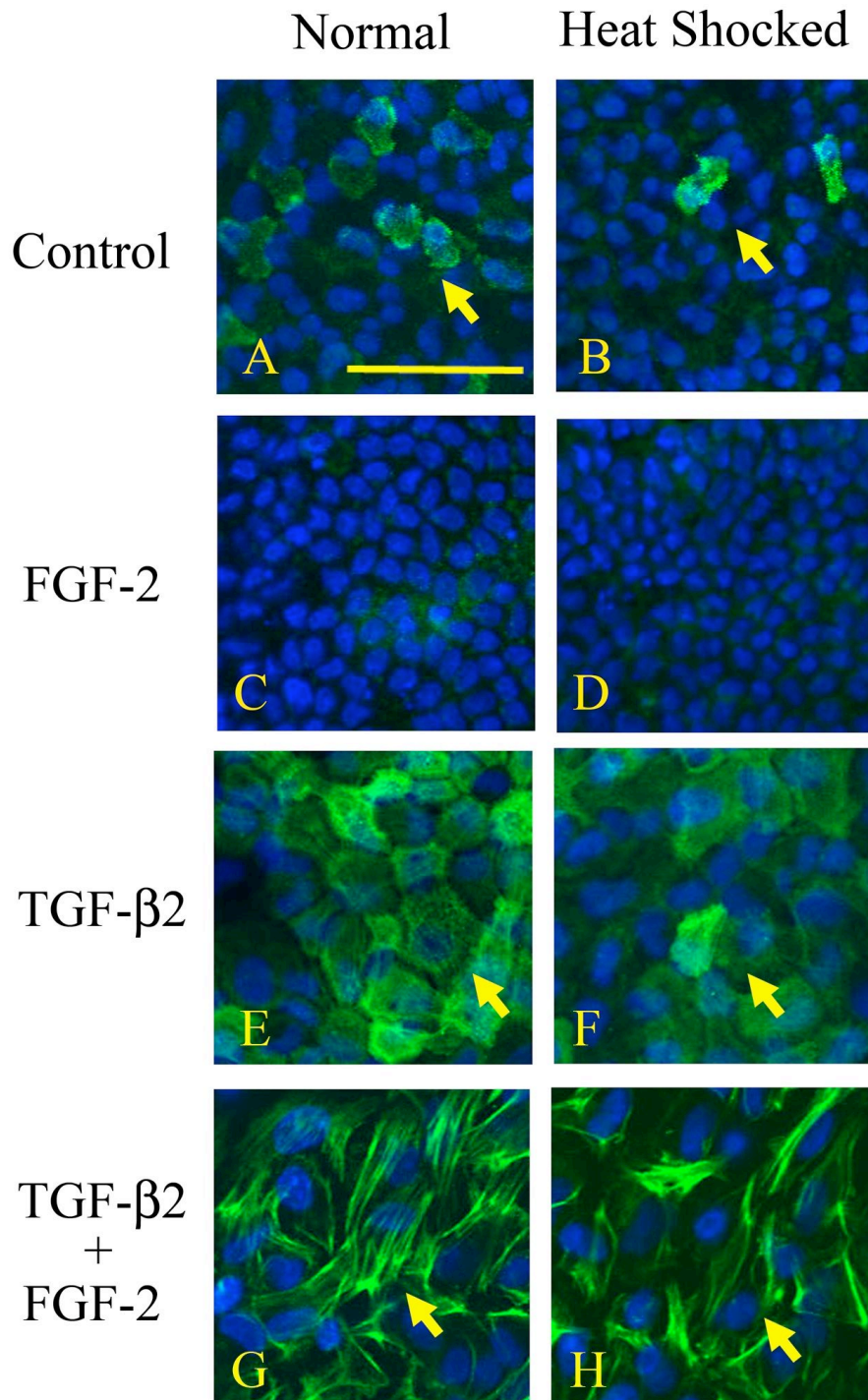
Figure 4. Immunohistochemical analysis of $\alpha$-Smooth muscle actin expression

The analysis of α-SMA immunoreactivity (Alexa fluor 488) using confocal microscopy. Control (A and B), FGF-2 (C and D), TGF-β2 (E and F) and TGF-β2/FGF-2 (G and H) lens epithelial explants under normal conditions (A, C, E and G) and after heat shock (B, D, F and H) treatment are shown. N=4 for each treatment group. Some control epithelial cells (A and B) show diffuse staining of α-SMA in the cytoplasm in a few cells, while FGF-2 treated explants (C and D) show negligible α-SMA immunoreactivity. The TGF-β2 (E and F (arrows)) treated explants demonstrate greater α-SMA immunoreactivity and more filamentous expression of α-SMA in the cell cytoplasm when compare to the controls (A and B). The simultaneous treatment of epithelial explants with TGF-β2 and FGF-2 (G and H (arrows)) induced the greatest α-SMA immunoreactivity with the formation of substantially longer and extended α-SMA filaments in the plaques. The heat shocked epithelial explants (B, F and H) show considerably lower α-SMA immunoreactivity than the same treatment groups under normal cultured conditions (A, E and G respectively). The scale bar represents 50 μm.

Figure 5. α-Smooth muscle actin protein expression

A total of twelve lens epithelial explants from each of the eight treatment groups were used for Western blot analysis of α-SMA (42 kDa) protein expression. Control (lanes 1 and 2), FGF-2 (lanes 3 and 4), TGF-β2 (lanes 5 and 6) and TGF-β2/FGF-2 (lanes 7 and 8) lens epithelial explants under normal conditions (lanes 1, 3, 5 and 7) and after heat shock (lanes 2, 4, 6 and 8) treatment are shown. β-actin (42 kDa) protein expression serves as an internal control and shows that equal amounts of total protein were loaded in all lanes.

The bar graph represents the α-SMA protein expression (percent of normal control, % ± SEM) for control, FGF-2, TGF-β2 and TGF-β2/FGF-2 treated lens epithelial explant extracts from normal culture and heat shocked conditions.  Statistical analysis (ANOVA: $p \leq 0.05$) shows that there is a significant treatment effect. [+]The heat shocked control (55.7±5.6%) and FGF-2 (normal (6.7±3.5%) and heat shocked (1.4±0.7%)) epithelial explants show significantly lower levels of α-SMA protein expression compared to the normal control (100%) epithelial explants.  [•]The treatment with TGF-β2 (normal (255.2±3.3%), heat shocked (170.0±.8.4%)) and TGF-β2/FGF-2 (normal (363.0±4.8%), heat shocked (293.4±.2.3%)) demonstrate a significant increase of α-SMA protein expression, with the greatest increase of α-SMA expression in the TGF-β2/FGF-2 explants.  [*]In addition, the α-SMA expression of heat shocked TGF-β2 and TGF-β2/FGF-2 explants are significantly lower than the same treatment groups under normal cultured conditions.
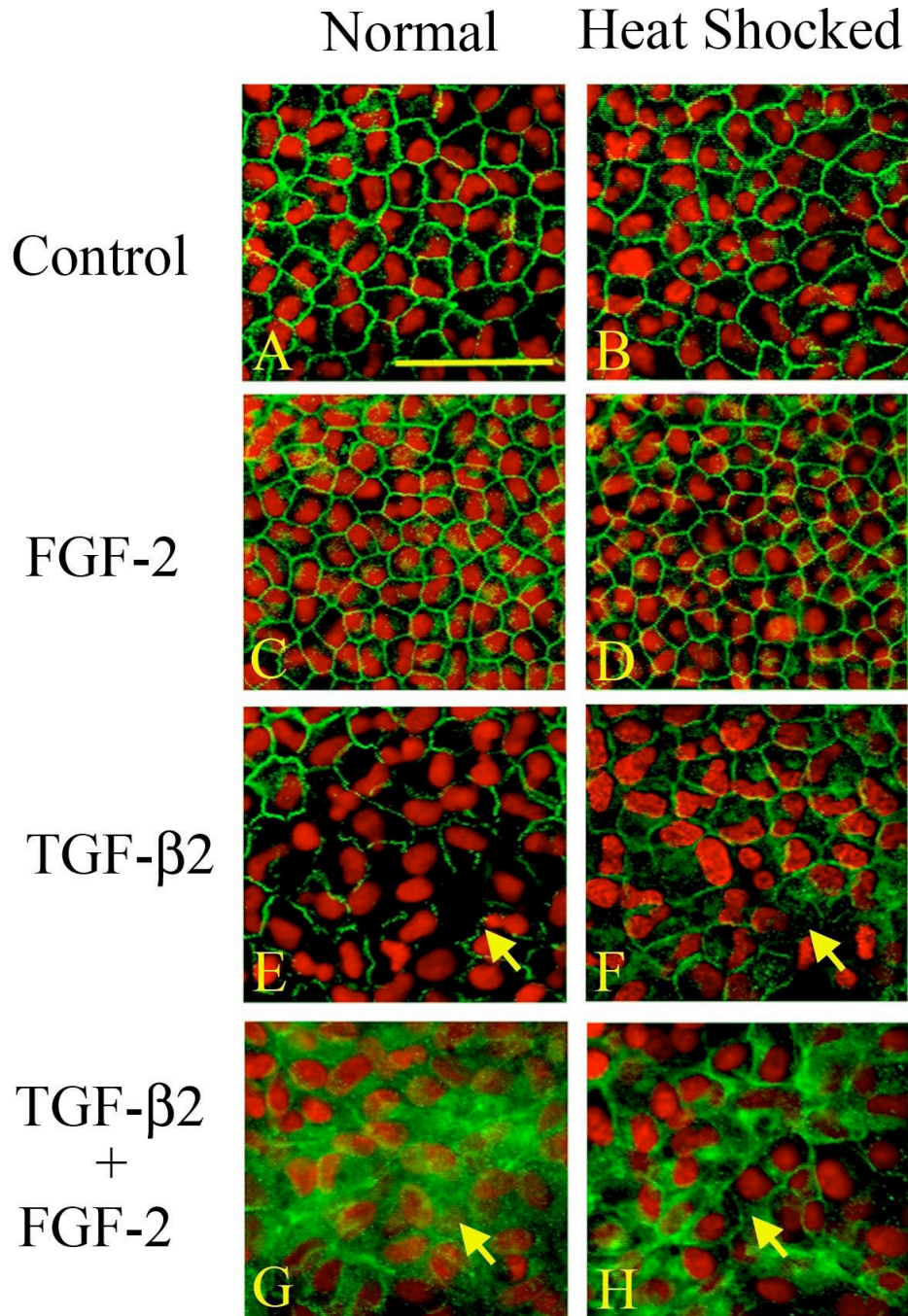
Figure 6. Immunohistochemical analysis of E-cadherin expression

The analysis of E-cadherin immunoreactivity (Alexa fluor 488) using confocal

microscopy. Control (A and B), FGF-2 (C and D), TGF-β2 (E and F) and TGF-β2/FGF-2

(G and H) lens epithelial explants under normal conditions (A, C, E and G) and after heat

shock (B, D, F and H) treatment are shown. N=4 for each treatment group. Both the control (A and B) and FGF-2 (C and D) treated explants show normal E-cadherin expression. The TGF-β2 (E and F (arrows)) treated explants demonstrate lower E-cadherin immunoreactivity when compare to the controls. The simultaneous treatment of epithelial explants with TGF-β2 and FGF-2 (G and H) induced substantial loss of E-cadherin organization and diffused staining (arrows). Heat shock treatment did not affect the E-cadherin expression levels in both the control and FGF-2 epithelial explants. However, the heat shock TGF-β2 and TGF-β2/FGF-2 (F and H) demonstrate higher immunoreactivity and organization of E-cadherin than the normal TGF-β2 and TGF-β2/FGF-2 (E and G) explants, respectively. The scale bar represents 50 μm.
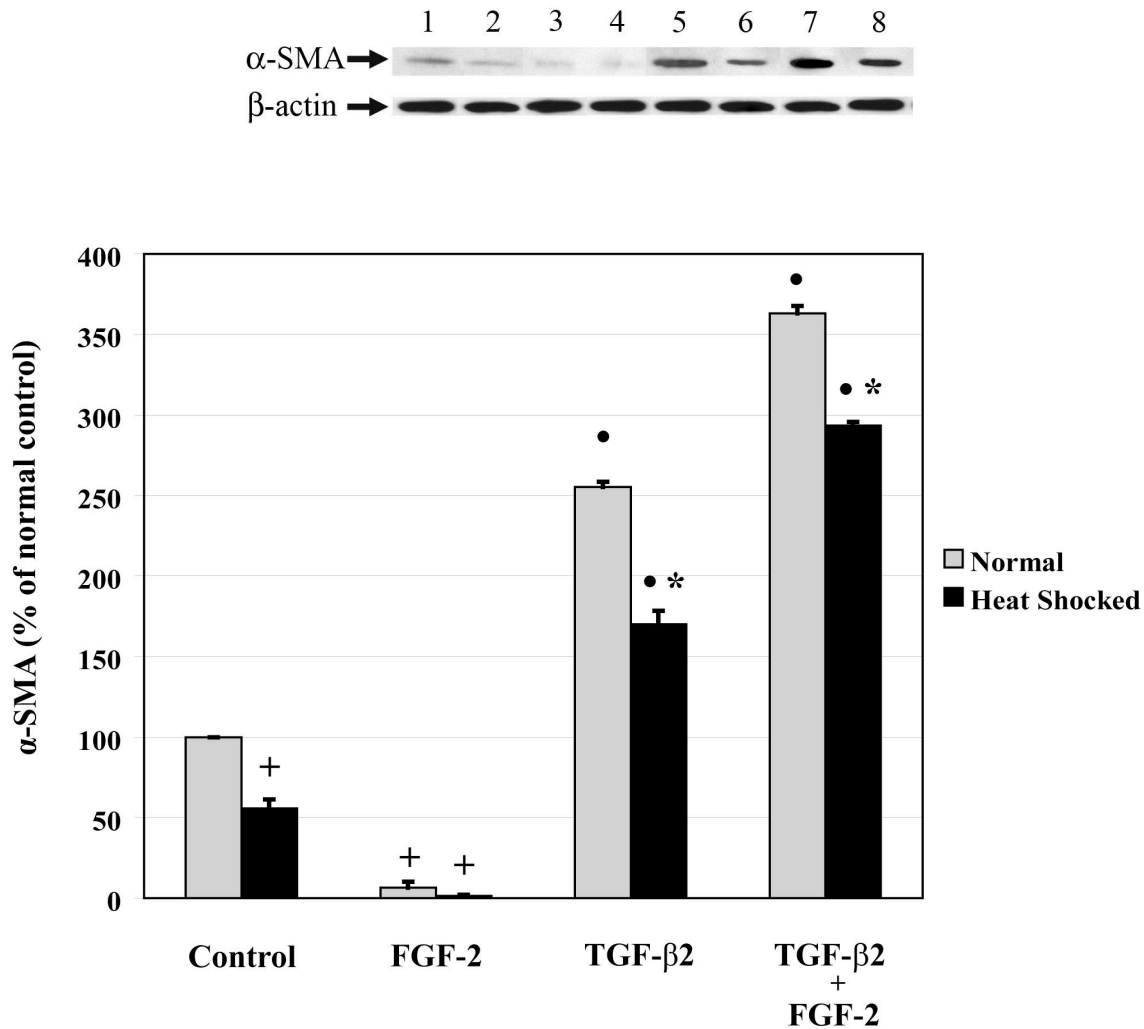
Figure 7. E-cadherin protein expression

A total of twelve lens epithelial explants from each of the eight treatment groups were used for Western blot analysis of E-cadherin protein (120 kDa) expression. Control (lanes 1 and 2), FGF-2 (lanes 3 and 4), TGF-β2 (lanes 5 and 6) and TGF-β2/FGF-2 (lanes 7 and 8) lens epithelial explants under normal conditions (lanes 1, 3, 5 and 7) and after heat shocked (lanes 2, 4, 6 and 8) treatment are shown. β-actin (42 kDa) protein expression serves as an internal control and shows that equal amounts of total protein were loaded in all lanes.

The bar graph represents the E-cadherin protein expression (percent of normal control, %

± SEM) for control, FGF-2, TGF-β2 and TGF-β2/FGF-2 treated lens epithelial explant extracts from normal culture and heat shock conditions. Statistical analysis (ANOVA: p ≤ 0.05) shows that there is a significant treatment effect. Both the normal control (100%) and heat shocked control (100.3±1.8%) explants express similar levels of E-cadherin protein. •FGF-2 treatment (normal (119.5±8.5%) and heat shocked (126.6±5.9%)) induced significant increase of E-cadherin expression when compared to the normal control epithelial explants. [+]Both treatment with TGF-β2 (normal (70.0±1.8%), heat shocked (86.7±.3.1%)) and TGF-β2/FGF-2 (normal (45.6±2.6%), heat shocked (72.6±.3.4%)) demonstrate a significant decrease of E-cadherin protein expression, with the greatest decrease of E-cadherin expression in the normal TGF-β2/FGF-2 explants. *However, the E-cadherin expression of heat shocked TGF-β2 and TGF-β2/FGF-2 explants are significantly higher than the same treatment groups under normal cultured conditions.
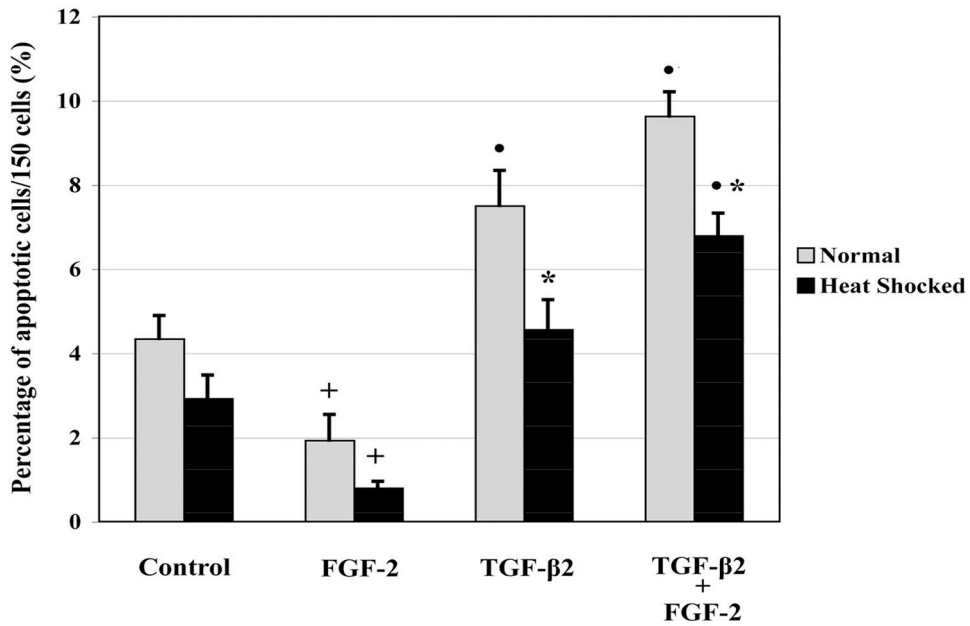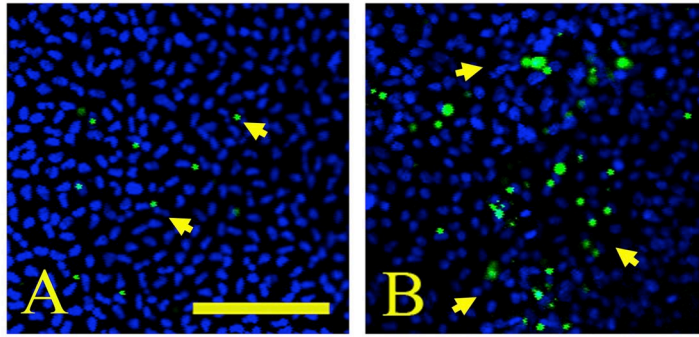
Figure 8. Apoptotic cell death in the rat lens epithelial explants

The photographs represent: a control (A) and a TGF-β2/FGF-2 (B) treated rat epithelial explant. The scale bar represents 100 μm. The TUNEL-positive nuclei are present as green nuclei. The control explant exhibited only a few TUNEL-positive nuclei. While the TGF-β1/FGF-2 treated epithelial explants show a greater number of TUNEL-positive nuclei located in the plaques (yellow arrows).

The bar graph represents the percentage of apoptotic nuclei per 150 cells for control, FGF-2, TGF-β2 and TGF-β2/FGF-2 treated lens epithelial explant extracts from normal culture and heat shock conditions. A total of three lens epithelial explants from each of the eight treatment groups were used for TUNEL analysis. Statistical analysis (ANOVA: $p \leq 0.05$) shows that there is a significant treatment effect. The heat shocked control (2.3±0.6%) epithelial explants demonstrate less apoptotic cell death than the control (4.3±0.5%) explants under normal cultured conditions, but the decrease is not significant. [+]FGF-2 treatment (normal (1.9±0.6%) and heat shocked (0.8±0.2%)) induced significant decrease of apoptotic cell death relative to the normal control epithelial explants. [•]The normal TGF-β2 (7.5±0.8%) and TGF-β2/FGF-2 (normal (9.6±0.6%), heat shocked (6.8±.0.5%)) explants demonstrate a significant increase of cell death. The increase of cell death in the heat shocked TGF-β2 (4.6±0.7%) explants is not significantly different from normal control explants. [*]In addition, the heat shocked TGF-β2 and TGF-β2/FGF-2 explants demonstrate significantly lower apoptotic cell death than the same treatment groups under normal cultured conditions.
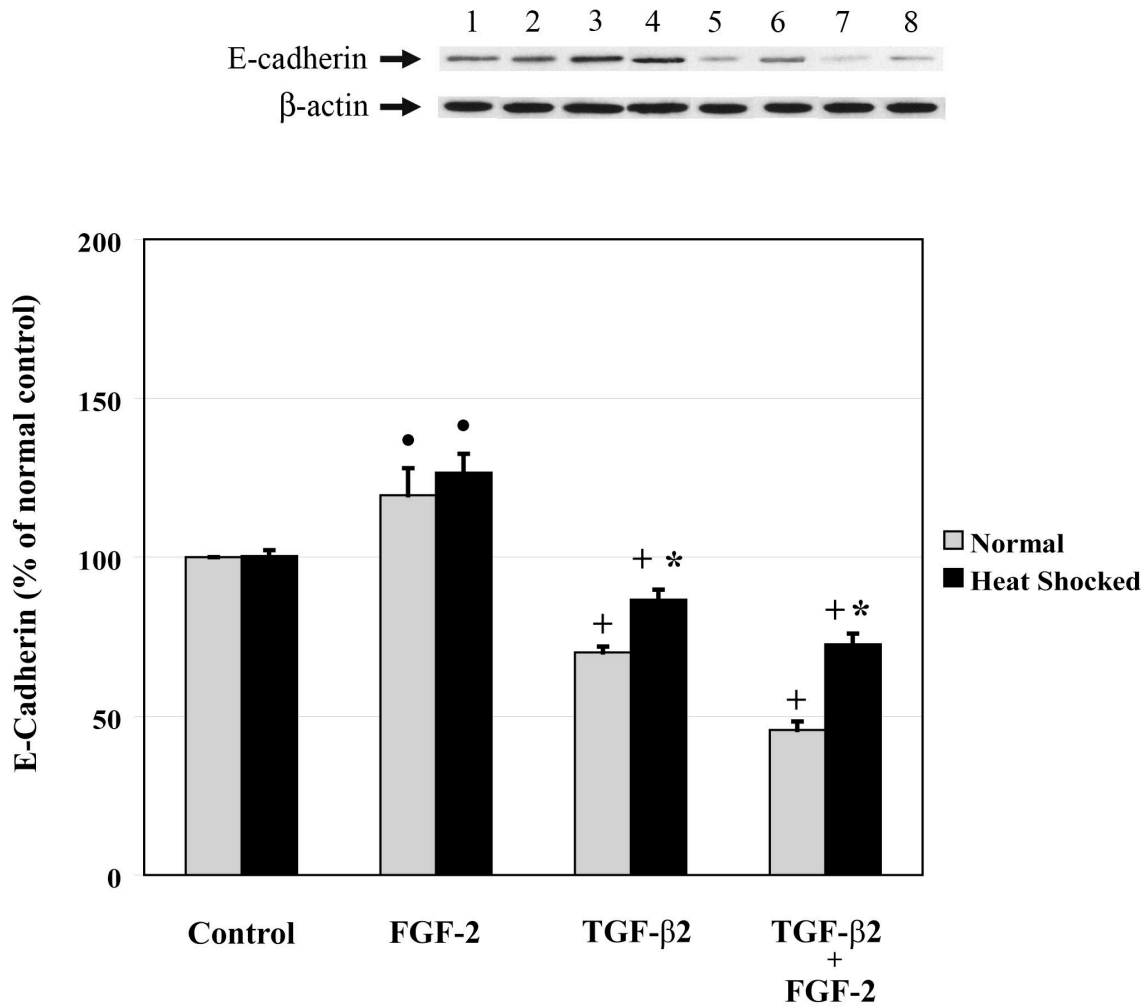
Figure 9. αA-crystallin protein expression

A total of twelve lens epithelial explants from each of the eight treatment groups were used for Western blot analysis of αA-crystallin (20 kDa) protein expression. Control (lanes 1 and 2), FGF-2 (lanes 3 and 4), TGF-β2 (lanes 5 and 6) and TGF-β2/FGF-2 (lanes 7 and 8) lens epithelial explants under normal conditions (lanes 1, 3, 5 and 7) and after heat shocked (lanes 2, 4, 6 and 8) treatment are shown. β-actin (42 kDa) protein expression serves as an internal control and show that equal amounts of total protein were loaded in all lanes.

The bar graph represents the αA-crystallin protein expression (percent of normal control,

% ± SEM) for control, FGF-2, TGF-β2 and TGF-β2/FGF-2 treated lens epithelial explant extracts from normal culture and heat shock conditions. Statistical analysis (ANOVA: p ≤ 0.05) shows that there is a significant treatment effect. [+]The heat shock treatment of control (48.9±1.3%), TGF-β2 (46.8±5.0%) and TGF-β2/FGF-2 (35.2±4.5%) epithelial explants significantly reduced the levels of αA-crystallin protein expression compared to the normal control (100%) epithelial explants. The decrease of αA-crystallin expression in normal TGF-β2 (87.1±2.3%) and TGF-β2/FGF-2 (94.1±2.3%) explants are not significant. *In addition, the heat shock treated TGF-β2 and TGF-β2/FGF-2 explants demonstrate significantly lower αA-crystallin expression than the same treatment groups under normal cultured conditions. •The FGF-2 (normal (124.0±1.2%), heat shock (114.8±.4.3%)) treated explants demonstrate a significant increase of αA-crystallin protein expression when compared to normal control explants.
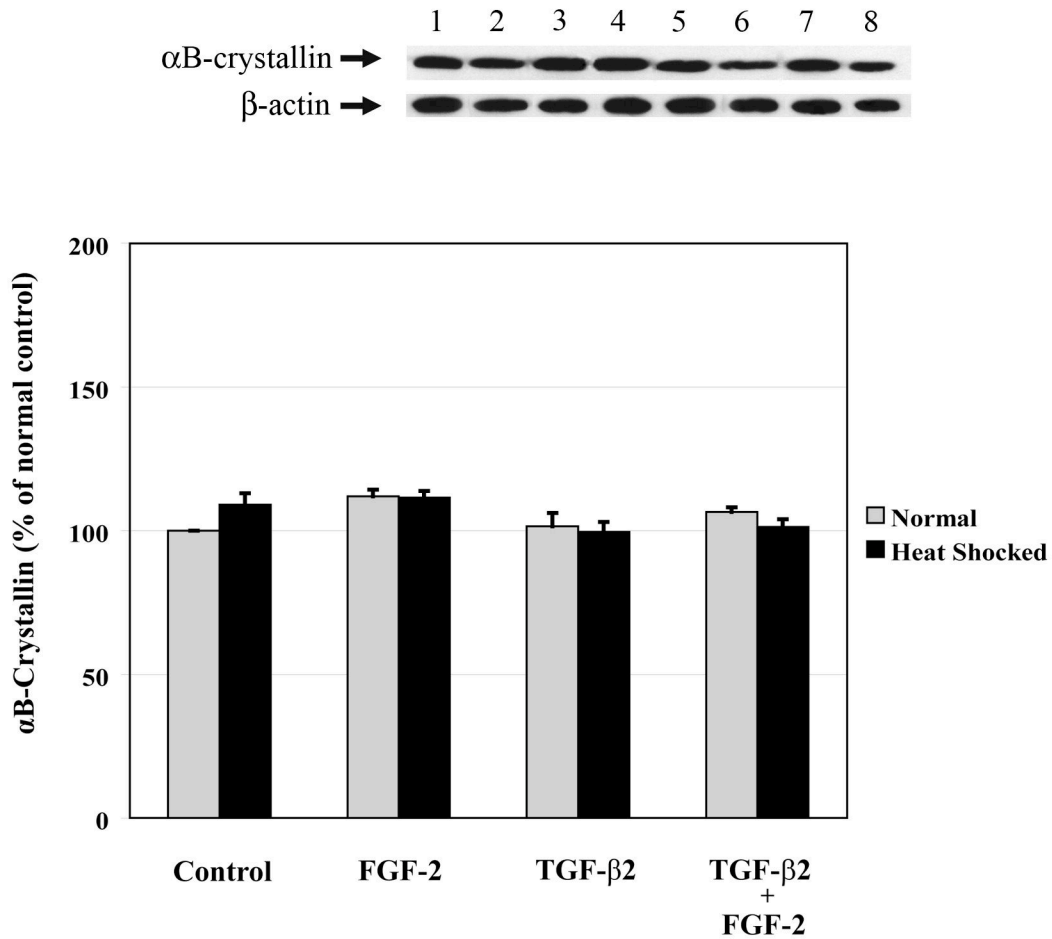
Figure 10. αB-crystallin protein expression

A total of twelve lens epithelial explants from each of the eight treatment groups were used for Western blot analysis of αB-crystallin (22 kDa) protein expression. Control (lanes 1 and 2), FGF-2 (lanes 3 and 4), TGF-β2 (lanes 5 and 6) and TGF-β2/FGF-2 (lanes 7 and 8) lens epithelial explants under normal conditions (lanes 1, 3, 5 and 7) and after heat shocked (lanes 2, 4, 6 and 8) treatment are shown. β-actin (42 kDa) protein expression serves as an internal control and shows that equal amounts of total protein were loaded in all lanes.

The bar graph represents the αB-crystallin protein expression (percent of normal control, % ± SEM) for control, FGF-2, TGF-β2 and TGF-β2/FGF-2 treated lens epithelial explant

extracts from normal culture and heat shocked conditions.  Statistical analysis (ANOVA: $p \leq 0.05$) shows that there is no significant treatment effect.  The $\alpha$B-crystallin protein expression of control (100%), FGF-2 (112.0±2.3%), TGF-$\beta$2 (101.6±4.6%) and TGF-$\beta$2/FGF-2 (106.5±1.6%) explants under normal culture conditions are similar to the heat shocked explants: control (109.0±4.0%), FGF-2 (111.5±2.3%), TGF-$\beta$2 (99.5±3.5%) and TGF-$\beta$2/FGF-2  (101.3±2.7%).
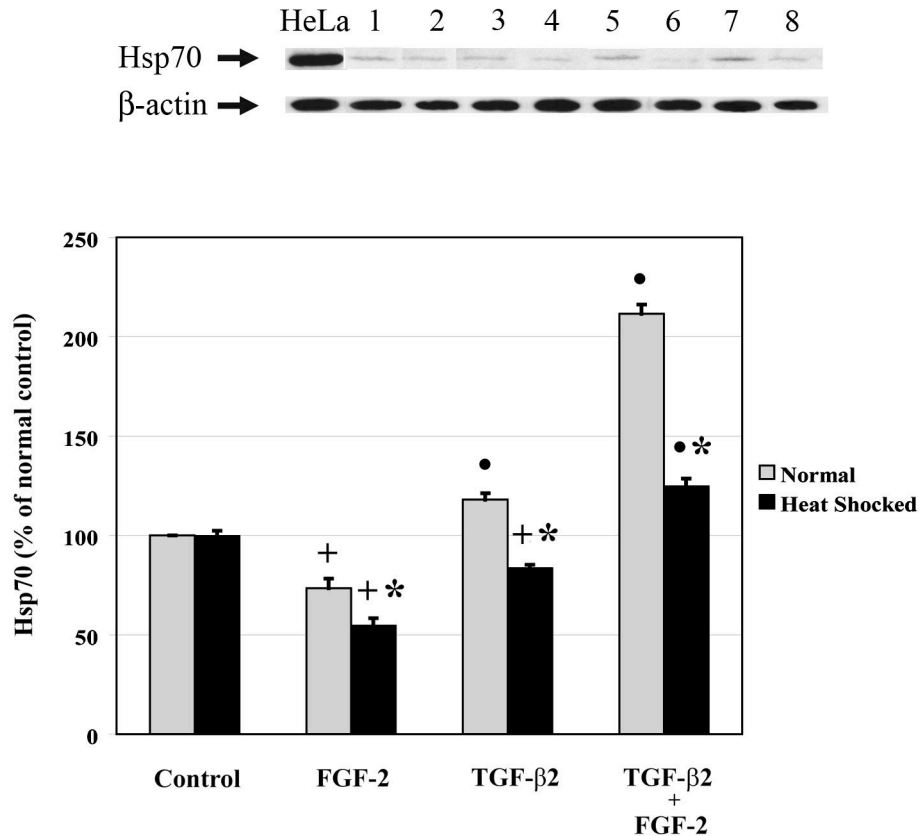
Figure 11. Hsp70 protein expression

A total of twelve lens epithelial explants from each of the eight treatment groups were used for Western blot analysis of Hsp70 (70 kDa) protein expression. HeLa cell lysate (positive control), control (lanes 1 and 2), FGF-2 (lanes 3 and 4), TGF-β2 (lanes 5 and 6) and TGF-β2/FGF-2 (lanes 7 and 8) lens epithelial explants under normal conditions (lanes 1, 3, 5 and 7) and after heat shock (lanes 2, 4, 6 and 8) treatment are shown. β-actin (42 kDa) protein expression serves as an internal control and shows that equal amounts of total protein were loaded in all lanes.

The bar graph represents the Hsp70 protein expression (percent of normal control, % ± SEM) for control, FGF-2, TGF-β2 and TGF-β2/FGF-2 treated lens epithelial explant extracts from normal culture and heat shocked conditions. Statistical analysis (ANOVA:

p ≤ 0.05) shows that there is a significant treatment effect. Both the normal control (100%) and heat shocked control (99.6±2.7%) explants express similar levels of Hsp70 protein. [+]FGF-2 (normal (73.5±4.7%) and heat shocked (54.6±3.7%)) and heat shocked TGF-β2 (83.5±1.6%) treated explants demonstrate significant lower levels of Hsp70 expression when compared to normal control epithelial explants. [•]The normal TGF-β2 (118.0±3.3%) and TGF-β2/FGF-2 (normal (211.6±4.5%), heat shocked (124.7±.4.0%)) explants show significant increases in Hsp70 protein expression, with the greatest increase in the TGF-β2/FGF-2 explants. *In addition, the Hsp70 expression of heat shocked FGF-2, TGF-β2 and TGF-β2/FGF-2 explants are significantly lower than the same treatment groups under normal cultured conditions.
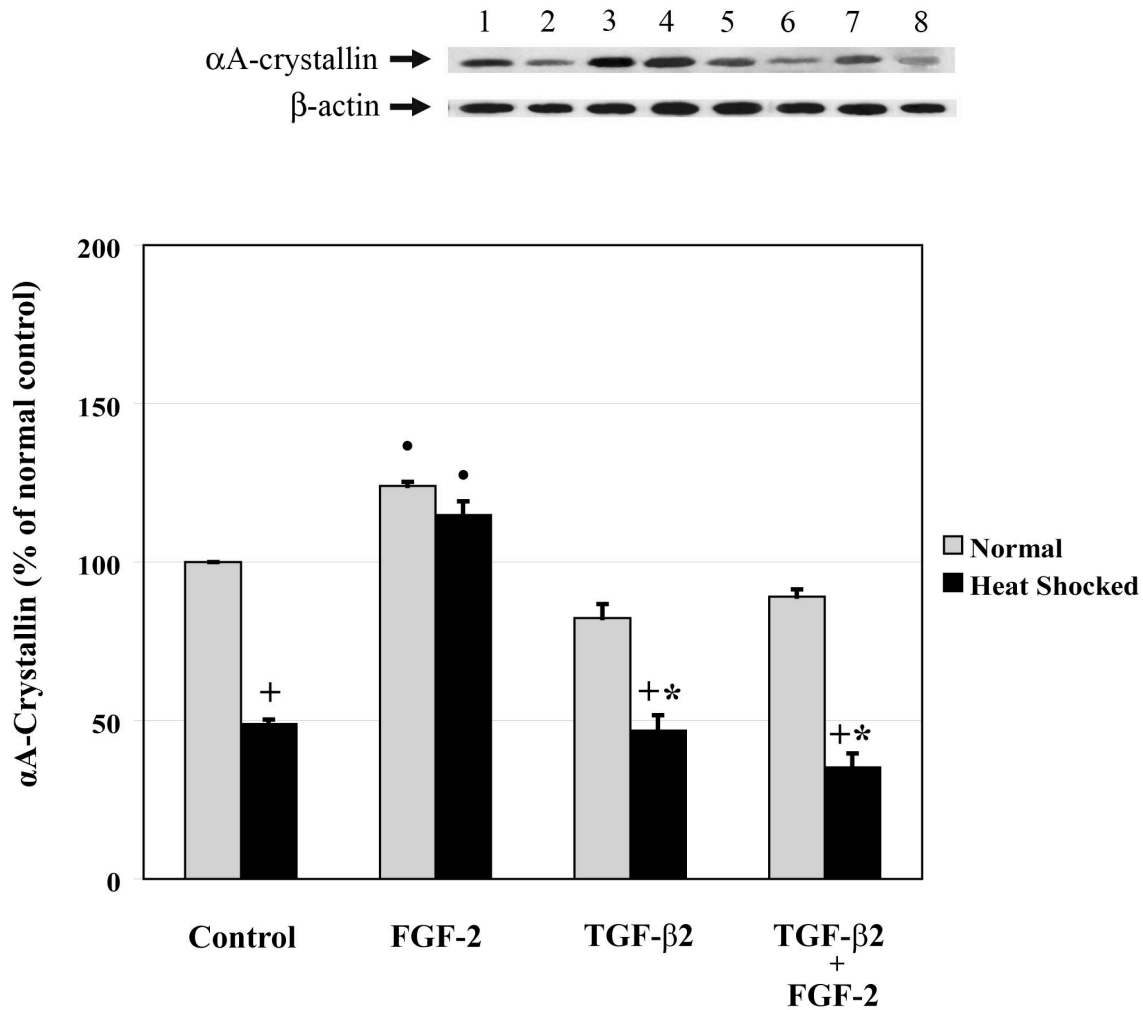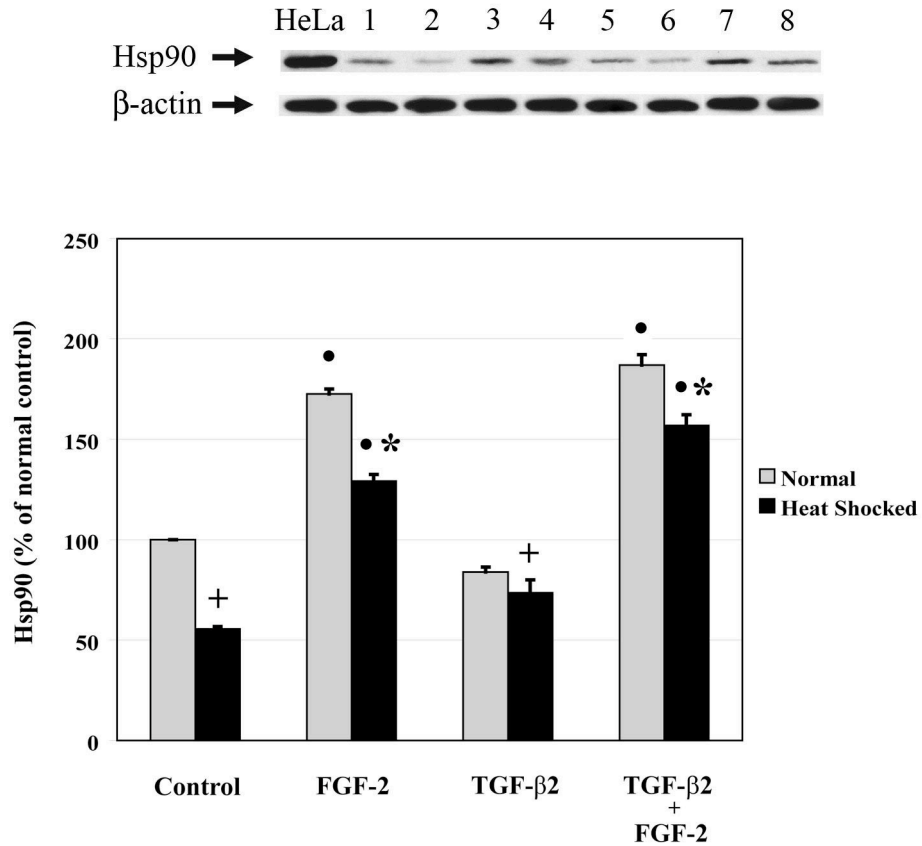
Figure 12. Hsp90 protein expression

A total of twelve lens epithelial explants from each of the eight treatment groups were used for Western blot analysis of Hsp90 (90 kDa) protein expression. HeLa cell lysate (positive control), control (lanes 1 and 2), FGF-2 (lanes 3 and 4), TGF-β2 (lanes 5 and 6) and TGF-β2/FGF-2 (lanes 7 and 8) lens epithelial explants under normal conditions (lanes 1, 3, 5 and 7) and after heat shock (lanes 2, 4, 6 and 8) treatment are shown. β-actin (42 kDa) protein expression serves as an internal control and shows that equal amounts of total protein were loaded in all lanes.

The bar graph represents the Hsp90 protein expression (percent of normal control, % ± SEM) for control, FGF-2, TGF-β2 and TGF-β2/FGF-2 treated lens epithelial explant extracts from normal culture and heat shocked conditions. Statistical analysis (ANOVA:

p ≤ 0.05) shows that there is a significant treatment effect.  [+]The heat shocked control (55.6±1.1%) and heat shocked TGF-β2 (73.6±6.0%) treated explants demonstrate significant lower levels of Hsp90 expression when compared to normal control (100%) epithelial explants.  Although there is also a decrease of Hsp90 expression in the normal TGF-β2 (93.9±2.5%), it is not significant.  [•]The FGF-2 (normal (172.6±2.5%), heat shocked (129.0±.3.3%)) and TGF-β2/FGF-2 (normal (187.0±5.3%), heat shocked (157.0±5.3%)) explants show a significant increase of Hsp90 protein expression, with the greatest increase in the TGF-β2/FGF-2 explants.  *In addition, the Hsp90 expression of heat shocked FGF-2, TGF-β2 and TGF-β2/FGF-2 explants are significantly lower than the same treatment groups under normal cultured conditions.

**Treatment**

| Protein Expression (%±SEM) | Normal | | | | Heat Shocked | | | |
|---|---|---|---|---|---|---|---|---|
| | Control | FGF-2 | TGF-β2 | TGF-β2 + FGF-2 | Control | FGF-2 | TGF-β2 | TGF-β2 + FGF-2 |
| α-SMA | 100% | 6.7±3.5% | 255.2±3.3% | 363.0±4.8% | 55.7±5.6% | 1.4±0.7% | 170.0±8.4% | 293.4±2.3% |
| E-cadherin | 100% | 119.5±8.5% | 70.0±1.8% | 45.6±2.6% | 100.3±1.8% | 126.6±5.9% | 86.7±3.1% | 72.6±3.4% |
| αA-crystallin | 100% | 124.0±1.2% | 87.1±2.3% | 94.1±2.3% | 48.9±1.3% | 114.8±4.3% | 46.8±5.0% | 35.2±4.5% |
| αB-crystallin | 100% | 112.0±2.3% | 101.6±4.6% | 106.5±1.6% | 109.0±4.0% | 111.5±2.3% | 99.5±3.5% | 101.3±2.7% |
| Hsp70 | 100% | 73.5±4.7% | 118.0±3.3% | 211.6±4.5% | 99.6±2.7% | 54.6±3.7% | 83.5±1.6% | 124.7±4.0% |
| Hsp90 | 100% | 172.6±2.5% | 93.9±2.5% | 187.0±5.3% | 55.6±1.1% | 129.0±3.3% | 73.6±6.0% | 157.0±5.3% |

Table 1. Summary of Western blot analysis

The table summarized the results for α-SMA, E-cadherin, αA-, αB-crystallins,

Hsp70 and Hsp90 protein expressions in rat lens epithelial explants (Fig. 5, 7, 9-10).

Protein expression is expressed as a percentage of normal control

and the standard error of the mean (%±SEM).

## 3.4 Discussion

### 3.4.1 TGF-β2-induced EMT in rat lens epithelial explants

TGF-β is a multifunctional cytokine that plays crucial roles during development, homeostasis and in certain pathological conditions, including ocular fibrotic diseases such as glaucoma, ASC and PCO formation.[6, 23, 59-61] Typically, TGF-β has inhibitory effects on cells of epithelial origin, while it is mitogenic for smooth muscle cells and fibroblasts.[60, 62] Although all three TGF-β isoforms induced cataractous effects in rat lens culture and epithelial explants, TGF-β2 is the predominant isoform expressed under normal and abnormal ocular conditions.[13, 14, 22, 63] Rat lenses in culture showed an age dependent response to TGF-β. Older rat lenses are more susceptible then younger rat lenses to TGF-β induced cataract formation.[52] Similarly, epithelial explants from 10 day old rats demonstrate minimal response to TGF-β stimulation while explants from weanling (21 day old) and adult rats show significant TGF-β-induced phenotype. TGF-β requires the presence of FGF to elicit a response in epithelial explants from 10 day old rats.[13] The age-dependent response to TGF-β is correlated with TGF-β receptor (TGF-βRI and TGF-βRII) expressions in LECs at different ages. Immunolocalization studies of type I and II TGF-β receptors demonstrate greater reactivity in the weanling rat lens than in the neonatal lens (3 day old). The same study also shows that FGF-2 up-regulated TGF-β receptor expression in 9 day old rat lens epithelial explants leads to an increase susceptibility to TGF-β-induced response.[64] The combined effects of TGF-β2 and FGF-2 in LECs is likely to occur *in situ* because both are present in the lens and aqueous

humor.[13, 22]  Hence, the interaction of FGF with TGF-β has been implicated in PCO development.[17, 23]  The *in-vitro* rat lens epithelial explant model has proven to be useful for uncovering the potential mechanisms involved in TGF-β-induced EMT in LECs. Histological analysis of lens epithelial explants from 7-10 day old rats showed similar morphology as described in previous experiments (Fig. 2).[13, 17, 23, 64]  Both control and FGF-2 treated explants demonstrated a confluent monolayer of LECs that maintained normal epithelial phenotype.  Treatment with TGF-β2/FGF-2 produced the greatest mutilayering effect, while treatment with only TGF-β2 induces minimal response and smaller distinct plaques.  Furthermore, the multilayer plaques developed in the heat shocked TGF-β2/FGF-2 lens epithelial explants are less diffuse and expansive than those found in the non-heat shocked TGF-β2/FGF-2 explants. The results from the current study show that heat shock treatment of rat lens epithelial explants caused a reduction of TGF-β-induced effects in the LECs.

*3.4.2 Heat shock proteins in LECs*

Heat shock proteins (Hsps) are ubiquitous proteins that are involved in maintaining native protein conformations. Hsps are involved in various processes such as refolding of damaged proteins, assisting in the folding of newly synthesized protein, intracellular transportation of proteins through the endoplasmic reticulum, prevention of protein aggregation and misfolding as well as the degradation of unfolded or partially degraded proteins during homeostasis and stress conditions.[30, 48, 65]  It is suggested that a decline of chaperone activities with age is associated with a loss of protein organization

and the appearance of age-related cataracts.[30] Hsp70, Hsp90 and α-crystallin exhibit chaperoning activities in the lens.[29] α-Crystallin binds to denatured proteins in the lens and prevents unspecific protein aggregation that leads to cataract formation.[39, 42, 65] Subsequently, Hsp70 can renature the α-crystallin bound target proteins in an ATP-dependent manner.[42] In addition, Hsp70 deficient mice has demonstrated delayed wound healing, increased corneal and lens opacity when compared to wild-type mice after photoablation.[50] Hsp90 is also present in the ocular system in the absence of stress. However, it's specific role in the LECs is less clear.[49] Hsps are also involved in regulating apoptosis. Both α-crystallin and Hsp70 are reported to protect cells from apoptosis.[66] On the other hand, Hsp90 can either promote or prevent apoptosis, depending on the apoptotic stimuli, tissue type, stages of development and the client proteins being chaperoned. For example, the inhibition of Hsp90 blocked lens apoptosis in the blind cavefish.[44] Hsp90 together with a client protein Akt (protein kinase B) can protect human vascular endothelial cells from stress-induced apoptosis by inhibiting apoptosis signal-regulating kinase 1 (ASK1) activity.[67] Although there is significant evidence showing the presence and localization of Hsps in the lens, their mechanisms and specific functions are still not well defined.

*3.4.3 Effect of heat shock treatment on TGF-β2-induced apoptosis*

Similar to previous findings, treatment with TGF-β induced a significant increase in apoptotic cell death in the rat lens epithelial explants (Fig. 8).[57, 58] The TGF-β2/FGF-2 treated explants show the greatest amount of apoptotic cell death. In contrast, the FGF-2 treated explants demonstrated the least amount of TUNEL positive nuclei in comparison to the control explants. All cultured rat lens epithelial explants that were preconditioned to heat stress show significant reduction of apoptotic cell death with respect to the non-heat shock explants. Therefore, heat shock treatment appeared to enhance the survival of rat LECs during both normal culture conditions and following TGF-β treatment.

*3.4.4 Effect of TGF-β on α-SMA expression, stress fibre and E-cadherin organization*

α-SMA expression served as the main EMT marker in this study (Figs. 4 and 5). The control cultured epithelial explants demonstrated a few positive α-SMA stained LECs. Similarly, non-cataractous human lenses have shown low-level expression of α-SMA mRNA and protein expression in the LECs.[68] The presence of α-SMA expression in control LECs may also be due to elevated stress levels under culture conditions. However, FGF-2 treated explants demonstrated negligible amount of α-SMA immunoreactivity. These results are in accordance with another study using 21 day old rat lens epithelial explants which show no α-SMA expression in the FGF treated explants and minimal α-SMA expression in the control explants.[19] In addition, α-SMA expression is a common feature found in primary bovine, rabbit and human cultured

134

LECs in serum free medium.[69] Treatment with TGF-β2 substantially increased the α-SMA immunoreactivity and filamentous actin morphology, with the greatest effect induced in the TGF-β2/FGF2 explants. Previously, it was shown that TGF-β and FGF have opposing effects on α-SMA expression. While TGF-β2 increased α-SMA expression, FGF-2 on the other hand decreased α-SMA expression in cultured bovine LECs [63]. Furthermore the results demonstrated significant reduction of α-SMA immunoreactivity and protein expression in the heat shocked control, TGF-β2 and TGF-β2/FGF-2 explants when compared to their respective non-heat shocked treatment groups. Thus, heat shock treatment successfully reduced the TGF-β induction of abnormal α-SMA expression in rat LECs.

E-cadherin is a transmembrane protein that is responsible for tight cell-to-cell adhesion and the suppression of epithelial cell dissociation, as well as maintaining cell polarity. E-cadherin initiates calcium dependent binding of E-cadherin extracellular domains on adjacent cells. It is stabilized by the interaction of intracellular E-cadherin domain with α, β and γ catenins and subsequently forms a link with F-actin to form functional adherens junctions.[54, 70] The loss of E-cadherin and F-actin stress fibre rearrangement are phenotypic changes associated with TGF-β mediated EMT.[54, 56, 71-73] As with previous studies, TGF-β treatment induced the loss of E-cadherin expression and delocalization E-cadherin from the cell junctions of the cultured rat LECs, with the greatest loss found in the TGF-β2/FGF-2 treated explants (Figs. 6 and 7).[56, 71, 72] However, the heat shocked TGF-β (TGF-β and TGF-β2/FGF-2) rat explants demonstrated significantly greater levels of E-cadherin expression and less severe E-

cadherin delocalization than the non-heat shocked TGF-β groups, while the control and FGF-2 explanted rat LECs show normal immunolocalization of E-cadherin. Interestingly, FGF-2 treated lens epithelial explants show significantly higher levels of E-cadherin protein expression relative to the control explants (Fig. 7). Our results are consistent with another study that demonstrated an up-regulation of E-cadherin expression in human pancreatic adenocarcinoma cell lines treated with FGF.[74] In addition to E-cadherin delocalization, substantial F-actin stress fibre formation and reorganization is also seen in TGF-β2/FGF-2 treated lens epithelial explants (Fig. 3). Although, heat shock treatment did not prevent TGF-β-induced stress fibre reorganization, it did however, diminish the loss of E-cadherin expression and organization in the TGF-β treated rat LECs.

*3.4.5 α-Crystallin expression in LECs duringTGF-β-induced EMT*

αA-crystallin is primarily lens specific, while αB-crystallin is also found in the heart, skeletal muscle, kidney, lung, and brain.[75-77] It has been shown that the expression of αB-crystallin is dramatically elevated under pathological conditions (heat disease, multiple sclerosis and Alzheimer's disease), thermal and chemical stress.[42, 76, 78, 79] In single α-crystallin knockout mice (αA- or αB-crystallin null), the remaining α-crystallin may fully or partially compensate for the functions of the missing protein in the lens.[80] Targeted disruption of the mouse αA-crystallin gene caused an early-onset of cataract development and significantly smaller lenses in comparison to the wild-type lenses. The αA-crystallin knockout mouse lenses also undergo slower proliferation and higher

136

apoptosis associated with mitosis,[38] while the disruption of the mouse αB-crystallin gene did not result in altered lens morphology or transparency. Thus, it is suggested that αA-crystallin plays a greater role in maintaining lens transparency than αB-crystallin.[38, 80, 81] Results from the current study show an abundance of αB-crystallin protein expression found in all the lens epithelial explants. No differential αB-crystallin expression was found between the treatment groups. Western blot analysis of cultured human, mouse, rat, rabbit, and bovine LECs also demonstrated an abundance of αB-crystallin, indicating increased stress in the cultured environment.[82] In contrast, results from this current study showed differential αA-crystallin protein expressions between treatment groups. Consistent with previous results, treatment of lens epithelial explants with FGF-2 significantly up-regulated the expression of αA-crystallin protein when compared to the control explants.[82] TGF-β2 reduces αA-crystallin protein expression, although the decrease was not significant in the non-heat shocked TGF-β explants. Another study has also shown that FGF stimulated αA-crystallin promoter activity in rat lens epithelial explants, while TGF-β inhibited the αA-crystallin promoter stimulation.[83] α-Crystallin can bind to actin filaments in the LECs and influence the cytoskeletal organization in the lens.[80] Thus, TGF-β induced reduction of αA-crystallin in the LECs may be associated with cytoskeletal disorganization and a loss of epithelial phenotype. Although α-crystallin has been reported to protect cells from apoptosis, there is evidence that suggest a decrease in αA-crystallin expression protect cells under stress conditions as part of the antiapoptotic mechanism of proteasome inhibition in Murine LECs.[66] In addition, the down-regulation of αA-crystallin expression observed in hydrogen peroxide-resistant αTN4 mouse LECs enhanced the survival of lens cells under harsh oxidative

137

conditions.[84] Hence, a decrease of αA-crystallin expression in the heat shocked control and TGF-β (TGF-β2 and TGF-β2/FGF-2) explants with respect to the non-heat shocked groups may also serve as protection against cultured and TGF-β-induced stresses.

*3.4.6 The role of Hsp70 and Hsp90 in rat LECs during TGF-β-induced EMT*

A basal level of inducible Hsp70 is expressed in the normal control rat epithelial explants.[30, 45] Treatment of lens explants with FGF-2 demonstrated reduced Hsp70 protein expression when compare to the control explants. By contrast, TGF-β induced significant increases in Hsp70 protein expression, with the greatest accumulation of Hsp70 found in the TGF-β2/FGF-2 explants. The increase in expression of Hsp70 in the TGF-β explants may be related to the increase in chaperoning functions needed to prevent aggregation and denaturation of proteins, as well as to increase cell survival during EMT. This is supported by a previous study, which demonstrated that an increase of Hsp70 expression is associated with lens cell differentiation in embryonic chicken lens cells. Furthermore, Hsp70 induction is also observed in apoptotic cells.[46] Hsp70 can also inhibit apoptosis by inhibiting caspase-3 and stress activated protein kinase/c-Jun N-terminal kinase (SAPK/JNK) activation.[85-87] Hence, The up-regulation of Hsp70 expression maybe due to an increased need for anitapoptotic functions of Hsp70 in the TGF-β treated explants. In addition, the Hsp70 accumulation may also induced by the apoptotic cells.[35] Hsp70 protein expression was diminished in the heat shocked TGF-β and FGF-2 explants when compared to the non-heat shocked explants. This corresponds with the reduction of apoptotic cell death found in the heat shocked TGF-β2 and TGF-

138

β2/FGF-2 treated explants.  Thus, less Hsp70 chaperoning activity is needed in the heat shocked TGF-β lens explants in respect to the non-heat shocked TGF-β lens explants.

It has been reported that heat shock induced Hsp70 mRNA accumulation in rat LECs progressively declines after three hours of recovery.[47]  The results of our study demonstrated that heat shock treatment enhanced the tolerance of LECs to TGF-β-induced effects even at day four of explant culture after initial exposure.

Hsp90 is another major chaperone present in the normal cultured rat LECs.  FGF-2 stimulated an up-regulation of Hsp90 expression in the rat lens epithelial explants, with the greatest accumulation of Hsp90 found in the TGF-β2/FGF-2 treated explants.  Treatment with TGF-β alone show similar levels of Hsp90 expression as the control explants.  The up-regulation of Hsp90 is related to increased cell proliferation and survival in the FGF-2 treated rat epithelial explants.  Hsp90 is required for the translocation of FGF-2 from the endosomes into the cytosol and cell nucleus where nuclear FGF-2 can increase cell proliferation and survival of carcinoma cells.[88]  It has been reported that inhibition of Hsp90 prevented FGF-2 induced mitogenic activity in human breast cancer epithelial cells.  Thus, it is suggested that Hsp90 chaperone activity is necessary for FGF-2 stimulated cell proliferation.[89]

The proteasome is a multicatalytic cytoplasmic and nuclear complex that is responsible for intracellular protein degradation and modulations of cell signaling

139

proteins, including those associated with TGF-β.[90] TGF-β induced apoptosis and α-SMA mRNA expression was blocked by proteasomal inhibition in human LECs. The proteasome inhibitor induced the accumulation of SnoN (Smad inhibitor protein) and repressed the TGF-β signal progression in LECs.[90] Another study shows that Hps90 and α-crystallin plays a protective role in human lens proteasome activities against oxidative insults.[91, 92] Therefore increased Hsp90 expression in the TGF-β2/FGF-2 treated explants may serve to protect proteasomal activities and enhanced TGF-β induced response. Hsp90 expression is lowered in the heat shock treated explants of all treatment groups in comparison to the respective non-heat shocked groups. This also serves as an indication that non-heat shocked LECs are under higher stress environment than the heat shocked LECs.

In addition, both Hsp90 and Hsp70 can interact with cytoskeletal elements including microtubules, microfilaments, actin and tublin.[49, 51, 93] Thus, it is suggested that Hsp90 and Hsp70 proteins are required during extensive cytoskeletal rearrangement and disassembly in the TGF-β2/FGF-2 treated rat lens epithelial explants.[51] Therefore TGF-β-induced α-SMA and F-actin disorganization as well as E-cadherin disassembly are concurrent with the up-regulation of Hsp70 and Hsp90 protein expressions along with reduced expression of αA-crystallin expression.

In conclusion, the findings of this current study show that preconditioning of cultured primary rat LECs to heat stress reduced the TGF-β induced EMT effect on the LECs. The most pronounced TGF-β induced EMT and plaque formation were found in

the TGF-β2/FGF-2 treated rat lens epithelial explants, while treatment with FGF-2 alone diminished the stress and enhanced the survival of LECs under normal culture conditions. The heat shocked TGF-β2/FGF-2 lens epithelial explants demonstrated lower α-SMA expression, E-cadherin disassociation and apoptosis than the non-heat shocked TGF-β2/FGF-2 explants. An increase in accumulation of Hsp70 and Hsp90 in these explants suggests that there is a greater need for molecular chaperone activities in the TGF-β2/FGF-2 treated LECs. TGF-β also reduced αA-crystallin expression while αB-crystallin expression produced no significant change relative to the control explants. The heat shocked LECs show lower αA-crystallin, Hsp70 and Hsp90 expressions when compared to their respective non-heat shocked groups. This study shows that molecular chaperones may play a protective role in rat LECs during both normal culture and TGF-β-induced stress. Further investigation is required to determine the exact roles that heat shock proteins play during TGF-β-induced EMT in the LECs. Understanding the mechanisms involved in lens epithelial cell transdifferentiation may provide potential therapeutic candidates to prevent ASC and PCO development.

## 3.5 References

1.      Yang Y, Chauhan BK, Cveklova K, Cvekl A. Transcriptional regulation of mouse alphaB- and gammaF-crystallin genes in lens: opposite promoter-specific interactions between Pax6 and large Maf transcription factors. *J Mol Biol* 2004;344:351-368.

2.      Harding JJ, Dilley KJ. Structural proteins of the mammalian lens: a review with emphasis on changes in development, aging and cataract. *Exp Eye Res* 1976;22:1-73.

3.      Bron AJ, Tripathi RC, Tripathi BJ, Wolff E. *Wolff's anatomy of the eye and orbit*. 8th ed. London: Chapman & Hall Medical; 1997:ix, 736.

4.      Marcantonio JM, Syam PP, Liu CS, Duncan G. Epithelial transdifferentiation and cataract in the human lens. *Exp Eye Res* 2003;77:339-346.

5.      Lovicu FJ, Schulz MW, Hales AM, et al. TGFbeta induces morphological and molecular changes similar to human anterior subcapsular cataract. *Br J Ophthalmol* 2002;86:220-226.

6.      Srinivasan Y, Lovicu FJ, Overbeek PA. Lens-specific expression of transforming growth factor beta1 in transgenic mice causes anterior subcapsular cataracts. *J Clin Invest* 1998;101:625-634.

7.      Yang X, Letterio JJ, Lechleider RJ, et al. Targeted disruption of SMAD3 results in impaired mucosal immunity and diminished T cell responsiveness to TGF-beta. *Embo J* 1999;18:1280-1291.

8.      Kurisaki A, Kose S, Yoneda Y, Heldin CH, Moustakas A. Transforming growth factor-beta induces nuclear import of Smad3 in an importin-beta1 and Ran-dependent manner. *Mol Biol Cell* 2001;12:1079-1091.

9.      Qing J, Zhang Y, Derynck R. Structural and functional characterization of the transforming growth factor-beta -induced Smad3/c-Jun transcriptional cooperativity. *J Biol Chem* 2000;275:38802-38812.

10.     Dunker N, Krieglstein K. Reduced programmed cell death in the retina and defects in lens and cornea of Tgfbeta2(-/-) Tgfbeta3(-/-) double-deficient mice. *Cell Tissue Res* 2003;313:1-10.

11.     Cousins SW, McCabe MM, Danielpour D, Streilein JW. Identification of transforming growth factor-beta as an immunosuppressive factor in aqueous humor. *Invest Ophthalmol Vis Sci* 1991;32:2201-2211.

12.     Wallentin N, Wickstrom K, Lundberg C. Effect of cataract surgery on aqueous TGF-beta and lens epithelial cell proliferation. *Invest Ophthalmol Vis Sci* 1998;39:1410-1418.

13.     Liu J, Hales AM, Chamberlain CG, McAvoy JW. Induction of cataract-like changes in rat lens epithelial explants by transforming growth factor beta. *Invest Ophthalmol Vis Sci* 1994;35:388-401.

14.     Gordon-Thomson C, de Iongh RU, Hales AM, Chamberlain CG, McAvoy JW. Differential cataractogenic potency of TGF-beta1, -beta2, and -beta3 and their expression in the postnatal rat eye. *Invest Ophthalmol Vis Sci* 1998;39:1399-1409.

15.     Banh A, Deschamps PA, Gauldie J, Overbeek PA, Sivak JG, West-Mays JA. Lens-specific expression of TGF-beta induces anterior subcapsular cataract formation in the absence of Smad3. *Invest Ophthalmol Vis Sci* 2006;47:3450-3460.

16.     Dwivedi DJ, Pino G, Banh A, et al. Matrix Metalloproteinase Inhibitors Suppress Transforming Growth Factor-{beta}-Induced Subcapsular Cataract Formation. *Am J Pathol* 2006;168:69-79.

17.     Mansfield KJ, Cerra A, Chamberlain CG. FGF-2 counteracts loss of TGFbeta affected cells from rat lens explants: implications for PCO (after cataract). *Mol Vis* 2004;10:521-532.

18.     Hales AM, Chamberlain CG, McAvoy JW. Cataract induction in lenses cultured with transforming growth factor-beta. *Invest Ophthalmol Vis Sci* 1995;36:1709-1713.

19.     Hales AM, Schulz MW, Chamberlain CG, McAvoy JW. TGF-beta 1 induces lens cells to accumulate alpha-smooth muscle actin, a marker for subcapsular cataracts. *Curr Eye Res* 1994;13:885-890.

20.     Kappelhof JP, Vrensen GF. The pathology of after-cataract. A minireview. *Acta Ophthalmol Suppl* 1992;13-24.

21.     de Iongh RU, Lovicu FJ, Overbeek PA, et al. Requirement for TGFbeta receptor signaling during terminal lens fiber differentiation. *Development* 2001;128:3995-4010.

22.     Cerra A, Mansfield KJ, Chamberlain CG. Exacerbation of TGF-beta-induced cataract by FGF-2 in cultured rat lenses. *Mol Vis* 2003;9:689-700.

23.     Symonds JG, Lovicu FJ, Chamberlain CG. Posterior capsule opacification-like changes in rat lens explants cultured with TGFbeta and FGF: Effects of cell coverage and regional differences. *Exp Eye Res* 2006;82:693-699.

24.     Blechinger SR, Evans TG, Tang PT, Kuwada JY, Warren JT, Jr., Krone PH. The heat-inducible zebrafish hsp70 gene is expressed during normal lens development under non-stress conditions. *Mech Dev* 2002;112:213-215.

25.     Zhang B, van Adel BA, Gabriele J, et al. Expression of the 40 kDa catecholamine regulated protein in the normal and injured rat retina. *J Chem Neuroanat* 2002;24:41-48.

26.     Lund PA. *Molecular chaperones in the cell*. New York: Oxford University Press; 2001:xx, 281.

27.     Basha E, Lee GJ, Demeler B, Vierling E. Chaperone activity of cytosolic small heat shock proteins from wheat. *Eur J Biochem* 2004;271:1426-1436.

28.     Chapple JP, Grayson C, Hardcastle AJ, Saliba RS, van der Spuy J, Cheetham ME. Unfolding retinal dystrophies: a role for molecular chaperones? *Trends Mol Med* 2001;7:414-421.

29.     Bagchi M, Katar M, Maisel H. A heat shock transcription factor like protein in the nuclear matrix compartment of the tissue cultured mammalian lens epithelial cell. *J Cell Biochem* 2001;80:382-387.

30.     Bagchi M, Katar M, Maisel H. Heat shock proteins of adult and embryonic human ocular lenses. *J Cell Biochem* 2002;84:278-284.

31.     Banh A, Vijayan MM, Sivak JG. Hsp70 in bovine lenses during temperature stress. *Mol Vis* 2003;9:323-328.

32.     Das KP, Surewicz WK. Temperature-induced exposure of hydrophobic surfaces and its effect on the chaperone activity of alpha-crystallin. *FEBS Lett* 1995;369:321-325.

33.     Andley UP, Song Z, Wawrousek EF, Bassnett S. The molecular chaperone alphaA-crystallin enhances lens epithelial cell growth and resistance to UVA stress. *J Biol Chem* 1998;273:31252-31261.

34.     Sun TX, Das BK, Liang JJ. Conformational and functional differences between recombinant human lens alphaA- and alphaB-crystallin. *J Biol Chem* 1997;272:6220-6225.

35.     Weinreb O, van Boekel MA, Dovrat A, Bloemendal H. Effect of UV-A light on the chaperone-like properties of young and old lens alpha-crystallin. *Invest Ophthalmol Vis Sci* 2000;41:191-198.

36.     Santhoshkumar P, Sharma KK. Analysis of alpha-crystallin chaperone function using restriction enzymes and citrate synthase. *Mol Vis* 2001;7:172-177.

37.     Regini JW, Grossmann JG, Burgio MR, et al. Structural changes in alpha-crystallin and whole eye lens during heating, observed by low-angle X-ray diffraction. *J Mol Biol* 2004;336:1185-1194.

38.     Xi JH, Bai F, Andley UP. Reduced survival of lens epithelial cells in the alphaA-crystallin-knockout mouse. *J Cell Sci* 2003;116:1073-1085.

39.     Bode C, Tolgyesi FG, Smeller L, Heremans K, Avilov SV, Fidy J. Chaperone-like activity of alpha-crystallin is enhanced by high-pressure treatment. *Biochem J* 2003;370:859-866.

40.     Horwitz J. The function of alpha-crystallin in vision. *Semin Cell Dev Biol* 2000;11:53-60.

41.     Hwang KH, Lee EH, Jho EH, et al. Accumulation and aberrant modifications of alpha-crystallins in anterior polar cataracts. *Yonsei Med J* 2004;45:73-80.

42.     Horwitz J. Alpha-crystallin. *Exp Eye Res* 2003;76:145-153.

43.     Thiagarajan G, Lakshmanan J, Chalasani M, Balasubramanian D. Peroxynitrite reaction with eye lens proteins: alpha-crystallin retains its activity despite modification. *Invest Ophthalmol Vis Sci* 2004;45:2115-2121.

44.     Hooven TA, Yamamoto Y, Jeffery WR. Blind cavefish and heat shock protein chaperones: a novel role for hsp90alpha in lens apoptosis. *Int J Dev Biol* 2004;48:731-738.

45.     Dean DO, Kent CR, Tytell M. Constitutive and inducible heat shock protein 70 immunoreactivity in the normal rat eye. *Invest Ophthalmol Vis Sci* 1999;40:2952-2962.

46.     Dash A, Chung S, Zelenka PS. Expression of HSP70 mRNA in the embryonic chicken lens: association with differentiation. *Exp Eye Res* 1994;58:381-387.

47.     Yao K, Rao H, Wu R, Tang X, Xu W. Expression of Hsp70 and Hsp27 in lens epithelial cells in contused eye of rat modulated by thermotolerance or quercetin. *Mol Vis* 2006;12:445-450.

48.     Bagchi M, Ireland M, Katar M, Maisel H. Heat shock proteins of chicken lens. *J Cell Biochem* 2001;82:409-414.

49.     Dean DO, Tytell M. Hsp25 and -90 immunoreactivity in the normal rat eye. *Invest Ophthalmol Vis Sci* 2001;42:3031-3040.

50.     Kim JM, Kim JC, Park WC, Seo JS, Chang HR. Effect of thermal preconditioning before excimer laser photoablation. *J Korean Med Sci* 2004;19:437-446.

51.     Takenaka IM, Hightower LE. Transforming growth factor-beta 1 rapidly induces Hsp70 and Hsp90 molecular chaperones in cultured chicken embryo cells. *J Cell Physiol* 1992;152:568-577.

52.      Hales AM, Chamberlain CG, McAvoy JW. Susceptibility to TGFbeta2-induced cataract increases with aging in the rat. *Invest Ophthalmol Vis Sci* 2000;41:3544-3551.

53.      Bradford MM. A rapid and sensitive method for the quantitation of microgram quantities of protein utilizing the principle of protein-dye binding. *Anal Biochem* 1976;72:248-254.

54.      Kasai H, Allen JT, Mason RM, Kamimura T, Zhang Z. TGF-beta1 induces human alveolar epithelial to mesenchymal cell transition (EMT). *Respir Res* 2005;6:56.

55.      Fischer RS, Lee A, Fowler VM. Tropomodulin and tropomyosin mediate lens cell actin cytoskeleton reorganization in vitro. *Invest Ophthalmol Vis Sci* 2000;41:166-174.

56.      Bhowmick NA, Zent R, Ghiassi M, McDonnell M, Moses HL. Integrin beta 1 signaling is necessary for transforming growth factor-beta activation of p38MAPK and epithelial plasticity. *J Biol Chem* 2001;276:46707-46713.

57.      Lee JH, Wan XH, Song J, et al. TGF-beta-induced apoptosis and reduction of Bcl-2 in human lens epithelial cells in vitro. *Curr Eye Res* 2002;25:147-153.

58.      Maruno KA, Lovicu FJ, Chamberlain CG, McAvoy JW. Apoptosis is a feature of TGF beta-induced cataract. *Clin Exp Optom* 2002;85:76-82.

59.      Rooke HM, Crosier KE. The smad proteins and TGFbeta signalling: uncovering a pathway critical in cancer. *Pathology* 2001;33:73-84.

60.      Flugel-Koch C, Ohlmann A, Piatigorsky J, Tamm ER. Disruption of anterior segment development by TGF-beta1 overexpression in the eyes of transgenic mice. *Dev Dyn* 2002;225:111-125.

61.      Lutjen-Drecoll E. Morphological changes in glaucomatous eyes and the role of TGFbeta(2) for the pathogenesis of the disease. *Exp Eye Res* 2005;81:1-4.

62.    Horowitz JC, Lee DY, Waghray M, et al. Activation of the pro-survival phosphatidylinositol 3-kinase/AKT pathway by transforming growth factor-beta1 in mesenchymal cells is mediated by p38 MAPK-dependent induction of an autocrine growth factor. *J Biol Chem* 2004;279:1359-1367.

63.    Kurosaka D, Kato K, Nagamoto T, Negishi K. Growth factors influence contractility and alpha-smooth muscle actin expression in bovine lens epithelial cells. *Invest Ophthalmol Vis Sci* 1995;36:1701-1708.

64.    de Iongh RU, Gordon-Thomson C, Chamberlain CG, Hales AM, McAvoy JW. Tgfbeta receptor expression in lens: implications for differentiation and cataractogenesis. *Exp Eye Res* 2001;72:649-659.

65.    Fink AL. Chaperone-mediated protein folding. *Physiol Rev* 1999;79:425-449.

66.    Awasthi N, Wagner BJ. Upregulation of heat shock protein expression by proteasome inhibition: an antiapoptotic mechanism in the lens. *Invest Ophthalmol Vis Sci* 2005;46:2082-2091.

67.    Zhang R, Luo D, Miao R, et al. Hsp90-Akt phosphorylates ASK1 and inhibits ASK1-mediated apoptosis. *Oncogene* 2005;24:3954-3963.

68.    Rungger-Brandle E, Conti A, Leuenberger PM, Rungger D. Expression of alphasmooth muscle actin in lens epithelia from human donors and cataract patients. *Exp Eye Res* 2005;81:539-550.

69.    Nagamoto T, Eguchi G, Beebe DC. Alpha-smooth muscle actin expression in cultured lens epithelial cells. *Invest Ophthalmol Vis Sci* 2000;41:1122-1129.

70.     Auersperg N, Pan J, Grove BD, et al. E-cadherin induces mesenchymal-to-epithelial transition in human ovarian surface epithelium. *Proc Natl Acad Sci U S A* 1999;96:6249-6254.

71.     Bhowmick NA, Ghiassi M, Bakin A, et al. Transforming growth factor-beta1 mediates epithelial to mesenchymal transdifferentiation through a RhoA-dependent mechanism. *Mol Biol Cell* 2001;12:27-36.

72.     de Iongh RU, Wederell E, Lovicu FJ, McAvoy JW. Transforming growth factor-beta-induced epithelial-mesenchymal transition in the lens: a model for cataract formation. *Cells Tissues Organs* 2005;179:43-55.

73.     Miettinen PJ, Ebner R, Lopez AR, Derynck R. TGF-beta induced transdifferentiation of mammary epithelial cells to mesenchymal cells: involvement of type I receptors. *J Cell Biol* 1994;127:2021-2036.

74.     El-Hariry I, Pignatelli M, Lemoine NR. FGF-1 and FGF-2 modulate the E-cadherin/catenin system in pancreatic adenocarcinoma cell lines. *Br J Cancer* 2001;84:1656-1663.

75.     Chepelinsky AB, Piatigorsky J, Pisano MM, et al. Lens protein gene expression: alpha-crystallins and MIP. *Lens Eye Toxic Res* 1991;8:319-344.

76.     Muchowski PJ, Bassuk JA, Lubsen NH, Clark JI. Human alphaB-crystallin. Small heat shock protein and molecular chaperone. *J Biol Chem* 1997;272:2578-2582.

77.     Reddy GB, Das KP, Petrash JM, Surewicz WK. Temperature-dependent chaperone activity and structural properties of human alphaA- and alphaB-crystallins. *J Biol Chem* 2000;275:4565-4570.

78. Muchowski PJ, Clark JI. ATP-enhanced molecular chaperone functions of the small heat shock protein human alphaB crystallin. *Proc Natl Acad Sci U S A* 1998;95:1004-1009.

79. Haley DA, Horwitz J, Stewart PL. The small heat-shock protein, alphaB-crystallin, has a variable quaternary structure. *J Mol Biol* 1998;277:27-35.

80. Boyle DL, Takemoto L, Brady JP, Wawrousek EF. Morphological characterization of the Alpha A- and Alpha B-crystallin double knockout mouse lens. *BMC Ophthalmol* 2003;3:3.

81. Brady JP, Garland D, Duglas-Tabor Y, Robison WG, Jr., Groome A, Wawrousek EF. Targeted disruption of the mouse alpha A-crystallin gene induces cataract and cytoplasmic inclusion bodies containing the small heat shock protein alpha B-crystallin. *Proc Natl Acad Sci U S A* 1997;94:884-889.

82. Wang X, Garcia CM, Shui YB, Beebe DC. Expression and regulation of alpha-, beta-, and gamma-crystallins in mammalian lens epithelial cells. *Invest Ophthalmol Vis Sci* 2004;45:3608-3619.

83. Ueda Y, Chamberlain CG, Satoh K, McAvoy JW. Inhibition of FGF-induced alphaA-crystallin promoter activity in lens epithelial explants by TGFbeta. *Invest Ophthalmol Vis Sci* 2000;41:1833-1839.

84. Carper D, John M, Chen Z, et al. Gene expression analysis of an $H_2O_2$-resistant lens epithelial cell line. *Free Radic Biol Med* 2001;31:90-97.

85. Li CY, Lee JS, Ko YG, Kim JI, Seo JS. Heat shock protein 70 inhibits apoptosis downstream of cytochrome c release and upstream of caspase-3 activation. *J Biol Chem* 2000;275:25665-25671.

86.     Mosser DD, Caron AW, Bourget L, Denis-Larose C, Massie B. Role of the human heat shock protein hsp70 in protection against stress-induced apoptosis. *Mol Cell Biol* 1997;17:5317-5327.

87.     Gabai VL, Meriin AB, Mosser DD, et al. Hsp70 prevents activation of stress kinases. A novel pathway of cellular thermotolerance. *J Biol Chem* 1997;272:18033-18037.

88.     Wesche J, Malecki J, Wiedlocha A, Skjerpen CS, Claus P, Olsnes S. FGF-1 and FGF-2 require the cytosolic chaperone Hsp90 for translocation into the cytosol and the cell nucleus. *J Biol Chem* 2006;281:11405-11412.

89.     Vercoutter-Edouart AS, Czeszak X, Crepin M, et al. Proteomic detection of changes in protein synthesis induced by fibroblast growth factor-2 in MCF-7 human breast cancer cells. *Exp Cell Res* 2001;262:59-68.

90.     Hosler MR, Wang-Su ST, Wagner BJ. Role of the proteasome in TGF-beta signaling in lens epithelial cells. *Invest Ophthalmol Vis Sci* 2006;47:2045-2052.

91.     Andersson M, Sjostrand J, Karlsson JO. Differential inhibition of three peptidase activities of the proteasome in human lens epithelium by heat and oxidation. *Exp Eye Res* 1999;69:129-138.

92.     Poppek D, Grune T. Proteasomal defense of oxidative protein modifications. *Antioxid Redox Signal* 2006;8:173-184.

93.     Ochoa GH, Clark YM, Matsumoto B, Torres-Ruiz JA, Robles LJ. Heat shock protein 70 and heat shock protein 90 expression in light- and dark-adapted adult octopus retinas. *J Neurocytol* 2002;31:161-174.

# General Conclusion

All three rodent models used in these experiments proved to be useful for examining TGF-β-induced subcapsular cataract development. The *in-vitro* rat whole lenses and the lens epithelial explants demonstrated similar TGF-β-induced effects as seen in the *in-vivo* TGF-β1 transgenic mice. Treatment with TGF-β2 and overexpression of TGF-β1 in rat and mouse lenses lead to multilayer plaque formation. These lenses subsequently exhibited an increase α-SMA expression and apoptosis in the LECs. This study also measured the optical quality of rat, transgenic TGF-β1 and Smad3 knockout mouse lenses during ASC formation. The results show that ASCs significantly reduced lens optical quality and focus (refer to data in Chapter 1 and 2). The *in-vitro* rat lens epithelial explants provided a primary lens epithelial cell culture to specifically detect TGF-β cellular effects during EMT (Chapter 3).

The development of these subcapsular cataracts involves EMT. EMT progression is characterized by the transdifferentiation of lens epithelial cells into myofibroblastic cells which cause the accumulation of ECM. [18-20] Under physiological conditions, TGF-β in the lens and ocular media mainly exists in its latent form, whereas biologically active TGF-β has been detected in the ocular media from patients suffering with ASC.[21, 22] Previously, *in-vitro* rat lens culture and lens epithelial explants have shown that all three TGF-β isoforms (TGF-β1, TGF-β2 and TGF-β3) can induce cataractous changes. However, TGF-β1 is 10 times less potent than TGF-β2 and TGF-β3.[14]

153

TGF-β modified ECM by inducing the expression of MMPs and other enzymes involved in matrix remodeling.[23]  A MMP inhibitor (Ilomastat) is also used in chapter 1 to investigate the role of MMPs in TGF-β-induced subcapsular cataract development. Through the breakdown and remodeling of extracellular matrix, MMPs play an essential role in normal physiological processes such as embryonic development, morphogenesis, reproduction, and tissue resorption and remodeling.[24]  MMPs are secreted as inactive zymogens (pro-MMPs) and require proteolytic removal of an amino-terminal pro-sequence for them to function.[25]  Various growth factors, hormones, cytokines, cell-to-matrix, cell-to-cell interactions and cellular transformation transcriptionally regulate MMP expression.[24, 26]  It has been suggested that over-expression of MMPs can promote tumor invasion and angiogenesis.[27]  Interestingly, MMP2 (gelatinase A, 72 kD) and MMP9 (gelatinase B, 92 kD) are the most widely studied members of the MMP family in the eye.[23, 28]  Both MMP2 and MMP9 are up-regulated during abnormal ocular conditions such as posterior capsule opacification, proliferative diabetic retinopathy and epithelial wound healing.[29-32]  The expression of MMP2 and MMP9 is both positively and negatively regulated by TGF-β.[23]  The results from this experiment show that prolonged exposure (6 days) of cultured rat lenses to TGF-β2 plus 25 μM Ilomastat effectively inhibited the formation of subcapsular plaques and lens opacities. Optical analysis demonstrated that there are no significant differences in BVD errors between the TGF-β2 + 25 μM Ilomastat treated lenses and control lenses.  Also the treatment with Ilomastat significantly reduced the effects of TGF-β2 on cultured rat lenses, as shown in the optical results.  Ilomastat is a general MMP inhibitor that has been shown to prevent lens capsule contraction, and human lens and corneal epithelial cell migration.[33, 34]  However, the

mechanisms that are involved in subcapsular cataract formation in respect to the relationship between MMPs and TGF-β are still not fully understood.

Chapter 2 shows that transgenic, *in vivo* expression of TGF-β1 in the lens promotes the formation of ASCs in the absence of Smad3. The fact that the subcapsular plaques in the TGF-β1/Smad3 null mice are reduced in size, with less α-SMA expression and substantially less collagen deposition, suggests that while Smad3 signaling is sufficient for the formation of ASC plaques, it is not necessary. In addition, all of the TGF-β1 (TGF-β1/Smad3^{+/+}, TGF-β1/Smad3^{-/-} and TGF-β1/Smad3^{+/-}) transgenic lenses which exhibited ASC plaques show significantly larger BVD errors (decreased sharpness of focus) relative to the BVD errors of the wild-type lenses, which are devoid of plaques. Importantly, the BVD errors of TGF-β1/Smad3^{-/-} lenses are significantly lower then both TGF-β1/Smad3^{+/+} and TGF-β1/Smad3^{+/-} lenses, demonstrating the ability of the scanning laser instrument to discern the effects of size of the subcapsular plaques on optical quality.

TGF-β signaling is mediated by a heterodimeric complex of two types of transmembrane serine/threonine kinase receptors. TGF-β binds to the receptor complex causing the type II receptor kinase to phosphorylate and thereby activate the type I receptor kinase. The type I receptor kinase then phosphorylates the receptor activated Smads (R-Smads), Smad2 and 3.[35, 36] Once activated, the R-Smads bind to Smad 4 and translocate into the nucleus and along with other transcription factors, bind to gene promoters to activate or repress transcription. Thus, it could be surmised that Smad2

155

activation may have compensated for the loss of Smad3 in the lens and contributed to the TGF-β-induced EMT in the TGF-β1/Smad3$^{-/-}$ lens epithelium. However, while both Smad2 and Smad3 can mediate TGF-β and activin signaling, they clearly have non-redundant functions. For example, homozygous mice with targeted disruptions in the Smad2 gene exhibit embryonic lethality during gastrulation [37, 38], whereas, homozygous Smad3 null mice are viable and survive to adulthood.[39, 40] Smad3 and Smad2 have also been shown to have different gene-regulatory functions and Smad3, not Smad2, has been linked to fibrotic events.[39, 41, 42] Future studies using the *in-vivo* transgenic mouse model will be aimed at determining the requirement for Smad-dependent and Smad-independent signaling pathways in various aspects of the ASC phenotype. Uncovering the specific TGF-β signaling mechanisms may provide potential therapeutic targets for ASC and closely related ocular fibrotic diseases, such as secondary cataract or PCO.

Finally the role of molecular chaperones in TGF-β2-induced EMT in rat lens epithelial explants was investigated in chapter 3. FGF-2 was also use to exacerbate the effects of TGF-β as mentioned previously. Heat shock proteins (Hsps) are ubiquitous proteins that are involved in maintaining native protein conformations. Hsps are involved in various processes such as refolding of damaged proteins, assisting in the folding of newly synthesized protein, intracellular transportation of proteins through the endoplasmic reticulum, prevention of protein aggregation and misfolding as well as the degradation of unfolded or partially degraded proteins during homeostasis and stress conditions.[2, 43, 44] It is suggested that a decline of chaperone activities with age is associated with a loss of protein organization and the appearance of age-related

156

cataracts.[2] Hsp70, Hsp90 and α-crystallin exhibit chaperoning activities in lens.[45] α-Crystallin binds to denatured proteins in the lens and prevents unspecific protein aggregation that leads to cataract formation.[43, 46, 47] Subsequently, Hsp70 can renature the α-crystallin bound target proteins in an ATP-dependent manner.[46] In addition, Hsp70 deficient mice has demonstrated delayed wound healing, increased corneal and lens opacity when compared to wild-type mice after photoablation.[48] Hsp90 is also present in the ocular system in the absence of stress. However it's specific role in the LECs is less clear.[49] Hsps are also involved in regulating apoptosis. Both α-crystallin and Hsp70 are reported to protect cells from apoptosis.[50] On the other hand, Hsp90 can either promote or prevent apoptosis depending on the apoptotic stimuli, tissue type, stages of development and the client proteins being chaperoned.[51]

The preconditioning of cultured primary rat LECs to heat stress reduced the TGF-β-induced EMT effect on the LECs. The most pronounced TGF-β-induced EMT and plaque formation were found in the TGF-β2/FGF-2 treated rat lens epithelial explants. Treatment with only FGF-2 diminished the stress and enhanced the survival of LECs under normal culture conditions. The heat shocked TGF-β2/FGF-2 lens epithelial explants demonstrated lower α-SMA expression, E-cadherin disassociation and apoptosis than the non-heat shocked TGF-β2/FGF-2 explants. An increased accumulation of Hsp70 and Hsp90 in these explants suggests that there is a greater need for molecular chaperone activities in the TGF-β2/FGF-2 treated LECs. TGF-β also reduced αA-crystallin expression while αB-crystallin expression showed no significant change relative to the control explants. The heat-shocked LECs shows lower αA-crystallin,

Hsp70 and Hsp90 expressions when compare to their respective non-heat shocked groups. This study shows that molecular chaperones may play a protective role in rat LECs during both culture and TGF-β-induced stress. Further investigation is required to determine the exact roles that heat shock proteins play during TGF-β-induced EMT in the LECs.

In conclusion, TGF-β induced the formation of subcapsular cataracts and reduced the optical function of the lens. Inhibition of MMPs prevented ASCs, while Smad3 gene knockout and heat shock treatment only diminished the effects of TGF-β. These results indicate that various proteins and signaling pathways are associated with subcapsular cataract development. MMPs, Smad proteins, and heat shock proteins may serve as therapeutic candidates for ASCs and PCO. However, more studies are required to determine the exact mechanisms involved.

# References to General Introduction and Conclusion

1.      Harding JJ, Dilley KJ. Structural proteins of the mammalian lens: a review with emphasis on changes in development, aging and cataract. *Exp Eye Res* 1976;22:1-73.

2.      Bagchi M, Katar M, Maisel H. Heat shock proteins of adult and embryonic human ocular lenses. *J Cell Biochem* 2002;84:278-284.

3.      WHO. Blindness and visual disability. World Health Organization; 1997.

4.      Lovicu FJ, Schulz MW, Hales AM, et al. TGFbeta induces morphological and molecular changes similar to human anterior subcapsular cataract. *Br J Ophthalmol* 2002;86:220-226.

5.      Srinivasan Y, Lovicu FJ, Overbeek PA. Lens-specific expression of transforming growth factor beta1 in transgenic mice causes anterior subcapsular cataracts. *J Clin Invest* 1998;101:625-634.

6.      Yang X, Letterio JJ, Lechleider RJ, et al. Targeted disruption of SMAD3 results in impaired mucosal immunity and diminished T cell responsiveness to TGF-beta. *Embo J* 1999;18:1280-1291.

7.      Kurisaki A, Kose S, Yoneda Y, Heldin CH, Moustakas A. Transforming growth factor-beta induces nuclear import of Smad3 in an importin-beta1 and Ran-dependent manner. *Mol Biol Cell* 2001;12:1079-1091.

8.      Qing J, Zhang Y, Derynck R. Structural and functional characterization of the transforming growth factor-beta -induced Smad3/c-Jun transcriptional cooperativity. *J Biol Chem* 2000;275:38802-38812.

9.      Dunker N, Krieglstein K. Reduced programmed cell death in the retina and defects in lens and cornea of Tgfbeta2(-/-) Tgfbeta3(-/-) double-deficient mice. *Cell Tissue Res* 2003;313:1-10.

10.     Lee EH, Seomun Y, Hwang KH, et al. Overexpression of the transforming growth factor-beta-inducible gene betaig-h3 in anterior polar cataracts. *Invest Ophthalmol Vis Sci* 2000;41:1840-1845.

11.     Maruno KA, Lovicu FJ, Chamberlain CG, McAvoy JW. Apoptosis is a feature of TGF beta-induced cataract. *Clin Exp Optom* 2002;85:76-82.

12.     de Iongh RU, Wederell E, Lovicu FJ, McAvoy JW. Transforming growth factor-beta-induced epithelial-mesenchymal transition in the lens: a model for cataract formation. *Cells Tissues Organs* 2005;179:43-55.

13.     Dwivedi DJ, Pino G, Banh A, et al. Matrix Metalloproteinase Inhibitors Suppress Transforming Growth Factor-{beta}-Induced Subcapsular Cataract Formation. *Am J Pathol* 2006;168:69-79.

14.     Gordon-Thomson C, de Iongh RU, Hales AM, Chamberlain CG, McAvoy JW. Differential cataractogenic potency of TGF-beta1, -beta2, and -beta3 and their expression in the postnatal rat eye. *Invest Ophthalmol Vis Sci* 1998;39:1399-1409.

15.     Hales AM, Chamberlain CG, McAvoy JW. Cataract induction in lenses cultured with transforming growth factor-beta. *Invest Ophthalmol Vis Sci* 1995;36:1709-1713.

16.     de Iongh RU, Lovicu FJ, Overbeek PA, et al. Requirement for TGFbeta receptor signaling during terminal lens fiber differentiation. *Development* 2001;128:3995-4010.

17.   Sun JK, Iwata T, Zigler JS, Jr., Carper DA. Differential gene expression in male and female rat lenses undergoing cataract induction by transforming growth factor-beta (TGF-beta). *Exp Eye Res* 2000;70:169-181.

18.   Hales AM, Chamberlain CG, McAvoy JW. Susceptibility to TGFbeta2-induced cataract increases with aging in the rat. *Invest Ophthalmol Vis Sci* 2000;41:3544-3551.

19.   Lee JH, Wan XH, Song J, et al. TGF-beta-induced apoptosis and reduction of Bcl-2 in human lens epithelial cells in vitro. *Curr Eye Res* 2002;25:147-153.

20.   Marcantonio JM, Syam PP, Liu CS, Duncan G. Epithelial transdifferentiation and cataract in the human lens. *Exp Eye Res* 2003;77:339-346.

21.   Cousins SW, McCabe MM, Danielpour D, Streilein JW. Identification of transforming growth factor-beta as an immunosuppressive factor in aqueous humor. *Invest Ophthalmol Vis Sci* 1991;32:2201-2211.

22.   Wallentin N, Wickstrom K, Lundberg C. Effect of cataract surgery on aqueous TGF-beta and lens epithelial cell proliferation. *Invest Ophthalmol Vis Sci* 1998;39:1410-1418.

23.   Richiert DM, Ireland ME. Matrix metalloproteinase secretion is stimulated by TGF-beta in cultured lens epithelial cells. *Curr Eye Res* 1999;19:269-275.

24.   Nagase H, Woessner JF, Jr. Matrix metalloproteinases. *J Biol Chem* 1999;274:21491-21494.

25.   Smine A, Plantner JJ. Membrane type-1 matrix metalloproteinase in human ocular tissues. *Curr Eye Res* 1997;16:925-929.

26.   Brew K, Dinakarpandian D, Nagase H. Tissue inhibitors of metalloproteinases: evolution, structure and function. *Biochim Biophys Acta* 2000;1477:267-283.

27.     Yu Q, Stamenkovic I. Cell surface-localized matrix metalloproteinase-9 proteolytically activates TGF-beta and promotes tumor invasion and angiogenesis. *Genes Dev* 2000;14:163-176.

28.     Wormstone IM. Posterior capsule opacification: a cell biological perspective. *Exp Eye Res* 2002;74:337-347.

29.     Tamiya S, Wormstone IM, Marcantonio JM, Gavrilovic J, Duncan G. Induction of matrix metalloproteinases 2 and 9 following stress to the lens. *Exp Eye Res* 2000;71:591-597.

30.     Noda K, Ishida S, Inoue M, et al. Production and activation of matrix metalloproteinase-2 in proliferative diabetic retinopathy. *Invest Ophthalmol Vis Sci* 2003;44:2163-2170.

31.     Wormstone IM, Tamiya S, Anderson I, Duncan G. TGF-beta2-induced matrix modification and cell transdifferentiation in the human lens capsular bag. *Invest Ophthalmol Vis Sci* 2002;43:2301-2308.

32.     Kawashima Y, Saika S, Miyamoto T, et al. Matrix metalloproteinases and tissue inhibitors of metalloproteinases of fibrous humans lens capsules with intraocular lenses. *Curr Eye Res* 2000;21:962-967.

33.     Wong TT, Daniels JT, Crowston JG, Khaw PT. MMP inhibition prevents human lens epithelial cell migration and contraction of the lens capsule. *Br J Ophthalmol* 2004;88:868-872.

34.     Daniels JT, Limb GA, Saarialho-Kere U, Murphy G, Khaw PT. Human corneal epithelial cells require MMP-1 for HGF-mediated migration on collagen I. *Invest Ophthalmol Vis Sci* 2003;44:1048-1055.

35.     Massague J, Wotton D. Transcriptional control by the TGF-beta/Smad signaling system. *Embo J* 2000;19:1745-1754.

36.     Piek E, Ju WJ, Heyer J, et al. Functional characterization of transforming growth factor beta signaling in Smad2- and Smad3-deficient fibroblasts. *J Biol Chem* 2001;276:19945-19953.

37.     Nomura M, Li E. Smad2 role in mesoderm formation, left-right patterning and craniofacial development. *Nature* 1998;393:786-790.

38.     Weinstein M, Yang X, Li C, Xu X, Gotay J, Deng CX. Failure of egg cylinder elongation and mesoderm induction in mouse embryos lacking the tumor suppressor smad2. *Proc Natl Acad Sci U S A* 1998;95:9378-9383.

39.     Datto MB, Frederick JP, Pan L, Borton AJ, Zhuang Y, Wang XF. Targeted disruption of Smad3 reveals an essential role in transforming growth factor beta-mediated signal transduction. *Mol Cell Biol* 1999;19:2495-2504.

40.     Ashcroft GS, Yang X, Glick AB, et al. Mice lacking Smad3 show accelerated wound healing and an impaired local inflammatory response. *Nat Cell Biol* 1999;1:260-266.

41.     Massague J. Wounding Smad. *Nat Cell Biol* 1999;1:E117-119.

42.     Greene RM, Nugent P, Mukhopadhyay P, Warner DR, Pisano MM. Intracellular dynamics of Smad-mediated TGFbeta signaling. *J Cell Physiol* 2003;197:261-271.

43.     Fink AL. Chaperone-mediated protein folding. *Physiol Rev* 1999;79:425-449.

44.     Bagchi M, Ireland M, Katar M, Maisel H. Heat shock proteins of chicken lens. *J Cell Biochem* 2001;82:409-414.

45.     Bagchi M, Katar M, Maisel H. A heat shock transcription factor like protein in the nuclear matrix compartment of the tissue cultured mammalian lens epithelial cell. *J Cell Biochem* 2001;80:382-387.

46.     Horwitz J. Alpha-crystallin. *Exp Eye Res* 2003;76:145-153.

47.     Bode C, Tolgyesi FG, Smeller L, Heremans K, Avilov SV, Fidy J. Chaperone-like activity of alpha-crystallin is enhanced by high-pressure treatment. *Biochem J* 2003;370:859-866.

48.     Kim JM, Kim JC, Park WC, Seo JS, Chang HR. Effect of thermal preconditioning before excimer laser photoablation. *J Korean Med Sci* 2004;19:437-446.

49.     Dean DO, Tytell M. Hsp25 and -90 immunoreactivity in the normal rat eye. *Invest Ophthalmol Vis Sci* 2001;42:3031-3040.

50.     Awasthi N, Wagner BJ. Upregulation of heat shock protein expression by proteasome inhibition: an antiapoptotic mechanism in the lens. *Invest Ophthalmol Vis Sci* 2005;46:2082-2091.

51.     Hooven TA, Yamamoto Y, Jeffery WR. Blind cavefish and heat shock protein chaperones: a novel role for hsp90alpha in lens apoptosis. *Int J Dev Biol* 2004;48:731-738.